

RADIO OVER MULTIMODE FIBER USING VCSELS

ASHOK PRABHU MASILAMANI

(B.Tech., Anna University)

A THESIS SUBMITTED

FOR THE DEGREE OF MASTER OF ENGINEERING

DEPARTMENT OF ELECTRICAL AND COMPUTER

ENGINEERING

NATIONAL UNIVERSITY OF SINGAPORE

2005

Acknowledgements

I would like to thank my advisor, Professor Michael Chia Yan Wah, for his excellent support and guidance throughout my graduate studies. Also I would like to thank to Yee Ming-Li of Institute for Infocomm Research for his extensive help in setting up the experiments for UWB and WLAN signal transmission over fiber. My thanks go out to Luo Bin (Institute for Infocomm Research) also for his valuable contribution in providing measurement data and data sheets related to VCSELs and multimode fibers.

I would like to acknowledge the support from “Agilent Asia Support” for providing assistance in resolving the SPICE program to ADS circuit import problems. Also I would like acknowledge the valuable comments from Siegfried Geckeler (Author of “Fiber Optic Transmission Systems” book) related to fiber optic system simulation.

This work was supported by Institute for Infocomm Research and I would like to thank the institute for providing the opportunity and facilities to conduct this research work. Also I would like to thank the institute staff and fellow graduate students for their support.

Table of contents

ACKNOWLEDGEMENTS	I
TABLE OF CONTENTS	III
SUMMARY	VI
LIST OF TABLES	VII
LIST OF FIGURES	IX
LIST OF SYMBOLS	XII
LIST OF ABBREVIATIONS	XII
1 INTRODUCTION TO ROF SYSTEMS	1
1.1 INTRODUCTION.....	1
1.2 OVERVIEW OF RADIO SYSTEMS.....	2
1.3 RADIO OVER FIBER SYSTEMS.....	4
1.3.1 <i>IMDD ROF links</i>	5
1.3.2 <i>ROF link performance</i>	8
1.3.3 <i>ROF link advantages</i>	9
1.4 ORGANISATION OF THE THESIS.....	10
2 MULTIMODE FIBER LINKS	12
2.1 EVOLUTION OF FIBER OPTIC LINKS.....	12
2.1.1 <i>LED based MMF links</i>	12
2.1.2 <i>CD Laser based MMF links</i>	13
2.2 VCSEL BASED MULTIMODE FIBER LINKS.....	14
2.2.1 <i>VCSELs</i>	14
2.2.2 <i>Laser optimized Multimode fibers</i>	16
2.2.3 <i>10 Gbps data rate and MMF based links</i>	23

2.3	MMF LINKS AS ROF MEDIUM	25
2.4	SUMMARY	26
3	CHARACTERIZATION AND MODELING OF THE ROF MMF LINK	28
3.1	INTRODUCTION.....	28
3.2	MMF LINK SPECIFICATIONS	28
3.3	MMF LINK COMPONENT MODELS.....	30
3.3.1	<i>VCSEL Model</i>	30
3.3.2	<i>Multimode Fiber Model</i>	37
3.3.3	<i>Photodiode Model</i>	44
3.4	MMF LINK SIMULATION RESULTS	45
3.5	SUMMARY	48
4	UWB OVER MMF LINK	49
4.1	INTRODUCTION TO UWB	49
4.2	UWB SPECIFICATIONS	49
4.3	UWB TRANSMISSION OVER FIBER.....	51
4.3.1	<i>UWB pulse Generation</i>	51
4.3.2	<i>Temporal Results of UWB downlink pulse over ROF</i>	54
4.3.3	<i>Spectral Results of UWB downlink pulse over ROF</i>	57
4.3.4	<i>Results of UWB uplink pulse transmission over ROF</i>	60
4.4	SUMMARY	62
5	WLAN TRANSMISSION OVER MMF LINK.....	63
5.1	INTRODUCTION TO WIRELESS LAN	63
5.2	WLAN PHYSICAL MEDIA AND ACCESS MODULATIONS	64
5.3	IEEE 802.11A SIGNAL GENERATION AND TESTING PARAMETERS	65
5.4	WLAN TRANSMISSION OVER FIBER	67
5.5	IEEE 802.11A/G ROF TRANSMISSION PERFORMANCE RESULTS	68
5.6	WLAN TRANSMISSION OVER FIBER IN THE PRESENCE OF UWB SIGNAL	71

5.6.1	<i>Performance results for IEEE 802.11a in the presence of UWB</i>	73
6	CONCLUSIONS AND FUTURE DIRECTIONS	78
6.1	CONCLUSIONS.....	78
6.1.1	<i>Conclusions for UWB</i>	79
6.1.2	<i>Conclusions for WLAN</i>	79
6.2	FUTURE DIRECTIONS OF ROF.....	80
	BIBLIOGRAPHY	82
	APPENDIX A: ENCIRCLED FLUX	82
	APPENDIX B: MODES OF CARRIER OPERATION IN WLAN	90

Summary

The aim of this research project is to address the transmission of radio signals like UWB or Wireless LAN signals over cheaper multimode fiber (MMF) links which are evolving along with the Gigabit / 10G Ethernet standards. These MMF links are based on 850nm VCSEL laser diodes and laser optimized graded index fibers and is meant for short distances up to 300 - 550 meters for 10Gbps data rate.

Large signal circuit models were created and implemented in ADS simulator to characterize the MMF link. The VCSEL model is a semiconductor rate equation model adopted for circuit simulation. The MMF model is a transfer function model based on modal delays and a simplified modal power distribution. The PIN diode model is a simple small signal equivalent circuit. The entire link was characterized and validated using the S-parameters and group delay simulations for small signal performance.

A pulsed UWB transmission over fiber is simulated and validated against the experimental results where the temporal signal qualities were analyzed. Also WLAN IEEE 802.11a/11g system's EVM performances for ROF transmission predicted by the simulation were consistent with experiments. This was further used to predict the EVM performance of the 802.11a system in the presence of UWB signal over ROF.

From the results it was concluded that the low cost MMF link could serve as a potential range extension structure for wireless networks.

List of Tables

TABLE 1.1 WIRELESS NETWORKS FOR PERSONAL USER COMMUNICATIONS	2
TABLE 1.2 UPCOMING WIRELESS NETWORKS.....	3
TABLE 1.3 IMDD LASER DIODES.....	7
TABLE 1.4 IMDD PHOTO DIODES AND CHARACTERISTICS.....	7
TABLE 1.5 IMDD FIBERS AND CHARACTERISTICS.....	8
TABLE 1.6 IMDD ROF LINK PERFORMANCES	8
TABLE 1.7 IMDD ROF COMPONENT PERFORMANCES	9
TABLE 2.1 LED BASED MULTIMODE FIBER LINKS IN LAN	13
TABLE 2.2 CD LASER BASED MULTIMODE FIBER LINKS IN LAN	13
TABLE 2.3 VCSELS Vs EDGE EMITTERS	15
TABLE 2.4 MULTIMODE FIBERS SPECIFIED IN IEEE 802.3z	17
TABLE 2.5 DMD MASK TEMPLATES	21
TABLE 2.6 FIBER TYPES IN THE PROPOSAL OF 10GB ETHERNET ALONG WITH SOURCES.....	25
TABLE 3.1 MMF LINK SPECIFICATIONS	29
TABLE 3.2 VCSEL RATE EQUATION PARAMETERS	31
TABLE 3.3 VCSEL OPTIMIZED COMPONENT VALUES	35
TABLE 3.4 MULTIMODE FIBER PARAMETERS USED TO CALCULATE MODAL DELAYS	42
TABLE 3.5 PHOTODIODE PARAMETERS AND THEIR VALUES.....	44
TABLE 4.1 AVERAGE RADIATED EMISSION LIMITS	49
TABLE 5.1 WLAN SPECIFICATIONS	64
TABLE 5.2 OFDM PARAMETERS.....	65
TABLE 5.3 TIMING PARAMETERS	65
TABLE 5.4 EVM AND CONSTELLATION ERROR REQUIREMENTS OF IEEE 802.11A [7].....	66
TABLE 5.5 RELATIVE CONSTELLATION ERROR RESULTS FOR WLAN ROF TRANSMISSION	70
TABLE 5.6 EVM RESULTS FOR WLAN ROF TRANSMISSION	70
TABLE 5.7 SIMULATION PARAMETERS FOR WLAN ROF TRANSMISSION WITH UWB PRESENCE	73

TABLE 5.8 RELATIVE CONSTELLATION ERROR AND EVM IN DB - UWB PRESENCE AT ROF TRANSMITTER. 75

TABLE 5.9 RELATIVE CONSTELLATION ERROR AND EVM IN DB - UWB PRESENCE AT ROF RECEIVER 77

List of Figures

FIGURE 1.1 IMPROVING COVERAGE RANGE IN A WLAN SCENARIO USING RF SIGNAL DISTRIBUTION WITH FIBER LINKS	4
FIGURE 1.2 DIRECT MODULATION IMDD LINK	6
FIGURE 2.1 OXIDE CONFINED TOP EMITTING VCSEL SCHEMATICS	14
FIGURE 2.2 LAUNCH CONDITIONS FOR LED AND VCSEL SOURCES	18
FIGURE 2.3 IDEAL MPD FOR LED SOURCES.....	19
FIGURE 2.4 A POSSIBLE MPD FOR VCSEL SOURCE WITH 0MM ALIGNMENT	19
FIGURE 2.5 DMD TEMPLATES	22
FIGURE 2.6 DMD TEMPLATES	22
FIGURE 3.1 SCHEMATICS OF THE MMF LINK.....	28
FIGURE 3.2 EQUIVALENT CIRCUIT MODEL OF VCSEL RATE EQUATIONS	33
FIGURE 3.3 PARASITIC CIRCUITRY OF VCSEL	34
FIGURE 3.4 ORIGIN OF PARASITICS IN VCSEL STRUCTURE	34
FIGURE 3.5 MEASURED AND SIMULATED L-I CURVE	36
FIGURE 3.6 MEASURED S11 CURVE.....	36
FIGURE 3.7 SPECTRAL ATTENUATION CURVE OF A 50 MICRON MMF	38
FIGURE 3.8 SIMULATED MODAL TRANSFER FUNCTION OF THE MULTIMODE FIBER.....	43
FIGURE 3.9 PHOTO DIODE MODEL.....	44
FIGURE 3.10 SIMULATED AND MEASURED S21 CURVES FOR 1M ROF LINK	45
FIGURE 3.11 SIMULATED AND MEASURED GROUP DELAYS FOR 1M ROF LINK	45
FIGURE 3.12 SIMULATED AND MEASURED S21 CURVES FOR 300M ROF LINK	46
FIGURE 3.13 SIMULATED AND MEASURED GROUP DELAYS FOR 300M ROF LINK	46
FIGURE 3.14 SIMULATED AND MEASURED S21 CURVES FOR 600M ROF LINK	47
FIGURE 3.15 SIMULATED GROUP DELAY VARIATION FOR 600M ROF LINK.....	47
FIGURE 4.1 IMPULSE RADIO UWB FCC SPECTRAL MASK FOR EMISSION	50
FIGURE 4.2 IMPULSE OUTPUT FROM AN IMPULSE FORMING NETWORK	52

FIGURE 4.3 GAUSSIAN MONOCYCLE PULSE OUTPUT FROM AN IMPULSE FORMING NETWORK.....	52
FIGURE 4.4 SETUP FOR AN IMPULSE RADIO UWB DOWN LINK PULSE GENERATION	53
FIGURE 4.5 UWB DOWNLINK SOURCE PULSE	53
FIGURE 4.6 UWB PULSE SPECTRUM	54
FIGURE 4.7 UWB DOWNLINK PULSE AFTER 1 METER ROF.....	55
FIGURE 4.8 UWB DOWNLINK PULSE AFTER 300 METER ROF.....	56
FIGURE 4.9 UWB DOWNLINK PULSE AFTER 600 METER ROF.....	57
FIGURE 4.10 MEASURED DOWNLINK SPECTRUM AFTER 1 METER ROF	57
FIGURE 4.11 SIMULATED DOWNLINK SPECTRUM AFTER 1 METER ROF	58
FIGURE 4.12 MEASURED DOWNLINK SPECTRUM AFTER 300 METER ROF.....	58
FIGURE 4.13 SIMULATED DOWNLINK SPECTRUM AFTER 300 METER ROF	59
FIGURE 4.14 SETUP FOR AN IMPULSE RADIO UWB UP LINK PULSE GENERATION.....	60
FIGURE 4.15 UWB UPLINK SOURCE PULSE	60
FIGURE 4.16 UWB UPLINK PULSE AFTER 1 METER ROF	61
FIGURE 4.17 UWB UPLINK PULSE AFTER 300 METER ROF.....	61
FIGURE 4.18 UWB UPLINK PULSE AFTER 600 METER ROF.....	62
FIGURE 5.1 A TYPICAL WIRELESS LAN SCENARIO.....	63
FIGURE 5.2 IEEE 802.11A TRANSMITTER SPECTRAL MASK.....	66
FIGURE 5.3 WLAN OVER FIBER SETUP.....	67
FIGURE 5.4 IEEE 802.11A SIGNAL AFTER 300 METER ROF	68
FIGURE 5.5 IEEE 802.11A SIGNAL SPECTRUM A) WITHOUT ROF B) WITH ROF	68
FIGURE 5.6 IEEE 802.11A CONSTELLATION A) WITHOUT ROF B) WITH ROF.....	69
FIGURE 5.7 IEEE 802.11G SIGNAL SPECTRUM A) WITHOUT ROF B) WITH ROF	69
FIGURE 5.8 IEEE 802.11G CONSTELLATION A) WITHOUT ROF B) WITH ROF.....	69
FIGURE 5.9 SPECTRUM OF IEEE WLAN AND UWB.....	71
FIGURE 5.10 WLAN AND UWB ADDED USING RF COMBINER	72
FIGURE 5.11 WLAN AND UWB ADDED USING OPTO-COUPLER.....	73
FIGURE 5.12 IEEE 802.11A SIGNAL SPECTRUM A) WITHOUT UWB B) WITH UWB	74

FIGURE 5.13 IEEE 802.11A CONSTELLATION WITH UWB PRESENCE	74
FIGURE 5.14 UWB PULSE TRAIN IN TIME DOMAIN WITH WLAN ADDED	75
FIGURE 5.15 IEEE 802.11A SIGNAL SPECTRUM A) WITHOUT UWB B) WITH UWB	76
FIGURE 5.16 IEEE 802.11A CONSTELLATION WITH UWB PRESENCE AT ROF RECEIVER	76

List of Symbols

Multimode Fiber

$\alpha(\lambda)$ - Attenuation Coefficient in dB/Km

n_1 - refractive index at $r = 0$

N_{eff} - Effective Group Index of Refraction

Δ - Normalized Refractive Index Difference

λ_0 - Zero dispersion wavelength in nm

S_0 - Zero dispersion slope in ps/(nm².km)

$D(\lambda)$ - chromatic dispersion coefficient in ps/(nm.km)

a - Core radius in μm

α - Profile Exponent

β_m - propagation constant of each mode group m

m - Mode group

$H_{\text{ch}}(\omega)$ - Chromatic dispersion transfer function

$H_{\text{mod}}(\omega)$ - Modal transfer function

$H_{\text{mmf}}(\omega)$ - Multimode fiber transfer function

σ_λ - Source spectral line width in nm

W_m - Modal power distribution in each mode group m

z - Length of the fiber

τ_m - Modal delays per unit length of each mode group m

VCSEL

$N(t)$ - Active region carrier density in cm⁻³

$S(t)$ - Photon density in cm⁻³

$P_o(t)$ - VCSEL output power in mW

$I(t)$ - Injection current in A

η_i - Current injection efficiency

V_a - Active volume of VCSEL Cavity in cm³

τ_n - Carrier lifetime in s

τ_s - Photon lifetime in s

v_g - Group velocity ms^{-1}
 g_0 - Differential gain cm^{-2}
 N_{tr} - Transparency carrier density cm^{-3}
 ε - Gain compression coefficient cm^3
 Γ - Optical confinement factor
 β - Spontaneous emission coefficient
 η_{opt} - Optical efficiency
 λ - Operating Wavelength in nm
 h - Planck's constant
 C_0 - Speed of light in vacuum in ms^{-1}
 z_n, k - arbitrary constants
 δ - a small constant
VCSEL Parasitics
 R_q - Driver output resistance in Ω
 C_q - Driver output capacitance in pF
 R_w - Bond-wire resistance in Ω
 L_w - Bond-wire inductance in nH
 R_p - Pad resistance in Ω
 C_p - Pad capacitance in pF
 R_s - Series Resistance in Ω
 R_a - Active layer resistance in Ω
 C_a - Active layer capacitance in pF
Photo diode
 I_{photo} - Photo current in A
 P_{pd} - Input optical power in W
 q - Electronic charge
 ν - Optical frequency in Hz
 η_{pd} - Quantum efficiency
 I_{sat} - Reverse saturation current (dark) in A

Photo diode parasitics

R_d - “Dark” or “Shunt” resistance

C_d - Junction capacitance

R_{ser} - Series diode resistance

L_{ser} - Parasitic Inductance

List of Abbreviations

ROF - Radio Over Fiber
VCSEL - Vertical Cavity Surface Emitting Laser
LW - Long Wavelength
FP - Fabry Perot
DFB - Distributed Feed Back
DBR - Distributed Bragg-Reflector
SMF - Single Mode Fiber
MMF - Multi Mode Fiber
WAN - Wide Area Network
LAN - Local Area Network
PAN - Personal Area Network
SAN - Storage Area Network
WLAN - Wireless Local Area Network
WPAN - Wireless Personal Area Network
UWB - Ultra Wide Band
SGS - Single mode-Graded-Single mode
PDA - Personal Digital Assistant
GSM - Global System for Mobile Communications
DCS - Digital Cellular System
PCS - Personal Communications Service
GPRS - General Packet Radio Service
EDGE - Enhanced Data Rates for GSM Evolution
CDMA - Code Division Multiple Access
WCDMA - Wideband Code Division Multiple Access
UMTS - Universal Mobile Telecommunications System
HTSG - High throughput study group
MBWA - Mobile Broadband Wireless Access
MBS - Mobile Broadband Services
SCM - Sun Carrier Multiplexing

IMDD - Intensity-Modulated Direct-Detection
FDDI - Fiber Distributed Data Interface
OFL - Over Filled Launch
MPD - Modal Power Distribution
RML - Restricted Mode Launch
EF - Encircled Flux
DMD - Differential Modal Delay
SFDR - Spurious free Dynamic Range
TIA - Trans Impedance Amplifier
SDD - Symbolic Defined Devices
WKB - Wentzel Kramers Brillouin
EMB - Effective Modal Bandwidth
EIRP - Effective Radiated Power
FHSS - Frequency Hopping Spread Spectrum
DSSS - Direct Sequence Spread Spectrum
CCK - Complementary Code Keying
PBCC - Packet Binary Convolutional Coding
OFDM - Orthogonal Frequency Division Multiplexing
BPSK - Binary Phase Shift Keying
QPSK - Quadrature Phase Shift Keying
DBPSK - Differential Binary Phase Shift Keying
DQPSK - Differential Quadrature Phase Shift Keying
QAM - Quadrature Amplitude Modulation
BER - Bit Error Rate
PER - Packet Error Rate
EVM - Error Vector Magnitude

1 Introduction to ROF systems

1.1 Introduction

Radio over fiber is a technology that allows a viable transmission of radio frequency signals over an optical fiber link within an acceptable degradation of the RF performance. Although ROF systems are already in use for distributed antennae systems [1], they are predominantly single mode fiber links based on Fabry-Perot or DFB laser diodes. This thesis explores the transmission of RF signals like wireless LAN and UWB over a low cost VCSEL laser diode based multimode fiber link. This involved designing a RF fiber optic system by characterizing, modeling and simulating the optical link-components like VCSEL laser diode, multimode fiber and PIN photo diode alongside the RF components. VCSEL laser diode is chosen as the ROF transmitter because of the reasons [2] [3] stated below:

- 1) Low cost availability, primarily because of microelectronic style manufacturing process and the possibility on-wafer testing.
- 2) The 50 Ohm series impedance of VCSEL is inline with the RF source impedances.
- 3) Due to low threshold current requirements, it can be driven directly by logic gates. This again leads to a lower link cost.
- 4) High relaxation oscillation frequency due to the smaller size of the cavity. Hence ideal choice for direct modulation, which again contributes to the lower link cost.

As the chapter progresses, it introduces the present and future radio systems and their necessities of range extension. It also gives an overview about the Radio over fiber technology – components, performance and advantages.

1.2 Overview of Radio systems

In the last decade radio systems witnessed an explosive growth backed by the second generation cellular networks like GSM [4], cdmaOne (IS-95) [5]. The applications provided by these networks have tremendously increased the personal user connectivity and has transformed the radio systems into a cheaper and viable system for individuals. In recent times, the cellular networks are offering enhanced connectivity services and the related applications like data packet services with 2.5G standards like GPRS for GSM and cdmaOne 1x for cdmaOne. In parallel the personal mobile computing devices like notebook computers, PDA computers had their share of wireless connectivity services based on Wireless Local Area Networks (IEEE802.11a, b, g) standards [6], [7], [8]. Table 1.1 provides a list of existing wireless networks and their capabilities.

Wireless Networks	Frequency band/span	Data rates
IEEE802.11b	2.400-2.480 GHz	Up to 11 Mbps
IEEE802.11a	5.150-5.350 GHz 5.725-5.825 GHz	Up to 54 Mbps
IEEE802.11g	2.400-2.480 GHz	Up to 54 Mbps
GSM 900	890-915 MHz 935-960 MHz	GPRS – 170 kbps EDGE – 384 kbps
GSM 1800 (DCS 1800)	1.710-1.785 GHz 1.805-1.880 GHz	GPRS – 170 kbps EDGE – 384 kbps
PCS 1900 (GSM in US)	1.850-1.990 GHz	GPRS – 170 kbps EDGE – 384 kbps
cdmaOne (IS-95)	824-849 MHz 869-894 MHz	Up to 144kbps with 1x

Table 1.1 Wireless networks for personal user communications

These cellular networks are expected to get revised soon with 3G standards like UMTS [9] and CDMA2000 [10]. These networks are already in deployment and would be offering services like customized information and entertainment, mobile internet access etc. In spite of all these improvements, the future wireless networks and the applications driving them like video-on-demand etc. are demanding very high data rates. This demand in the data rate can be attributed to the development of upcoming standards like

1. IEEE802.15.3a - Ultra Wide Band (UWB) technology for personal area networks (PAN) [11].
2. IEEE802.11n - evolved from High Throughput Study Group (HTSG) investigating WLAN data rates over 100Mbps [12].
3. IEEE802.20 - Mobile Broadband Wireless Access (MBWA) working group [13].

Table 1.2 gives a list of new wireless standards getting deployed or developed.

Wireless Networks	Frequency band/span	Data rates	
UMTS	1.885-2.025 GHz 2.110-2.200 GHz	Up to 1.920 Mbps	
CDMA2000	1.900 GHz PCS band	1x	307 kbps
		1xEV-DO	384 kbps - 2.4 Mbps
		1xEV-DV	4.8 Mbps
IEEE802.15.3a (UWB)	3.10-10.6 GHz	Demonstrated up to 1 Gbps	
IEEE802.11n	-	Up to 100 Mbps	
IEEE802.20 (MBWA)	3.5 GHz band	Up to 1 Mbps	
Mobile Broadband Services (MBS)	60 GHz band	155 Mbps	
Vehicle Communication and Control	63-64 GHz 76-77 GHz	-	

Table 1.2 Upcoming Wireless networks

Alongside the demand for data rates, the sharp increase in the user density within the networks has to be accommodated. This demands the increase in the number of base stations to improve the coverage range.

1.3 Radio over fiber systems

The previous section discussed about the rapid expansion of wireless networks in WAN, WLAN and WPAN scenarios. This expansion leads to more demanding physical media restrictions due to the co-existence of different wireless networks. Also in the WLAN and WPAN scenarios due to shorter coverage range (few meters to 100 meters), rapid increase in users will lead to the installation of more base stations raising the cost of the network. One solution to overcome these problems is to use a cheap alternative physical media which can distribute these RF/microwave signals for example 1) from a base station (BS) to many remote antennas (RA) as shown in Figure 1.1 and 2) from a central processing site to a base station.

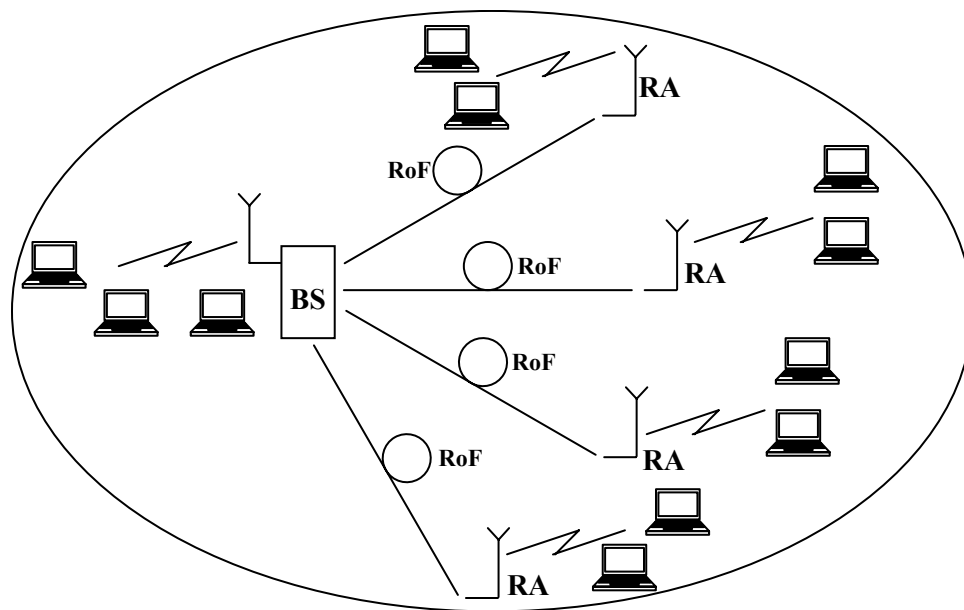


Figure 1.1 Improving Coverage range in a WLAN scenario using RF signal distribution with fiber links

One such media which is capable of carrying RF/Microwave signals is a fiber optic link. The recent drive in the use of fiber optic links as campus backbone networks in different high speed LAN environments like 10Gbps Fibre channel [14], 10GB Ethernet [15] has led to the standardization of a reliable cheaper fiber optic solution for high bandwidth scenarios. With enormous bandwidth availability and cheaper costs, RF fiber optic links promise a greater role in the RF signal distribution.

ROF links are similar to digital fiber optic links except that they are operated at the laser diode's linear region in most of the cases. Also much of the signals driving these links would be of small signal nature, hence small signal models would be good enough to characterize these links. The use ROF links started a decade back for distribution of CATV video signals using subcarrier multiplexing (SCM) technique [16]. In SCM, several RF subcarriers modulated with the different data channels are combined and modulated over a high frequency RF carrier and sent over the fiber link. Then ROF links were started getting used widely for antenna remoting for satellite earth stations and wireless cellular networks [1]. Generally, these fiber links were Intensity-Modulated Direct-detection (IMDD) links.

1.3.1 IMDD ROF links

An intensity modulated direct detection link as the name suggests operates based on an amplitude/intensity modulated laser diode, a fiber and a photo receiver based on direct detection. The intensity modulation can be a direct modulation or an external modulation technique. In direct modulation, the laser diode is driven directly by the signal current along with the bias current which correspondingly varies the output optical power directly. A direct modulation IMDD link is shown in Figure 1.2.

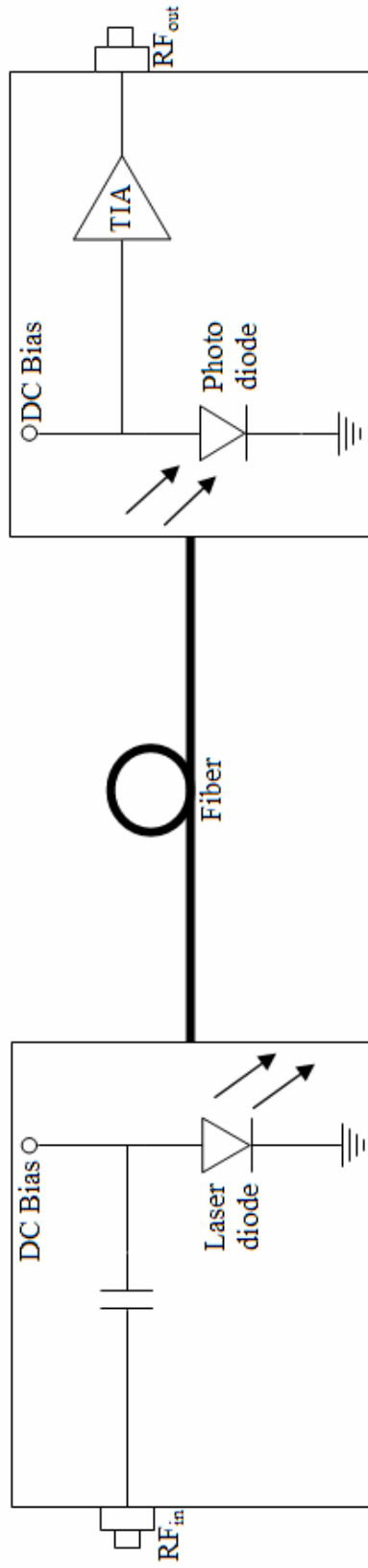


Fig. 1.2 Direct modulation IMDD link

The Table 1.3, 1.4 and 1.5 shows the possible components and their characteristics used in an IMDD ROF link.

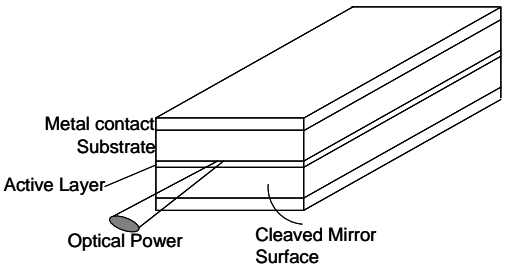
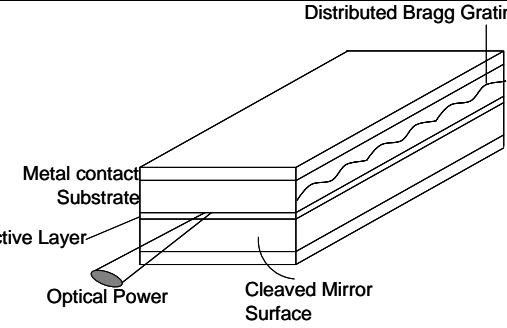
Types	Structure	Properties
Fabry Perot Laser		<ul style="list-style-type: none"> • Simple structure • Feedback occurs as reflection at mirror ends • Multiple longitudinal modes leading to broad optical spectrum (3-6 nm at 1300nm) • High Power up to 10dBm • Modulation bandwidth > 1GHz
DFB Laser		<ul style="list-style-type: none"> • Distributed Feedback occurs at Bragg gratings • Single longitudinal mode leading to narrow optical spectrum (0.05nm at 1500nm) • High linearity • Modulation bandwidth > 10GHz
VCSEL	See Figure 2.1	See Chapter 2 Table 2.3

Table 1.3 IMDD Laser Diodes [2] [17] [18] [3]

Parameter	Symbol	Unit	Type	Material		
				Si	Ge	InGaAs
Wavelength	λ	nm		0.4-1.1	0.8-1.8	1.0-1.7
Responsivity	R	A/W	p-i-n	0.4-0.45	0.8-0.87	0.5-0.95
Quantum Efficiency	η	%	p-i-n	75-90	50-55	60-70
APD gain	M	-	APD	-	50-200	10-40
Dark Current	I_d	nA	p-i-n	1-10	50-500	1-20
Bandwidth	BW	GHz	APD	0.1-1	50-500	1-5
			p-i-n	0.125-1.4	0-0.0015	0.0025-40
Bit rate	BR	Gbit/s	p-i-n	0.01	-	0.1555-53
			APD	-	-	2.5-4
Reverse voltage	V	V	p-i-n	50-100	6-10	5-6
k-factor	kA	-	APD	200-250	20-40	20-30
			APD	0.02-0.05	0.7-1.0	0.5-0.7

Table 1.4 IMDD Photo Diodes and characteristics [17]



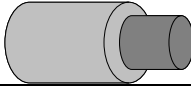
Properties	SMF		Silica MMF			Polymer MMF	
							
Core diameter	~10 μ m		50 μ m	62.5 μ m	120 μ m		
Attenuation dB/km	1300nm	~ 0.50	850nm	~ 2.5	~ 3.0	850nm	~ 40
	1500nm	~ 0.25	1300 nm	~ 0.7	~ 0.7	1300 nm	~ 25
Bandwidth MHz.km	1300nm	-	850nm	400 - 1000	160 - 300	850nm	Above 300
	1500nm	-	1300 nm	400 - 1500	500 - 1000	1300 nm	Above 300
Numerical Aperture	0.13		0.2	0.275	0.185		
Light sources	DFB lasers, FP lasers, VCSEL diodes		VCSEL diodes, LED			VCSEL diodes, LED	

Table 1.5 IMDD fibers and characteristics [2] [17] [18] [19]

1.3.2 ROF link performance

The performances of the ROF links are evaluated based on link gain, noise figure and spurious free dynamic range etc. The performances of the single mode fiber links are discussed in the literature which is tabulated in the Table 1.6 [20].

Parameter		Direct Modulation	External Modulation
Wavelength		850nm, 1300nm, 1550nm	1300nm, 1550nm
Maximum modulation frequency		30 GHz	100 GHz
Link Gain		-5dB to -35 dB	-30dB to 30dB
Noise Figure		20dB to 60dB	4dB to 30dB
Spurious Free dynamic Range	Standard	100 to 114 dBHz ^{2/3}	112 dBHz ^{2/3}
	Linearized	120 dBHz ^{2/3}	130 dBHz ^{2/3}

Table 1.6 IMDD ROF link performances [20]

The following Table 1.7 [1] discusses reports the best available component performances by various components which could be used in a ROF links. It can be seen that the IMDD links are constrained by the intrinsic modulation bandwidth of the semiconductor laser diodes. Also it can be noted that with the efficiency at 61% and modulation bandwidth at 36GHz VCSEL would be better choice for an IMDD ROF link.

Component	Highest reported Efficiency	Highest Reported Bandwidth
Photo detector		
Surface-Illuminated	0.94 A/W	375 GHz
Edge-Illuminated	0.84 A/W	520 GHz
Semiconductor Laser		
Vertical-Cavity Surface Emitter (VCSEL)	0.61 W/A	36 GHz
Fabry-Perot (FP)Edge Emitter	0.38 W/A	40 GHz
Distributed Feedback (DFB) Edge Emitter	0.44 W/A	20 GHz
External Intensity Modulators		
Mach-Zehnder modulator	15 W/A	70 GHz
Electro-Absorption modulator	15 W/A	60 GHz

Table 1.7 IMDD ROF component performances [1]

1.3.3 ROF link advantages

- Low Attenuation Loss
 - Single mode fiber - 0.2 dB/km and 0.5 dB/km in the 1.5 μm and the 1.3 μm transmission window respectively.
 - Polymer optical fiber - 10 to 40 dB/km in the 500 - 1300 nm region
- Large Bandwidth

- 50 THz of bandwidth available of which only 1.6 THz is commercially used. Multiplexing techniques like Wavelength Division Multiplexing, Sub-Carrier Multiplexing can improve this deficiency.
- Immunity to radio frequency interference and cross talk.

1.4 Organization of the thesis

Chapter 1 introduces the existing and the future wireless networks and undermines the necessities for the coverage range extensions. Also it proposes a low cost solution in the form of ROF links. Then it gives a detailed account on the types of ROF links, the components involved, and their performances and concludes with their advantages.

Chapter 2 deals with the multimode fiber links in depth. It starts with the evolution of multimode fibers in the LAN networks as short distance data communication medium. Then it explores how the multimode fiber links entered the high speed arena of 10 Gbps Ethernet. In parallel it explores in detail about the vertical cavity surface emitting laser which was a potential reason for the evolution of MMF links into a low cost, high speed physical medium. At the end a brief description is given on ROF MMF link demonstrations in the literature.

Chapter 3 deals with characterization and modeling of the multimode fiber links. It starts with the VCSEL model and its adaptation from the rate equations and slowly explains the transformation into equivalent circuit model adopted for the ADS simulator. Then the multimode fiber and its characteristics are dealt in details before arriving at a transfer function model for it. A brief explanation about the photo diode model is also given before dealing with the simulated results. A comparison of model performances alongside the measurements is also given.

Chapter 4 deals with UWB transmission over MMF links. First the UWB standard and the characteristic nature of the UWB signals are dealt in detail. Then UWB signal generation using an experimental setup is explained for both uplink and downlink cases. The UWB transmission over MMF is evaluated both in simulations and experiment for 1, 300, 600 meters link length. The temporal qualities of the received pulses are analyzed in detail by comparing the simulated and measured results. It also explores the model capabilities and the errors induced by the model.

Chapter 5 deals with the transmission of Wireless LAN signals over MMF and evaluates the performance in terms of transmitter spectral mask, constellation diagrams and error vector magnitude. Both simulation and experimental setup are dealt in detail with a conclusive display of results. After this it deals with the co-existence scenario for WLAN along with UWB in a ROF link. Here again WLAN performance is evaluated and presented in detail.

2 Multimode Fiber links

2.1 Evolution of Fiber Optic links

The use of fiber optic technology for telecommunication systems started with graded Index multimode fibers and LEDs operating at 800-900nm band. But the modal dispersion as well as the high attenuation (> 5 dB/Km) limited the bandwidth and the transmission distance largely [2] [18] [21]. After the development of single mode fibers, they took centre stage in telecommunication networks as they had no modal dispersion and an attenuation of ~ 0.4 dB/Km at 1300nm and 0.2 dB/Km at 1550nm [2] [18]. With the development of 1300nm and 1550nm semiconductor lasers, single mode fibers became the sole choice for long distance telecommunication applications which eventually scaled trans-oceanic distances of the order of tens of thousands of kilometers. But this was not the end of multimode fiber links. In parallel with the single mode fiber links, the LED based multimode fiber links saw their potential use in back bone links, in spite of their lower bandwidth distance product. The forthcoming sections would be discussing these MMF links, their components and their evolution towards 10Gbps operation.

2.1.1 LED based MMF links

These links span over from few meters up to 2km for the Local Area networks like FDDI, Fibre Channel and Fast Ethernets [22], [23]. This interest was sparked by the lower cost of these links. And it is due to the 1) large core of the multimode fiber which led to easy installation and maintenance and 2) the low cost LED transmitters. All of

these links were using 62.5 μm core multimode fibers and operated at either 850nm or 1300nm. Table 2.1 lists out the LED based MMF links used in LANs.

LAN		Physical Media specification	Maximum Data rate And Distance
FDDI		1300nm LED, 62.5/125 μm MMF	100 Mbps and 2000m
Ethernet	10BASE-FL	850nm LED, 62.5/125 μm MMF	10 Mbps and 2000m
	100BASE-F	1300nm LED, 62.5/125 μm MMF	100 Mbps and 2000m
Fibre Channel		1300nm LED, 62.5/125 μm MMF	266Mbps and 1500m

Table 2.1 LED based multimode fiber links in LAN

2.1.2 CD Laser based MMF links

One major criterion for the popularity of multimode fiber links was the low cost transmitter. But due to the increase in demand for improving the data rates in these links, the exploration of producing a cost effective transmitter started. This was temporarily satisfied by an innovative approach. The low cost CD lasers which were operating at 780nm wavelength were combined with a telecommunication-grade 50 μm core multimode fiber to achieve higher bandwidth distance product [24]. Soon these multimode fiber links were put into use in Fibre Channel and IBM OptiConnect LAN [22]. Table 2.2 lists out the CD Laser based MMF links used in LANS.

LAN		Physical Media specification	Maximum Data rate And Distance
Fibre Channel		780nm Laser Diode, 50/125 μm MMF	266Mbps and 2000m / 532Mbps and 1000m / 1062.5 Mbps and 500m
OptiConnect		780nm Laser Diode, 50/125 μm MMF	266Mbps and 2000m / 1062.5 Mbps and 500m
OptiConnect		780nm Laser Diode, 62.5/125 μm MMF	266Mbps and 700m / 1062.5 Mbps and 170m

Table 2.2 CD Laser based multimode fiber links in LAN

Even though the CD laser based MMF links scaled the data rates up to 1Gbps, the laser reliability issues marred these links from getting widely accepted. Almost in parallel the low cost 850nm VCSELs with high reliability were getting commercialized. These VCSEL based multimode fiber links became highly popular in LANs as well as in Storage Area Networks (SAN) [22], [23]. Because of their high reliability and high speed operations as well as lower costs they also became a potential medium in Radio over fiber links. The next section discusses the VCSEL based multimode fiber links in detail with component descriptions.

2.2 VCSEL based Multimode fiber links

2.2.1 VCSELs

VCSELs are surface emitting semiconductor lasers having a vertical cavity formed by several epitaxial layers consisting of a narrow active region with quantum wells flanked by reflective mirror stack regions on both sides as shown in Figure 2.1.

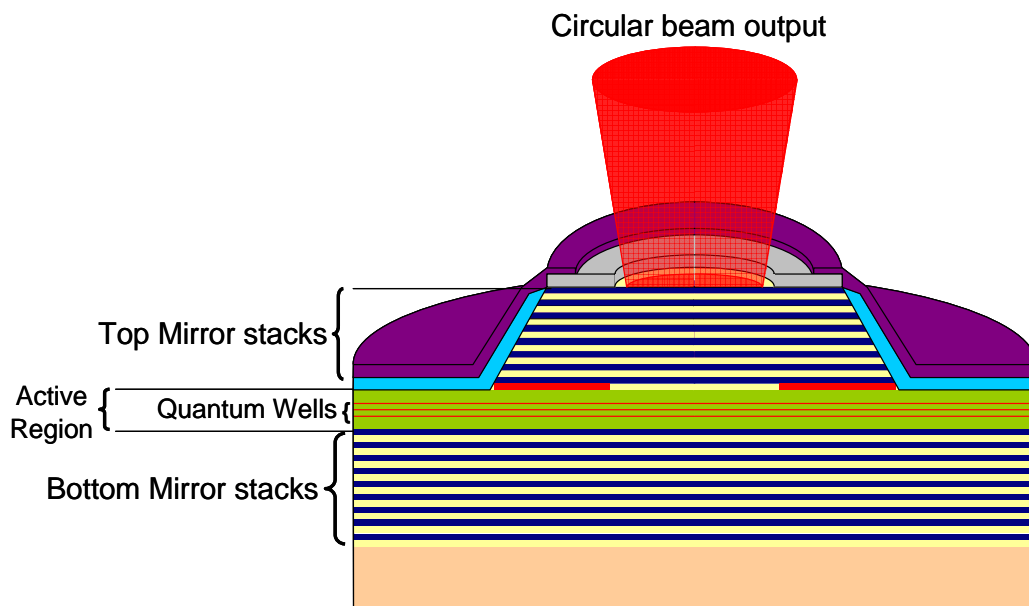


Figure 2.1 Oxide confined top emitting VCSEL schematics [25]

The major difference from edge emitting lasers is the cavity length which is of wavelength scale requires highly reflective mirrors (reflectivity greater than 99.9 %) to reach lasing condition. The major advantage of this is the reduced threshold current due to the small cavity size. A comparison of features of VCSEL with edge emitters like DFB and FP Lasers are given in Table 2.3.

	VCSEL	Edge Emitters
Cavity Length	Wavelength scale $\sim(1-3)\lambda$	$\sim 300\mu\text{m}$ [25]
Mirror reflectivity	Greater than 99.9% achieved by growing Distributed Bragg Reflectors	Typically 30% [25]
Growth on Wafer	The growth of VCSEL structure on wafer is complete.	Edge emitters have to be separated and cleaved to form facets before they can be complete.
Cost	Microelectronic style manufacturing process and On-wafer testing is possible, leading to low cost	Testing/processing is possible only after packaging leading to higher cost
Power	Low threshold current ($<1\text{mA}$) due to smaller cavity size hence low Power consumption	High threshold current and high power consumption
Driver	Due to low threshold current requirements, it can be driven directly by logic gates.	Driver circuits needed.
Intrinsic Bandwidth	High Relaxation oscillation frequency due to the smaller size of the cavity. Ideal choice for direct modulation.	Low Relaxation oscillation frequency.
Modulation Bandwidth reported (max)	36 GHz [1] due to electrical parasitics and the package parasitics.	20GHz for DFB Lasers and 40 GHz for FP Lasers [1]
Beam	Asymmetric beam	Low divergent symmetric circular beams facilitates efficient coupling to fiber.
Integration	Not easily integrable with devices like photo detectors	Integration with photo detectors and coupling lens is easier due to the planar structure.

Table 2.3 VCSELs Vs Edge Emitters [3], [25]

With these advantages mentioned above, commercialized 850nm VCSELs started to replace the edge emitting CD lasers used in short wavelength multimode fiber links for 1Gbps operation. VCSELs emerged as the dominant optical transmitters especially for short wavelength solution in the Fibre Channel as well as Gigabit Ethernet physical media. In parallel, due to the perpendicular emission of VCSEL to its surface it was easy to produce 1D and 2D VCSEL arrays. This array producibility alongside with VCSEL's symmetric circular beams enabled them to be easily coupled with ribbon fiber interconnects. These arrays especially 1D array of 4 or 10 VCSELs were used to achieve higher data rates using parallel optics. The arrival of commercial VCSELs operating up to 10GHz enabled the emerging 10Gbps LAN standards like 10Gbps Ethernet and 10Gbps Fibre channel to choose VCSELs as the only optical transmitter in short wavelength physical media solution. Also 10Gbps Ethernet specifies a parallel optics solution using a 1D array of 10 VCSELs each having 1GHz modulation bandwidth as one of its physical media. With this VCSELs have completely swept the short wavelength based data communication domain. There are also reports in the literature [26] about the long wavelength VCSELs in 1300nm [27] and 1550nm [28], but none is yet to be commercialized. But in future VCSELs can be expected to emerge as a dominant optical transmitter solution even for long distance telecommunication links.

2.2.2 Laser optimized Multimode fibers

The LAN applications continued to drive the usage of multimode fibers as a solution for their campus backbone links of distances up to 500 meters. The predominantly used multimode fibers were pertaining to the FDDI grade specified by ISO 11801 standard. This standard specified two multimode fibers: 62.5µm core MMF

and 50 μ m core MMF. Both support a bandwidth length product of 500 MHz.Km at 1300 nm while 62.5 μ m MMF supports 160 MHz.Km and 50 μ m MMF 500 MHz.Km at 850 nm. Then LAN standards were revived for 1Gbps data rate. The IEEE 802.3z (Gigabit Ethernet) – a standard for 1Gbps data rate Ethernet specified multimode fiber as a physical media for both long and short wavelength as given in Table 2.4. This physical media specification was adopted from the Fibre channel physical media specification.

Wavelength	Fiber	Modal Bandwidth	Max. Length
850 nm	65.2 μ m MMF	160 MHz.Km	220 Meters
	65.2 μ m MMF	200 MHz.Km	275 Meters
	50 μ m MMF	400 MHz.Km	500 Meters
	50 μ m MMF	500 MHz.Km	550 Meters
1300 nm	65.2 μ m MMF	500 MHz.Km	550 Meters
	50 μ m MMF	400 MHz.Km	550 Meters
	50 μ m MMF	500 MHz.Km	550 Meters

Table 2.4 Multimode fibers Specified in IEEE 802.3z [23] Modal Bandwidth – Bandwidth Length Product

A. Overfilled Launch (OFL) Bandwidth

The minimum overfilled modal bandwidth is a way of estimating the bandwidth of a multimode fiber evolved out from LED based multimode fiber links. The basic assumption is the light power launched from the transmitter fills the entire core. But this overfilled modal bandwidth may not represent the real bandwidth achieved in a Laser/VCSEL based multimode fiber links. The difference arises in the way the optical power is launched into the fiber core. This can be explained with the help of Figure 2.2:

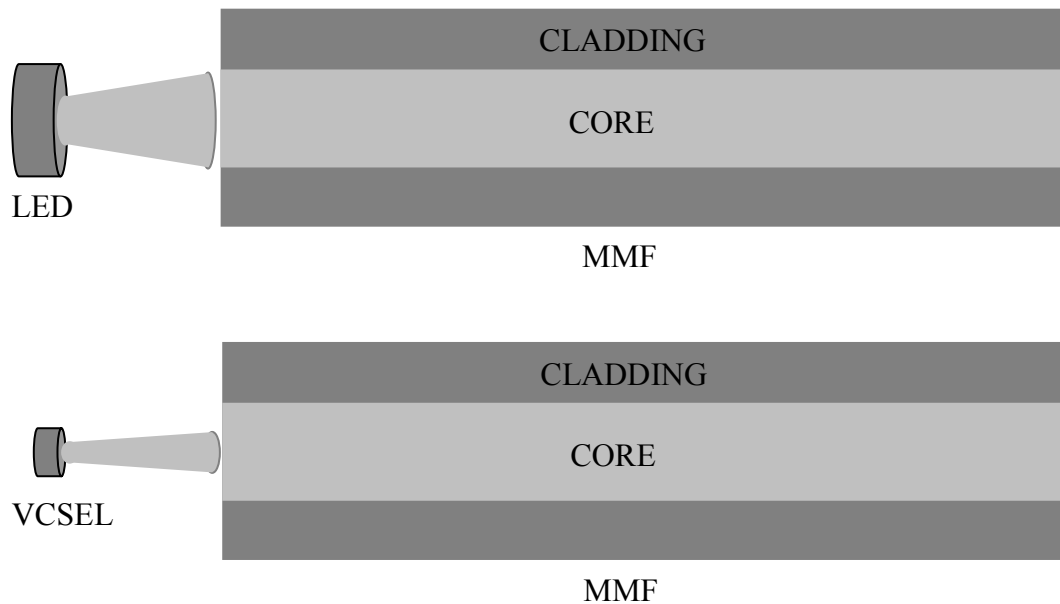


Figure 2.2 Launch Conditions for LED and VCSEL sources

From Figure 2.2 it can be seen that the light emission from LED is wide enough (high numerical aperture and larger area) to cover the entire core cross-sectional area of the multimode fiber. This induces a modal excitation which fills approximately equal power in all the propagation modes of the fiber. This kind of power launch is called over filled launch (OFL) condition, representing the overfilling of power in all the modes. The modal bandwidth calculated based on this launch condition is termed as OFL bandwidth was good enough to characterize the LED based MMF links. However VCSELs or any laser diodes have smaller spot size across the core cross-section and they tend to fill the modes partially or under fill. This can be explained considering that the emission is coincided with the center of the fiber core. Near the fiber center the lower order modes propagate and hence much of the power is launched into these modes alone. This could be understood with the modal power distribution (MPD) given in Figures 2.3 and 2.4.

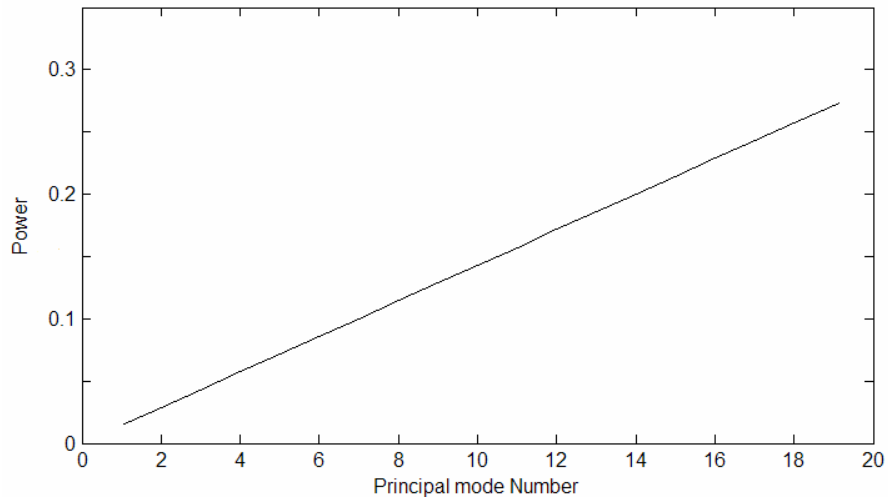


Figure 2.3 Ideal MPD for LED sources

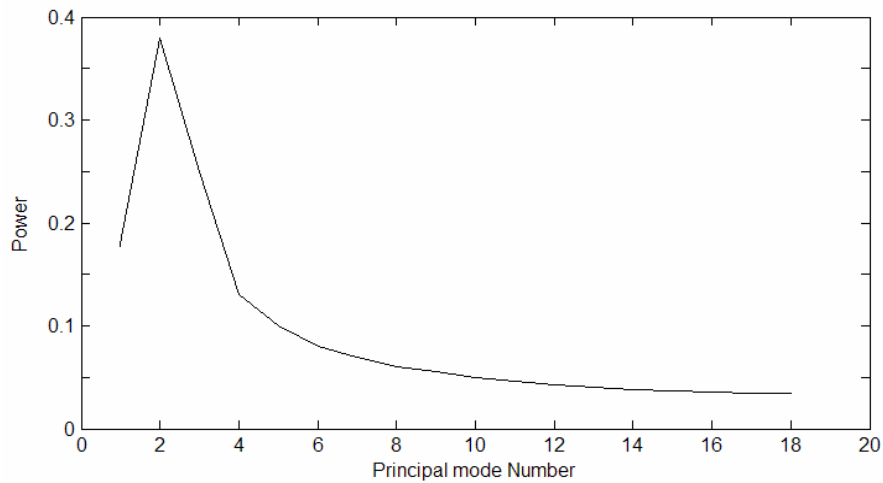


Figure 2.4 A possible MPD for VCSEL source with 0μm alignment

It can be seen that the modal power distribution for LED is uniform whereas for a VCSEL source it's highly non uniform because of the dependence on the alignment of the emitted power with the center of the MMF core. The Figure 2.4 shows the VCSEL MPD for a case where the alignment is perfect, measured as 0μm. There will be a huge variation in the modal power distribution with every micron deviation in the alignment of

the VCSEL with the fiber which is possible due to the presence of connectors. This is easily understandable because a slight deviation in the connector causes a different launch of power in different set of modes. So characterizing the VCSEL MPD with an ideal equation as done in the LED case is not possible. In general VCSEL based MMF link has a higher bandwidth due to the propagation happening at fewer modes. But in some cases due to the fiber perturbations at the fiber axis the effective bandwidth can go well below the overfilled bandwidth case. In these cases instead of a center launch, an offset launch technique was proposed [29]. Overall the variations in signal launch conditions leads to an uncertainty in bandwidth prediction.

B. Restricted Modal Launch(RML) Bandwidth

In an attempt to overcome the problems related to characterizing the bandwidth of VCSEL based MMF links, specific launch conditions alongside with restrictions on the encircled flux (Appendix A) of the transmitter were specified in the TIA FOTP-204 [30] and TIA FOTP-203 [31]. The bandwidth characterization based on this specification is termed as Restricted Modal Launch (RML) bandwidth.

C. DMD and 10Gbps Laser optimized fiber

The migration from the gigabit LAN network to a 10Gbps LAN network (Fibre channel, 10Gbps Ethernet) needed a better specification for the bandwidth, since the RML Bandwidth method was not adopted widely as a standard. So the TIA proposed a new specification which would combine the restrictions placed on the encircled flux of the transmitter (VCSEL) defined in TIA FOTP-203 [31] and the fiber delay structure in terms of the differential model delay (DMD) measurement defined in TIA FOTP 220

[32]. The encircled flux (EF) specifications for an 850 nm VCSEL coupled to a 50 μm laser optimized multimode fiber are specified as:

- At radius 4.5 μm : $\text{EF} \leq 30\%$ which requires the VCSEL to concentrate lesser power within the given radius. This implies that the lower order fiber modes which travel through the region defined by the radius should be imparted with lesser power by the VCSEL.
- At radius 19 μm : $\text{EF} \geq 86\%$ which requires the VCSEL to concentrate more power within the given radius. This implies that the higher order fiber modes which travel through the outer region of 19 μm radius should be imparted with lesser power by the VCSEL.

The DMD specifications for 50 μm laser optimized multimode fiber are characterized by the following test method. The modal delay structure of the fiber is found out by scanning the fiber core using a small spot size and a very short pulse. The corresponding output pulses are monitored and the delays are noted. The DMD pattern calculated has to confine within one of the six DMD mask templates defined in Table 2.5.

Max. DMD at 850 nm [ps/m]		
Template	Inner Mask (radius 5-18 μm)	Outer Mask (radius 0-23 μm)
1	≤ 0.23	≤ 0.70
2	≤ 0.24	≤ 0.60
3	≤ 0.25	≤ 0.50
4	≤ 0.26	≤ 0.40
5	≤ 0.27	≤ 0.35
6	≤ 0.33	≤ 0.33

Table 2.5 DMD mask templates [32]

Figures 2.5 and 2.6 give a better visualization of the DMD mask templates.

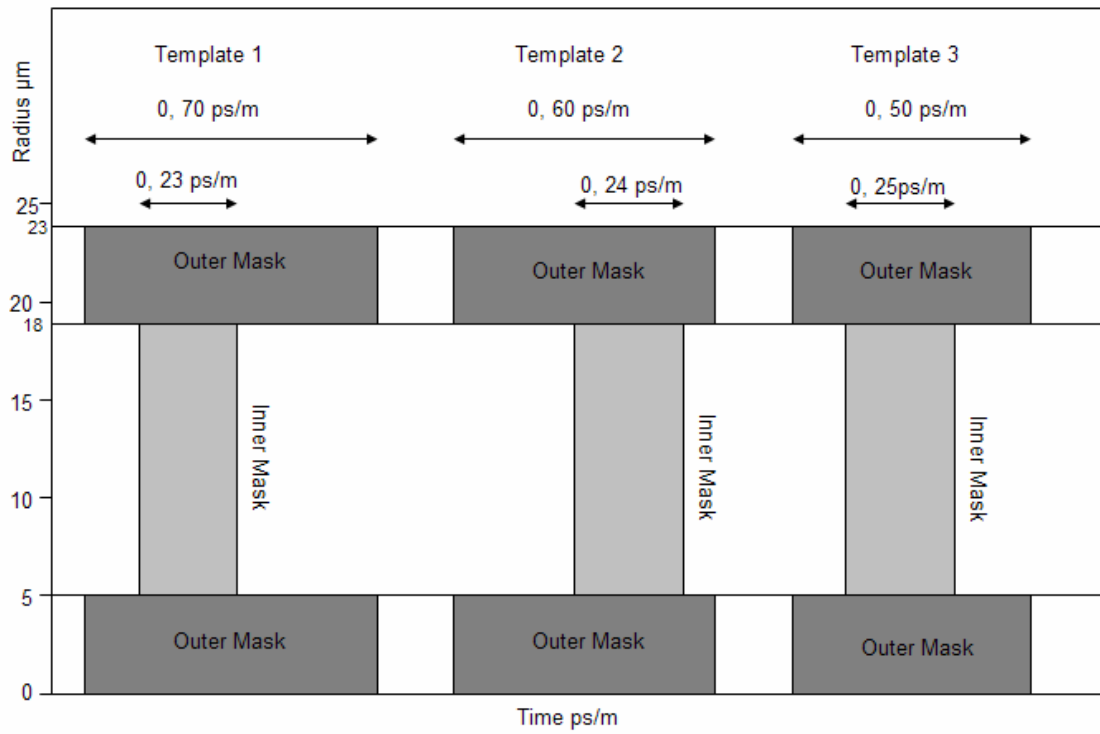


Figure 2.5 DMD Templates [32]

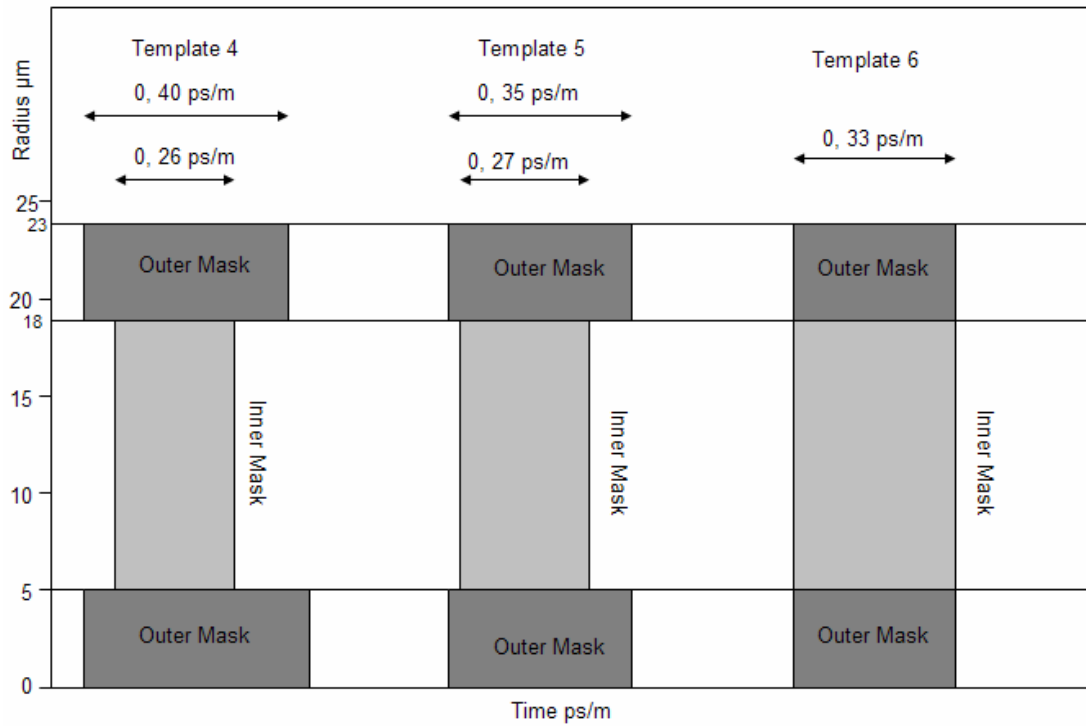


Figure 2.6 DMD Templates [32]

According to FOTP 220 [32] DMD is defined as the maximum difference in the 25% threshold of the leading and trailing edges of the output pulses collected by scanning a single mode spot light between radius r_1 and r_2 . The radius r_1 and r_2 are categorized as inner region specified by 5 μm and 18 μm correspondingly. There is an outer region which is specified by 0 μm and 23 μm . According to template 1 the inner region has to take care of DMD not exceeding above 23 ps/m and the outer region has to take care of DMD not exceeding above 70 ps/m. This in effect restricts the fiber manufacturers to design the core of the MMF with a refractive index profile which would confine to any one of the DMD templates.

If these above criterion are met the link would eventually meet the IEEE minimum modal bandwidth of 2000 MHz.Km at 850 nm so that a distance of 300 meters could achieved for a data rate of 10 Gbps.

2.2.3 10 Gbps data rate and MMF based links

This section summarizes the MMF based physical medium solutions for 10Gbps data rate to get a better understanding about the influence of MMF based links in high speed data communications, which later could be extended to low cost short distance Tele-communication links. Also a tabulation of the 10 Gbps Ethernet physical media solutions shows the predominant presence of MMF based links in Table 2.6.

- The 62.5 μm MMF is the cheapest option among the applicable choices of fibers.
 - Most of the existing fiber infrastructures for links up to 300 meters are 62.5 μm MMFs.
 - It supports operations in the 850 nm and 1300 nm wavelength bands.

- The performance of this type of fiber is typically limited at about 200 MHz.km limiting the link distance to less than 50 meters for a data rate about 10Gbps
 - In practice, a parallel solution is needed to achieve the data rate of about 10Gbps over the existing 62.5 μm MMF based links.
 - It has more attenuation and lesser modal bandwidth comparing with the 50 μm MMF.
 - The typical applications of the 62.5 μm MMFs are the in-building and building-to-building networks.
- The traditional 50 μm MMF has slightly better performance than the 62.5 μm MMF.
 - The attenuation is 0.5 dB/km lesser than the 62.5 μm MMF
 - The modal bandwidth above 400 MHz.km which is much better than the 62.5 μm MMF.
 - In general link distance is limited to less than 65 meters at about 10 Gbps data rate.
 - However, the new laser optimized 50 μm MMFs can scale up to 300 to 550 meters at 10 Gbps data rate.
 - Standardization of this new type of fibers is done confining to FOTP 220 [32] as explained in previous section. For this type of fibers, the bandwidth-distance product will be as high as 2000 MHz.km, enabling a data rate of 12.5 Gbps for link distance up to 300 meters.

Fiber Type	Wavelength (nm)	Laser Type	Line Rate (GBaud)	Distance
62.5 μm MMF	850	VCSEL	12.5	25 m
	850	DFB	4 x 3.125 WDM	100 m
	850	VCSEL	10 x 1.25 parallel optics	300 m
	1300	DFB	12.5	50 m
	1300	DFB	4 x 3.125 WDM	300 m
50 μm MMF	850	VCSEL	12.5	65 m
	1300	F-P	12.5	65 m
Enhanced MMF	850	VCSEL	12.5	> 300 m
	1300	LW-VCSEL	12.5	2 km
SMF	1300	F-P	12.5	2 km
	1300	DFB LW-VCSEL	12.5	10 km
	1300	Cooled-DFB	12.5	40 km
	1500	Cooled-DFB	12.5	40 km

Table 2.6 Fiber types in the proposal of 10GB Ethernet along with sources [15]

2.3 MMF links as ROF medium

This section deals with the usage of multimode fiber as a potential medium for RF signal transmissions. Using MMF as a ROF link dates back to 1981 where a 700 MHz analog fiber optic link has been demonstrated over a 1.1 km graded-index fiber [33]. Then recently in late 90's demonstrations of RF signal over MMF link were demonstrated successfully. This is largely due to the fact that Gigabit and 10 Gbps ethernet standards adopted MMF as a potential medium and eliminated the bottlenecks in the modal bandwidth to provide a reliable high speed data communications up to 10 Gbps. The MMF ROF demonstrations in recent times from literature are discussed next in detail.

- In 2002 transmission of GSM signal over a 1Gbps multimode fiber link along with the presence of 1Gbps ethernet signal was demonstrated. [34]
- In 2003 transmission of GSM-1800 signal over a 1Gbps multimode fiber link along with the presence of W-CDMA signal was demonstrated. [35]
- In the same year the transmission of IEEE 802.11a, b, g WLAN signals over 10Gbps multimode fiber link has been demonstrated. [36]
- In the same year the transmission of UWB signals over 10Gbps multimode fiber link has been demonstrated. [37]
- In 2004 a co-existence scenario of WLAN, 1 Gbps Ethernet, and UWB signals have been demonstrated. [38]

It should be noted that all these demonstrations were experimental and if these signals had to be distributed over a large network of multimode fiber links it is very important that the link has to be modeled and simulated. Some literatures have characterized the MMF ROF link as a linear link and evaluated its performance in terms of the link gain, noise figure and spurious free dynamic range (SFDR) [39]. Still, to simulate the above mentioned wireless systems including the co-existence scenarios, a extensive characterization and modeling work has to be done which is the major work involved in this thesis.

2.4 Summary

This chapter described the evolution of multimode fiber links as a potential high speed and low cost medium for bandwidth demanding applications. It also explained in detail about the attempts of radio signal transmission over multimode fiber links. In the

next chapters it will be shown how these links are characterized and modeled as well as used to extend the range of the Wireless networks like UWB and WLAN.

3 Characterization and Modeling of the ROF MMF link

3.1 Introduction

Characterization of a system is an important aspect of a system design and verification, because it is required to create a good operating model of the system and hence to predict the performance of the system. It is also very useful to optimize the performance of the system or the individual components. In case of an analog or RF fiber optic system the fiber optic link is considered to be linear and it is characterized using a small signal model for its individual components. This is mainly due to the small signal nature of the signals used. In this thesis, the performance of the Ultra Wide Band (UWB) signal transmission over a multimode fiber link of 300 meters length is evaluated. The UWB (pulsed) signal for wireless communication is a broadband radio signal spanning from 3.1 GHz to 10.6 GHz and it is a large signal (~200mV P-P) with respect to the downlink scenario. Hence large signal modeling is required for an accurate characterization to predict the performance of UWB signals over fiber. The next sections discuss the details of the MMF link used in this project as well as the choice of ADS [40] as the simulator and the ADS simulation models.

3.2 MMF link specifications

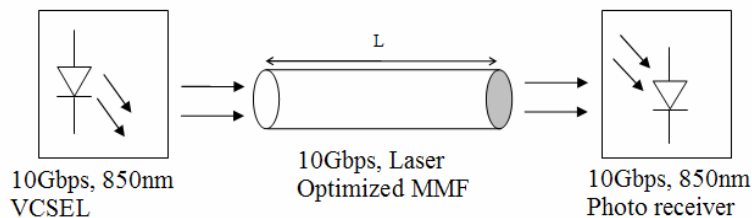


Figure 3.1 Schematics of the MMF link

The multimode fiber link for the radio over fiber application shown in Figure 3.1 is a direct modulation direct detection link. It consists of 3 major components – a 10Gbps VCSEL diode operating at 850nm wavelength, a laser-optimized graded index fiber (300 meters) and an optical receiver comprising of a 10Gbps photodiode and a trans-impedance amplifier. The VCSEL is operated without any laser driver circuitry. The specifications for the above mentioned components are given in Table 3.1.

VCSEL Specifications		
Wavelength	850 nm	
Output power	800 μ W typical	
Bandwidth	7.5 GHz typical	
Low Frequency cutoff	10 kHz	
Small signal gain	1.4 mW/V typical	
RMS noise	2.2 %	
Input impedance	60 Ω	
Output fiber	50 μ m multimode	
PIN Photo Receiver Specifications		
Wavelength	400-870 nm	
3-dB Bandwidth	12 GHz typical	
Low Frequency cutoff	10 kHz	
Rise Time	34 ps	
Conversion gain	-400 V/W	
Responsivity	0.4 A/W	
Trans-impedance gain	1000 V/A	
Noise Equivalent power	50 pW/ $\sqrt{\text{Hz}}$	
Maximum pulse power	1.5 mW	
Output impedance	50 Ω	
Input Fiber	50 μ m multimode	
MMF Specifications		
Wavelength	850 nm	
Core diameter	50 μ m	
Effective Modal Bandwidth	2000 MHz.km	
Attenuation Coefficient ($\alpha(\lambda)$)	2.4 dB/km	
Effective Group Index of Refraction (N_{eff})	1.481	
Refractive Index difference	1%	
Chromatic Dispersion	Zero dispersion wavelength (λ_0)	$1300 \text{ nm} \leq \lambda_0 \leq 1320 \text{ nm}$
	Zero dispersion slope (S_0)	$\leq 0.101 \text{ ps}/(\text{nm}^2 \cdot \text{km})$

Table 3.1 MMF link specifications

3.3 MMF link component models

This section discusses how to characterize and model the components specified in the previous section. The system verification for Radio over fiber systems needs a combination of a sophisticated RF system simulation engine along with the capability to handle optical component models. One such simulator is the Agilent's Advanced Design System (ADS) simulator [40] which provides the possibility of co-simulating two different environments. The built-in model library of ADS consists of a wide set of RF systems like GSM, WCDMA, WLAN, UWB etc. Also the co-simulation with SPICE like circuit simulation engine, Matlab etc makes it an ideal choice for characterizing RF optical links. The RF signals can be generated from the built-in libraries which could be co-simulated with the optical components modeled either in Matlab or as equivalent circuits. Also the high speed circuitry like TIA and laser drivers can be included along with the parasitics of the bond wires. In this project it was chosen to model the optical components as equivalent circuit behavioral models as they can be realized using the Symbolic Defined Devices (SDD) of ADS. Also using the ADS optimizer the model parameters can be tuned to fit with the measurement data so that they characterize the fiber link accurately.

3.3.1 VCSEL Model

The VCSEL model is based on the semiconductor laser rate Equations 3.1, 3.2, 3.3 [41], [42].

$$\frac{dN(t)}{dt} = \frac{\eta_i I(t)}{qV_a} - \frac{N(t)}{\tau_n} - v_g g_0 \frac{N(t) - N_{tr}}{1 + \epsilon S(t)} S(t) \quad (3.1)$$

$$\frac{dS(t)}{dt} = -\frac{S(t)}{\tau_s} + \Gamma v_g g_0 \frac{N(t) - N_{tr}}{1 + \varepsilon S(t)} S(t) + \frac{\Gamma \beta N(t)}{\tau_n} \quad (3.2)$$

$$Po(t) = \frac{S(t) V_a \eta_{opt} h c_0}{\Gamma \lambda \tau_p} \quad (3.3)$$

These equations depict the relationship between the injection current, the electron density, the photon density and the emitted optical power. The parameters of these equations are explained in Table 3.2.

Parameters	Description
$N(t)$	Active region carrier density in cm^{-3}
$S(t)$	photon density in cm^{-3}
$Po(t)$	VCSEL output power in mW
$I(t)$	Injection current in A
η_i	Current Injection efficiency
V_a	Active Volume in cm^3
τ_n	Carrier lifetime in s
τ_s	Photon lifetime in s
v_g	Group Velocity in ms^{-1}
g_0	Differential gain in cm^{-2}
N_{tr}	Transparency Carrier density in cm^{-3}
ε	Gain compression coefficient cm^3
Γ	Optical confinement factor
β	Spontaneous emission coefficient
η_{opt}	Optical efficiency

Table 3.2 VCSEL rate equation parameters

The equivalent circuit of the above mentioned rate equations are derived as mentioned in mena [41], [42]. The Equation 3.1 is the carrier rate equation and the Equation 3.2 is the photon rate equation. Here the carrier density $N(t)$ and the photon density $S(t)$ are considered to be node voltages V_s and V_n . Since their values could be very high they are scaled with arbitrary constants z_n , k for attaining convergence in the ADS circuit simulator. Also the V_s is added with a small constant δ and squared to avoid negative solutions for the equations. These transformations are given in equations 3.4 and 3.5

$$N = z_n V_n \quad (3.4)$$

$$S = \frac{(V_s + \delta)^2}{k} \quad (3.5)$$

Substituting Equations 3.4 and 3.5 in Equations 3.1 and 3.2 and rearranging

$$I(t) = \frac{qV_a Z_n}{\eta_i} \frac{dV_n}{dt} + \frac{qV_a Z_n}{\eta_i \tau_n} V_n + \frac{\nu_g g_0}{k} \frac{qV_a}{\eta_i} \frac{(Z_n V_n - N_{tr})(V_s + \delta)^2}{1 + \frac{\epsilon}{k}(V_s + \delta)^2} \quad (3.6)$$

$$2\tau_s \frac{dV_s}{dt} + V_s = \frac{\tau_s \Gamma \nu_g g_0 (Z_n V_n - N_{tr})(V_s + \delta)}{1 + \frac{\epsilon}{k}(V_s + \delta)^2} - \delta + \frac{\tau_s}{\tau_n} \frac{\Gamma \beta Z_n V_n k}{(V_s + \delta)} \quad (3.7)$$

The equations 3.6 and 3.7 represent the current flowing in and out of two nodes whose voltages are represented by V_s and V_n . Basically they are Kirchoff's current law equations. Now adopting them into circuit elements is much easier as shown in Figure 3.2

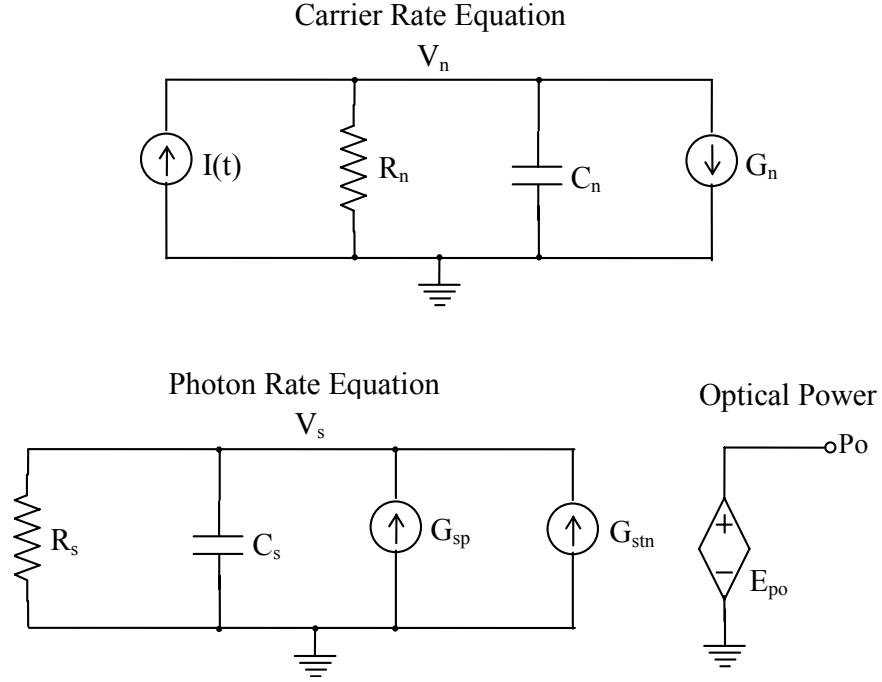


Figure 3.2 Equivalent Circuit model of VCSEL Rate Equations

The corresponding equations for the circuit elements are given below.

$$C_n = \frac{qV_a Z_n}{\eta_i} \quad C_s = 2\tau_s$$

$$R_n = \frac{\eta_i \tau_n}{qV_a Z_n} \quad R_s = 1$$

$$G_n = \frac{\nu_g g_0}{k} \frac{qV_a}{\eta_i} \frac{(Z_n V_n - N_{tr})(V_s + \delta)^2}{1 + \frac{\epsilon}{k}(V_s + \delta)^2}$$

$$G_{stn} = \frac{\tau_s \Gamma \nu_g g_0 (Z_n V_n - N_{tr})(V_s + \delta)}{1 + \frac{\epsilon}{k}(V_s + \delta)^2} - \delta$$

$$G_{sp} = \frac{\tau_s}{\tau_n} \frac{\Gamma \beta Z_n V_n k}{(V_s + \delta)}$$

where G_n , G_{sp} , G_{stn} are voltage dependent current behavioral sources. E_{po} is a voltage dependent voltage source which gives out optical power from photon density based on equation 3.3. These behavioral sources are implemented in ADS using the SDD components. Along with this, the VCSEL parasitics due to cavity, bond wires etc. are to be included. The parasitic component model and its origin are adopted from [25] as shown in the Figure 3.3 and 3.4. R_a and C_a characterize the parasitics of the active region of the VCSEL cavity, R_p and C_p characterize the parasitics of the pads, R_s characterizes the series resistance arising due to the DBR mirror stacks, R_w and L_w characterize the parasitics of the bondwire and R_q and C_q represent the simplified model of the source output impedance of the driver.

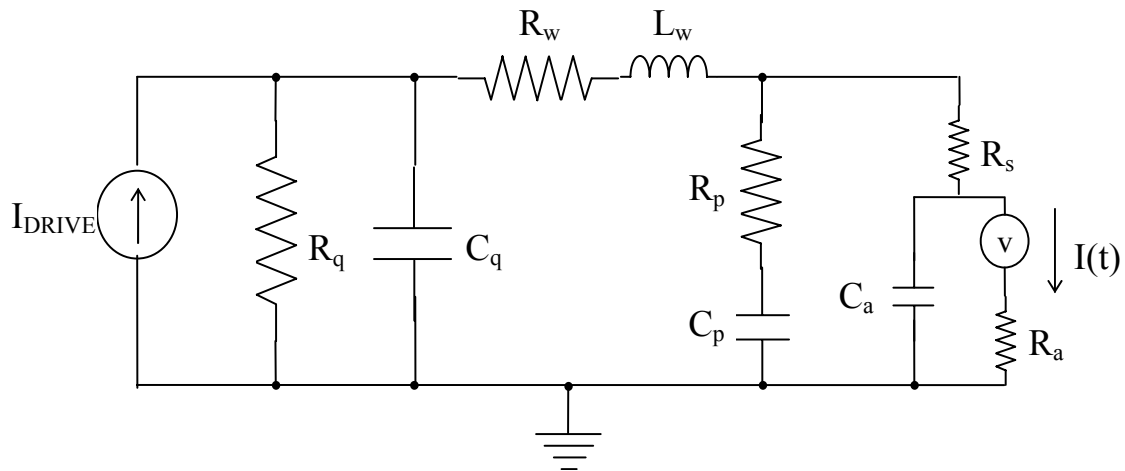


Figure 3.3 Parasitic circuitry of VCSEL [25]

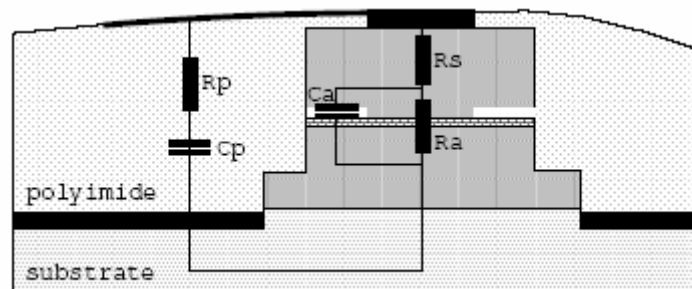


Figure 3.4 Origin of parasitics in VCSEL structure [25]

To represent the VCSEL module used, the component values of the VCSEL equivalent circuit and its parasitic circuit should be optimized to match the measured characteristics of the VCSEL. The DC characteristic curves of the VCSEL are used to obtain the equivalent circuit component values. The S-parameter curves are used to obtain the parasitic circuit component values.

Parasitic component values	
R_q , Driver output resistance	50 Ω
C_q , Driver output capacitance	0.5 pF
R_w , Bond-wire resistance	1 Ω
L_w , Bond-wire inductance	0.05 nH
R_p , Pad resistance	250 Ω
C_p , Pad capacitance	0.25 pF
R_s , Series Resistance	30 Ω
R_a , Active layer resistance	40 Ω
C_a , Active layer capacitance	0.5 pF
VCSEL Rate Equation parameter values	
η_i , Current injection efficiency	0.75
V_a , Active volume	2.5e-13 cm ³
τ_n , Carrier lifetime	2.5e-9 s
τ_s , Photon lifetime	1.9e-12 s
v_g , Group velocity	71.43e6 m/s
g_0 , Differential gain	3.5e-16 cm ² /s
N_{tr} , Transparency carrier density	1.2e18 cm ⁻³
ε , Gain compression coefficient	3e-17 cm ⁻²
Γ , Optical confinement factor	0.025
β , Spontaneous emission coefficient	1.5e-4
η_{opt} , Optical efficiency	0.4

Table 3.3 VCSEL optimized component values

Figure 3.5 Shows the measured DC optical power vs injected current curve agrees well with the simulated curve after obtaining optimized values for the rate equation parameters. Figure 3.6 shows measured S11 curves used to optimize the parasitic component values

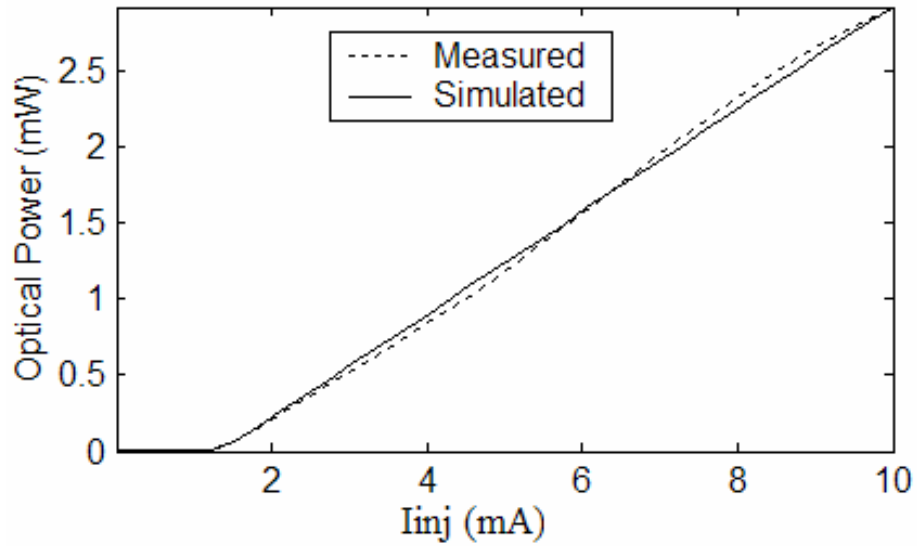


Figure 3.5 Measured and simulated L-I curve

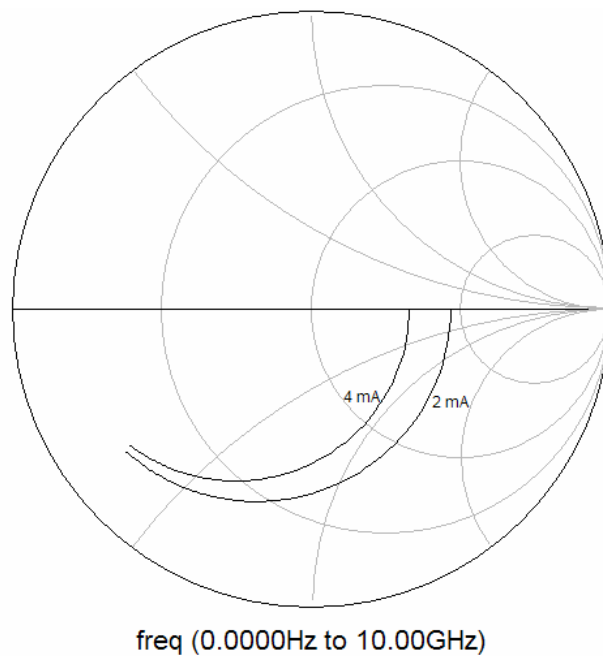


Figure 3.6 Measured S11 curve

3.3.2 Multimode Fiber Model

Multimode fiber mentioned here specifically denotes a “Circularly symmetric Graded index fiber”. These fibers have been modeled in several possible ways of which two prominent models are the “Impulse response model” and the “Transfer function model”. The former operates in time domain while the later is associated with frequency domain. For both these models several common transmission parameters are to be obtained as well as calculated. They are discussed below.

Propagation constant:

The index profile of a circularly symmetric graded index fiber is as given below:

$$n(r, \lambda) = \begin{cases} n_1(\lambda) \left[1 - 2\Delta(\lambda) (r/a)^\alpha \right]^{\frac{1}{2}} & \text{for } (0 \leq r \leq a) \\ n_1(\lambda) \left[1 - 2\Delta(\lambda) \right]^{\frac{1}{2}} & \text{for } (r \geq a) \end{cases} \quad (3.8)$$

Where

n_1 - refractive index at $r = 0$

a - Core radius

α - Profile Exponent

Δ - Normalized Refractive Index Difference

Some of the propagating modes of a multimode fiber have similar propagation constants. They are grouped into mode groups or principal mode number which is represented by m . Each m^{th} mode group has $2(m+1)$ degenerate modes. For example a 50/125 μm grade index fiber has 19 mode groups and supports approximately 400 propagation modes. Each of these mode groups are characterized by a propagation constant β_m whose WKB approximation [43] is given in equation 3.9 and 3.10:

$$\beta_m = 2\pi \frac{n_1}{\lambda} \left[1 - 2\Delta \left(\frac{m}{M(\alpha)} \right)^{2\alpha/(\alpha+2)} \right]^{\frac{1}{2}} \quad (3.9)$$

$$M(\alpha) = 2\pi a \frac{n_1}{\lambda} \left(\frac{\alpha\Delta}{\alpha+2} \right)^{\frac{1}{2}} \quad (3.10)$$

Attenuation:

The most important power loss parameter is the wavelength dependent attenuation ($\alpha(\lambda)$) which caused by Rayleigh scattering is given in equation 3.11.

$$\alpha(\lambda) = a + \frac{b}{\lambda^4} + c(\lambda) \quad (3.11)$$

Where a is a constant, the 2nd term accounts for Rayleigh scattering and $c(\lambda)$ accounts for absorption by impurities [24]. The typical curve fit for the attenuation equation of a 50/125 μm core MMF is shown in Figure 3.7. It can be seen that at 850 nm the attenuation is approximately 2.4 dB/Km.

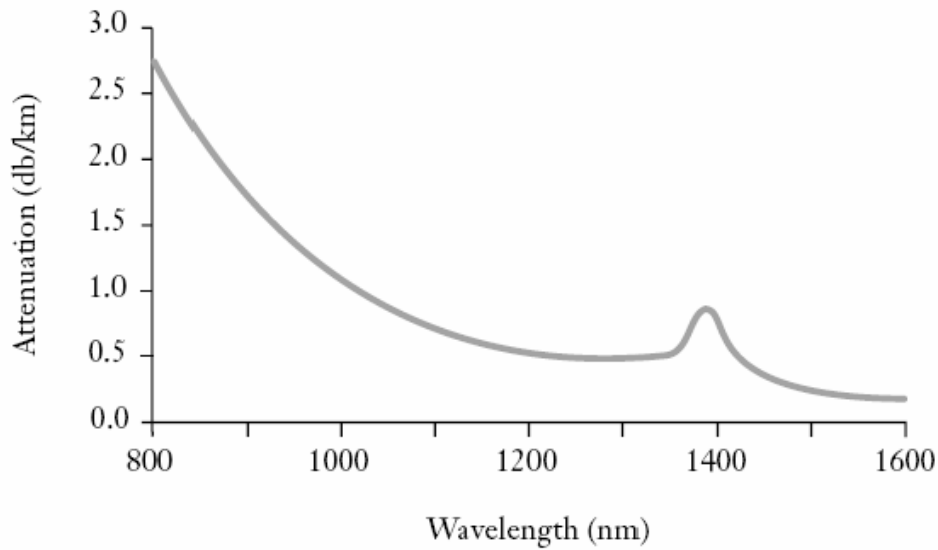


Figure 3.7 Spectral Attenuation curve of a 50 micron MMF

The other important parameter of the multimode fiber is dispersion, which is a combination of two dispersion parameters – the chromatic dispersion and the modal dispersion. While the attenuation relates with the power loss with distance, the dispersion parameter relates with the available bandwidth with distance.

Chromatic Dispersion:

The chromatic dispersion also called as intermodal dispersion is defined as the pulse broadening due to the changes in the refractive index of the glass with wavelength. This is due to the difference in the velocities of different wavelengths with which the pulse is composed of. It should be noted that this is confined within a propagating mode of the fiber. This dispersion is characterized by the chromatic dispersion coefficient given in equation 3.12:

$$D(\lambda) = \frac{S_0}{4} \left\{ \lambda - \frac{\lambda_0^4}{\lambda^3} \right\} \quad (3.12)$$

Where:

$D(\lambda)$ - chromatic dispersion coefficient in ps/(nm.km)

λ - Operating wavelength in nm

λ_0 - Zero dispersion wavelength in nm

S_0 - Zero dispersion slope in ps/(nm².km)

From this coefficient and the source spectral linewidth, the chromatic dispersion transfer function of a multimode fiber [44] could be solved and hence the bandwidth restriction due to chromatic dispersion could be found out. The chromatic dispersion transfer function is as given in equation 3.13:

$$H_{ch}(\omega) = \frac{1}{\left(1 + i\omega/\omega_2\right)^{\frac{1}{2}}} \exp\left[-\frac{\left(\omega/\omega_1\right)^2}{2\left(1 + i\omega/\omega_2\right)}\right] \quad (3.13)$$

where

$$\omega_1 = -(\sigma_\lambda D(\lambda)z)^{-1}$$

$$\omega_2 = \left[\sigma_\lambda^2 (S_0 + 2D(\lambda)/\lambda)z\right]^{-1}$$

z - Length of the fiber

σ_λ - Source spectral line width

Modal Dispersion:

The other dispersion which occurs in MMF is called the modal dispersion which relates to the pulse broadening during a multimode fiber transmission due to the difference in velocities in between the modes of propagation. This leads to different time delays for the pulse energy distributed across different propagation modes. So to calculate the modal dispersion, the modal delays have to be calculated. From various methods of calculating the modal delays, the WKB approximation [43] is used due to its simplicity. The modal delay per unit length of the fiber is defined as given in equation 3.14:

$$\tau_m = -\lambda^2 \beta'_m / (2\pi C) \quad (3.14)$$

Using Equation 3.19 and WKB approximation the above equation is deduced [43] into equation 3.15:

$$\tau_m = \frac{N_1}{C} \left[1 + \frac{\alpha - 2 - \varepsilon}{\alpha + 2} \Delta \left(\frac{m}{M(\alpha)} \right)^{2\alpha/(\alpha+2)} + \frac{1}{2} \frac{3\alpha - 2 - 2\varepsilon}{\alpha + 2} \Delta^2 \left(\frac{m}{M(\alpha)} \right)^{4\alpha/(\alpha+2)} \right]$$

where

$$N_1 = n_1 - \lambda \frac{dn_1}{d\lambda} \quad (3.15)$$

and

$$\varepsilon = -\frac{2n_1}{N_1} \frac{\lambda}{\Delta} \frac{d\Delta}{d\lambda}$$

The modal transfer function [45] [46] of a multimode fiber is given by the equation 3.16:

$$H_{\text{mod}}(\omega) = \sum_{m=1}^K w_m \exp(-j\omega z \tau_m) \quad (3.16)$$

Where

W_m - Modal power distribution in each mode group m

z - Length of the fiber

τ_m - Modal delays per unit length of each mode group m

Equation 3.16 has to be evaluated to find the modal bandwidth of the MMF. The modal delays are calculated using a Matlab script implementing equation 3.15. Even though 19 mode groups are supported in the “850 nm Laser optimized 50 μm ” MMF used, only 17 mode groups are significant. The calculations were performed 17 mode groups with the parameters as shown in the Table 3.4

Parameters	Value
Diameter of the Core in um	50
Diameter of the Cladding in um	125
Profile Exponent, g	2
Maximum Refractive Index in the Core, n_1	1.481
Numerical Aperture, NA	0.2
Normalized Refractive Index Difference, Δ	0.01
Operating Wavelength in nm, λ	850
Deformation Parameter, b	0
Profile Dispersion Parameter, p	0
Length of fiber in m, L	300
Source spectral line width in nm, σ_λ	0.4
Zero Dispersion Wavelength in nm, λ_0	1300
Zero Dispersion Slope in ps/(nm ² .km), S_0	0.101

Table 3.4 Multimode fiber parameters used to calculate modal delays

The modal power distribution depends on the launch condition as described in chapter 2 and it can vary widely affecting the modal bandwidth very much. So the overfilled launch condition (OFL) used for LEDs cannot be used, where the power launched into the multimode fiber modes are equal. This Flux of a VCSEL and the corresponding detailed modeling of the power coupling to the fiber, a simpler approximated approach for modeling the modal power distribution is adopted. Assuming a centre launch condition from VCSEL the power distribution is approximated as a SGS (Single-Graded-Single) mode scrambler modal power distribution [47] as given in equation 3.17.

$$w(m) = 1 - x(m / M) \quad (3.17)$$

The value of x is optimized such that the calculated 3dB bandwidth of the multimode fiber is approximately the same as the effective modal bandwidth of the fiber (given in the fiber specification). With this modal power distribution model, the simulated modal transfer function of the multimode fiber is shown in Figure 3.8 for a length of 1000m. It can be seen that the 3dB point approximately lies around 2GHz which is the same as the EMBc of 2000MHz.Km of the fiber.

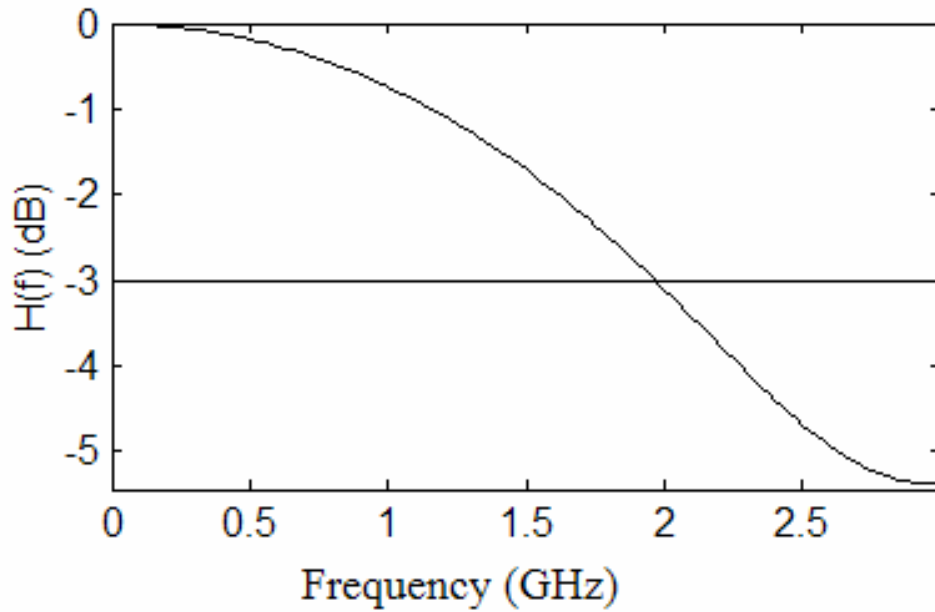


Figure 3.8 Simulated Modal Transfer function of the multimode fiber

With the chromatic transfer function and the modal transfer function, the MMF transfer function can be derived as equation 3.18:

$$H_{MMF}(\omega) = H_{ch}(\omega) \cdot H_{mod}(\omega) \quad (3.18)$$

This transfer function was directly implemented in the ADS simulator using the weighing function option of the symbolic defined devices (SDD) [40], where a user defined frequency dependent expression can be used to scale the spectrum of a port current.

3.3.3 Photodiode Model

The Photodiode is PIN diode model is a small signal equivalent circuit model which includes the package parasitic components as shown in the Figure 3.9 and the parameters are explained in Table 3.5 .

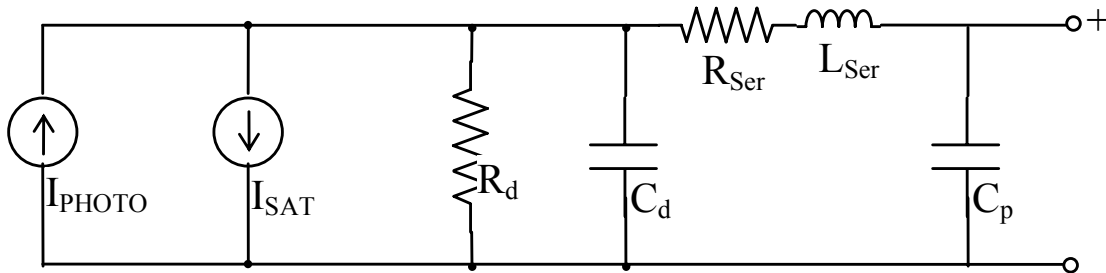


Figure 3.9 Photo diode model

Where

$$I_{photo} = \frac{q\eta_{pd}P_{pd}}{h\nu} \quad \text{- Photo current} \quad (3.19)$$

Parameters		Values
P_{pd}	Input optical power	-
q	Electronic charge	$1.6021e-19$ C
h	Planck's constant	$6.6261e-34$ J*s
ν	Optical frequency	$3.53e14$ Hz
η_{pd}	Quantum efficiency	0.8
I_{sat}	Reverse saturation current (dark)	0.5 nA
R_d	“Dark” or “Shunt” resistance	5 M Ω
C_d	Junction capacitance	175.7 fF
R_{ser}	Series diode resistance	10.6 Ω
L_{ser}	Parasitic Inductance	0.04 nH
C_p	Parasitic capacitance	40.6 fF

Table 3.5 Photodiode parameters and their values

3.4 MMF link simulation results

Using the above models the link was characterized for 1, 300, 600 meter lengths and S-paramater, group delay simulations were performed. These results along with the measured results are shown in Figures 3.10, 3.11, 3.12, 3.13, 3.14, 3.15.

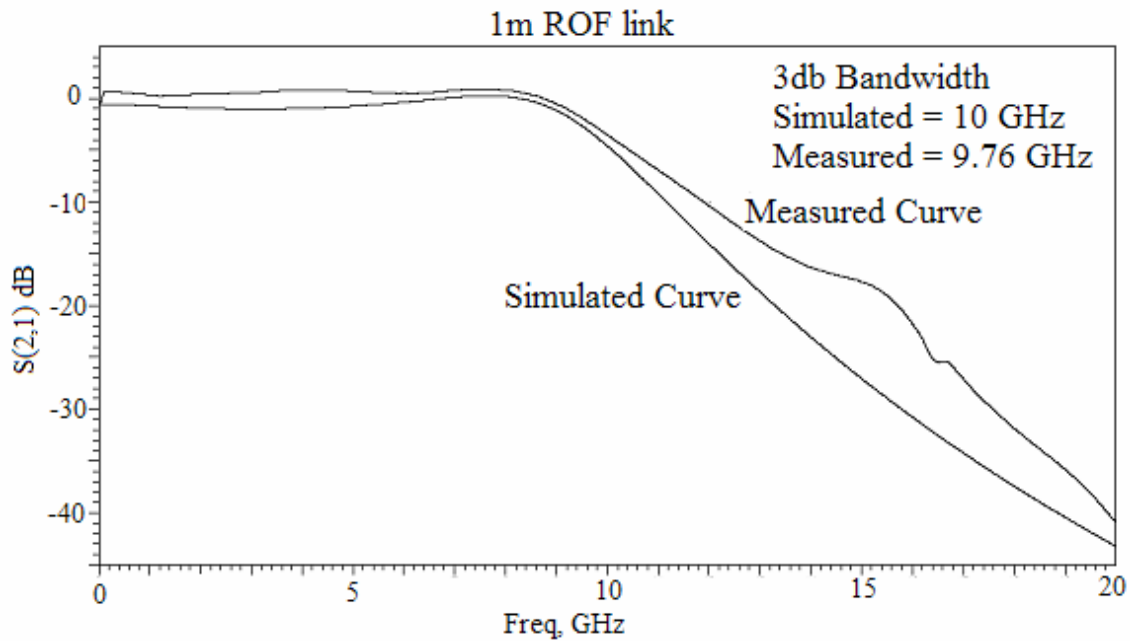


Figure 3.10 Simulated and measured S21 Curves for 1m ROF link

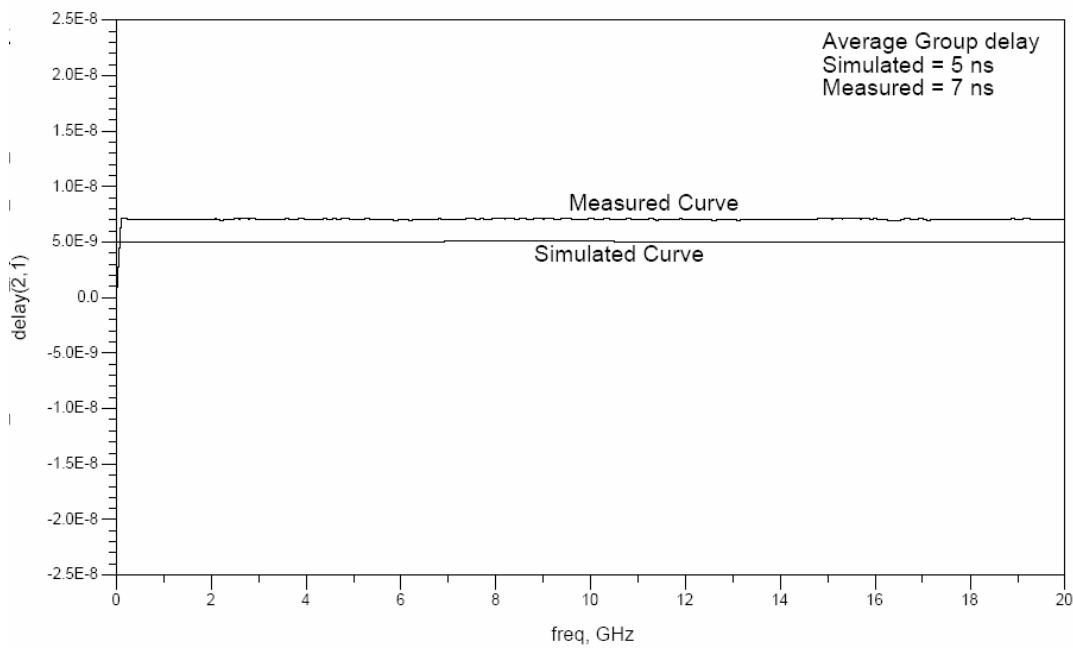


Figure 3.11 Simulated and measured group delays for 1m ROF link

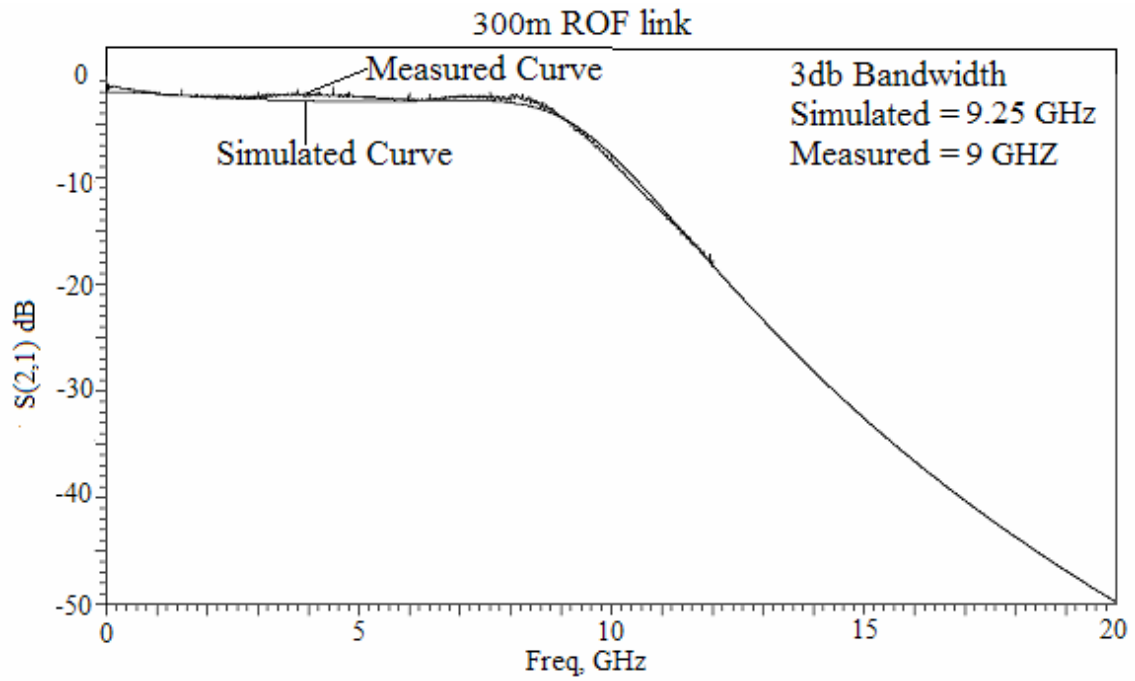


Figure 3.12 Simulated and measured S21 Curves for 300m ROF link

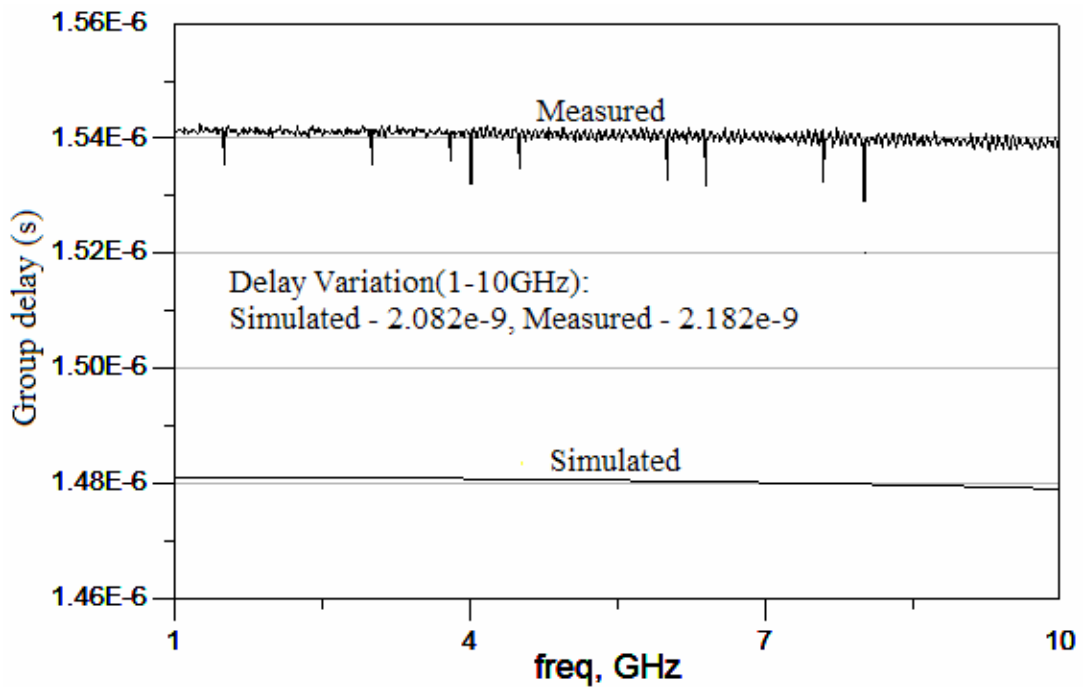


Figure 3.13 Simulated and measured group delays for 300m ROF link

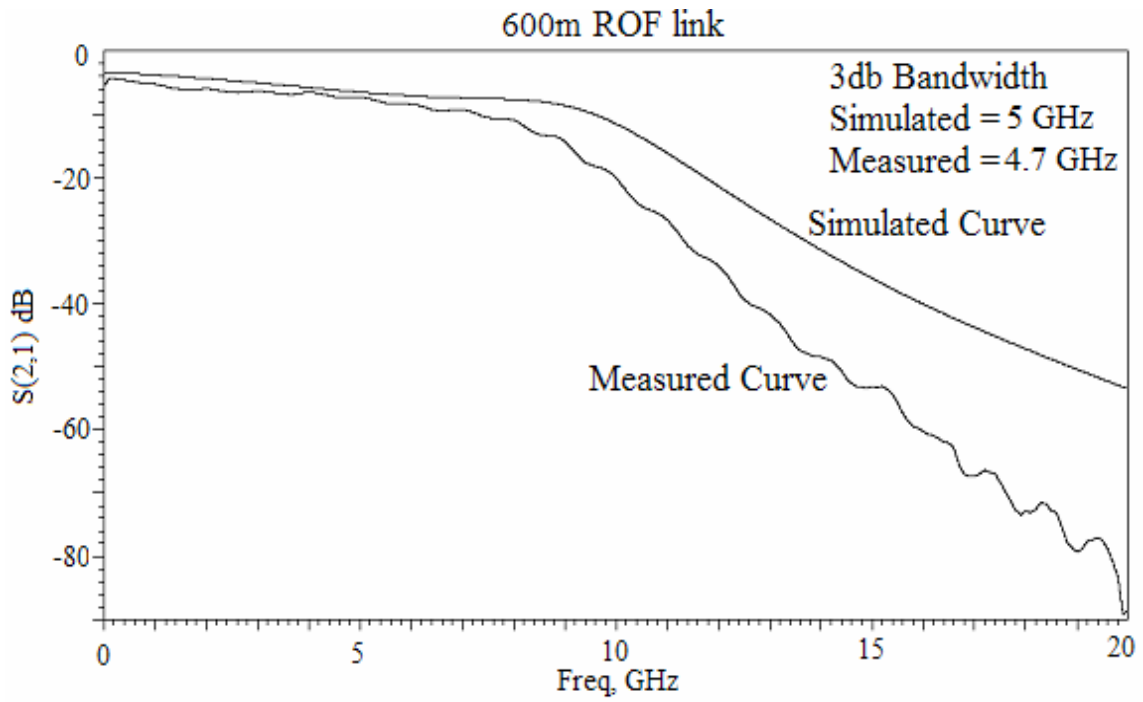


Figure 3.14 Simulated and measured S21 Curves for 600m ROF link

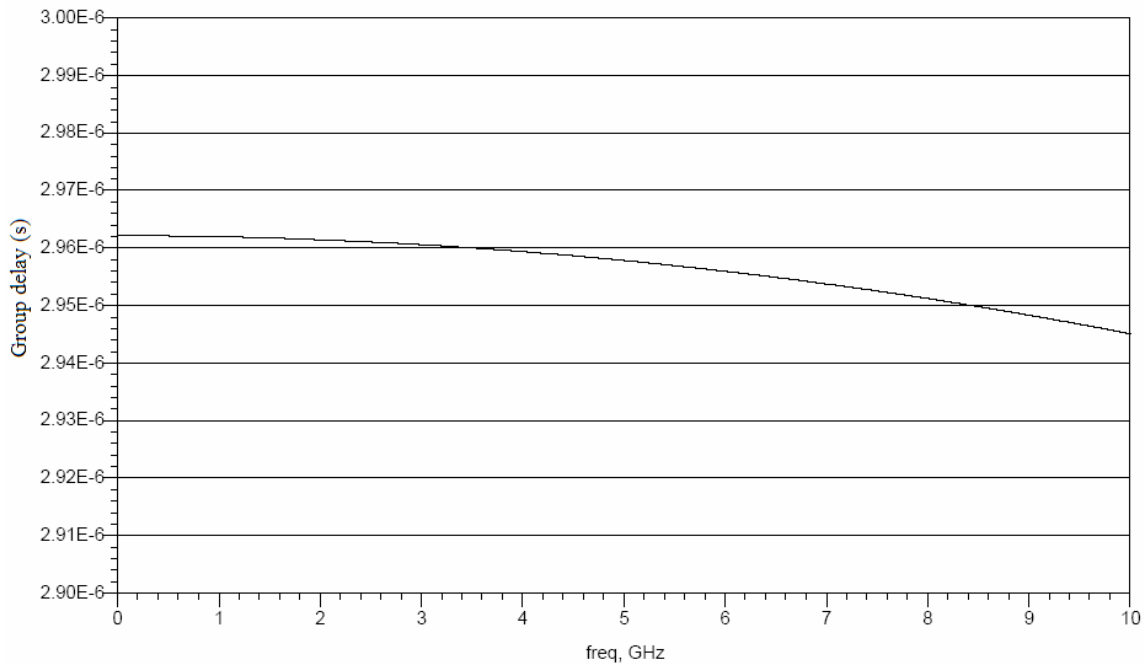


Figure 3.15 Simulated group delay variation for 600m ROF link

The simulated group delay for a 600 meter ROF link is 2.96 micro seconds. The measured value for a 600m link is not available for a comparison. Also roll off characteristics of the 600m link which starts after 6 GHz doesn't match with measured value. This could be attributed to the simplification of the multimode fiber model by assuming a single link length rather than representing the physical scenario which is segmented and connectorized for the 600 meter case. Overall the simulation curves agree well with the measured values and especially for the link length of 300 meters.

3.5 Summary

In this chapter the characterization and modeling of the MMF link components were done based on the measurements and simulations. These models were validated for the measured link performances. The transmission distances were chosen to be in multiples of 300m. This would be in consistent with the IEEE 10gbps specification for short wavelength, enhanced MMF physical media. Also the enhanced MMFs are practically available in bundles of 300m lengths. Above 600m, the results were very insignificant to report. In the next chapter these models are used to attempt UWB signal transmission over 1m, 300m and 600m lengths of fiber.

4 UWB over MMF link

4.1 Introduction to UWB

Ultra wide band (UWB) communications are the emerging wireless technology targeting at the wireless personal area networks (WPAN) standards. The IEEE 802.15.3a [11] task group is developing the WPAN standard which would cater the high speed connectivity needs of an indoor environment, typically a home environment, where the transmission distances would be of the order of few meters to 10 meters. A basic definition of UWB would be: it is a radio modulation technique where the data is represented by pulses of very short duration in time of the order of nanoseconds or less, whereas they occupy a very large span of the spectrum. This chapter discusses UWB transmission over MMF link for range extension by analyzing the UWB temporal signal.

4.2 UWB specifications

The FCC defines UWB signals as having a fractional bandwidth i.e. the ratio of the base band bandwidth to the RF carrier frequency, to be greater than 0.2 [48]. The operating frequency range is from 3.1GHz to 10.6 GHz. Also the transmitted power should comply with spectral mask with mean EIRP of -41.3 dBm/MHz. Table 4.1 shows the average radiated emission limits.

Frequency Range (MHz)	Mean EIRP (dBm/MHz)
960 – 1610	-75.3 / -75.3
1610 – 1900	-53.3 / -63.3
1900 – 3100	-51.3 / -61.3
3100 – 10600	-41.3 / -41.3
Above 10600	-51.3 / -61.3

Table 4.1 Average Radiated emission limits [48]

The enormous bandwidth offers very high data rates possible within very short ranges of less than 10 meters constrained by the emission limits. The IEEE 802.15.3a Working Group has come up with the technical requirements [11] of

- Data rates up to 110, 200 and a optional 480 Mbps
- Ranges of 10m, 4m and below
- Power consumption of 100 and 200 mW

But there two approaches in contention for IEEE 803.15.a [11], one based on direct sequence and the other based on multi band OFDM

- Direct sequence or Impulse radio UWB
 - Very short duration impulses that occupy a bandwidth of several GHz
 - Data is modulated using pulse position modulation or Bi phase modulation
 - Dual bands from 3.2-5.15 GHz and 5.825-10.6 GHz
- Multi band OFDM UWB
 - The entire UWB band is divided into several smaller bands each of 520 MHz to comply with FCC definition of UWB.
 - Each band uses frequency hopping OFDM

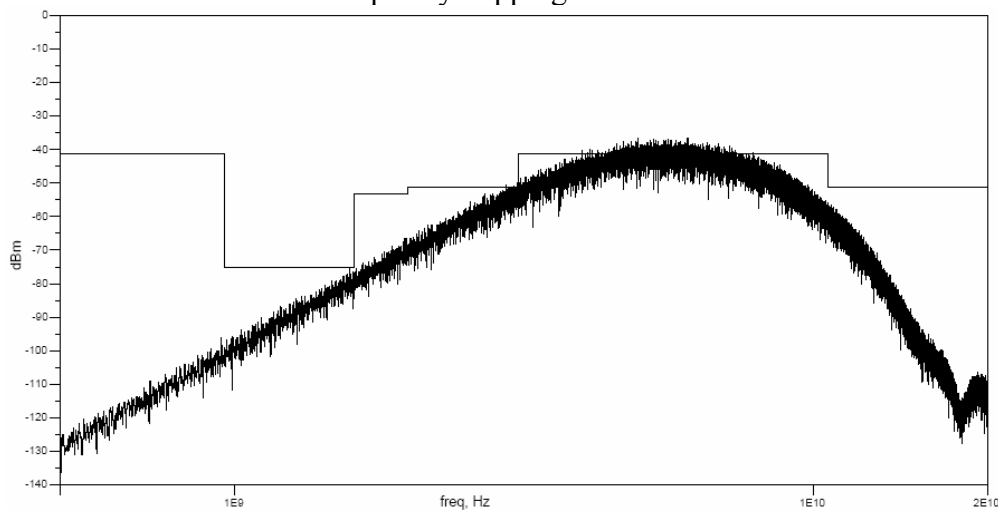


Figure 4.1 Impulse radio UWB FCC spectral mask for emission [48]

4.3 UWB transmission over Fiber

In IEEE 802.15.3a specifications it can be noted that as the data rates goes higher, the range of the UWB communications comes down drastically. At 480 Mbps data rate the range is expected to be around 2 meters. Similar to any other wireless system, the range enhancement of UWB systems can be performed using a low cost multimode fiber links. In general RF signals are typically narrow band and of small signal nature. But the UWB signal has an extremely wideband occupying the band from 3.1 GHz to 10.6 GHz and the temporal pulses are of large signal nature (downlink scenario) with peak to peak voltage ranging from few hundreds of millivolts to few volts. This could drive the VCSEL diode into non-linearity and correspondingly have the non-linear effects propagated across the link. To study this scenario a conventional linear small signal fiber optic link model cannot be used. This is the reason why, the MMF link was characterized as a large signal model in Chapter 3. Here a UWB temporal pulse is captured and its effect on transmission over MMF link is studied both with simulations and experimental setup.

4.3.1 UWB pulse Generation

The impulse Radio UWB does not have any separate RF carrier modulation. Instead it is the simplest form of achieving the desired ultra wide bandwidth spectrum by just shaping the digital base band pulses into a sharp and narrow time domain pulses. As it is known that the digital pulses have a very broad spectral distribution, it is a matter of removing the unwanted spectral energies below 3.1 GHz and above 10.6 GHz. This could be achieved by a combination of filters and pulse shaping circuits. The UWB pulse shape chosen to be used in this project is a Gaussian monocycle impulse signal. This signal

would satisfy the FCC spectral emission limits. This pulse could be generated as given below. The edge of a base band signal is used to form a Gaussian impulse described as:

$$g(t) = \frac{1}{\sigma\sqrt{2\pi}} \exp\left(-0.5\left(\frac{t-\mu}{\sigma}\right)^2\right) \quad (4.1)$$

This is done using an impulse forming network [49]. Basically an impulse forming network is a circuit component which provides the derivative of the input waveform.

$$V_{out} \approx T_c \cdot \frac{dV_{in}}{dt} \quad [49] \quad (4.2)$$

where, T_c is the derivative time coefficient. When a trailing edge of a digital pulse is sent across an impulse forming network it generates an impulse as shown in Figure 4.2.

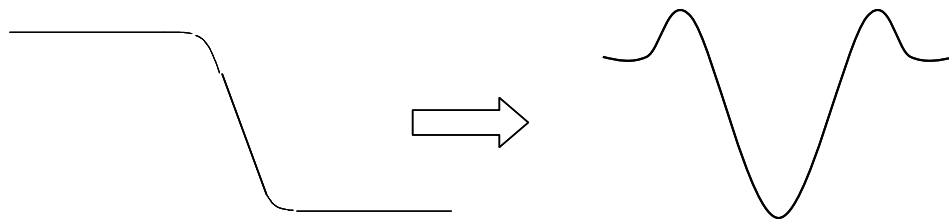


Figure 4.2 Impulse Output from an impulse forming network

When this Impulse is sent across an impulse forming network it generates a Gaussian monocycle pulse as shown in Figure 4.3.

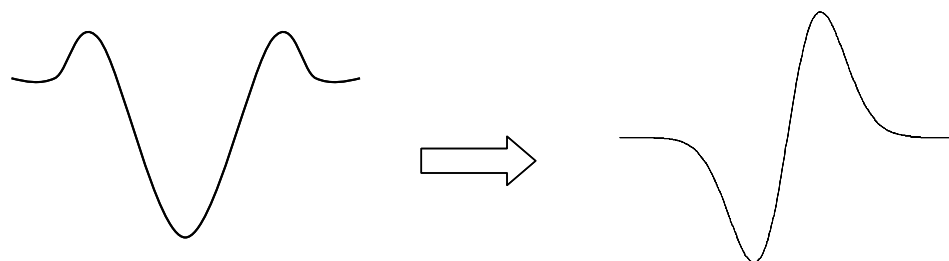


Figure 4.3 Gaussian monocycle pulse Output from an impulse forming network

The entire setup for generating a series of UWB monocycle pulses representing a digital base band pulse series of data rate 100 Mbps is shown in Figure 4.4

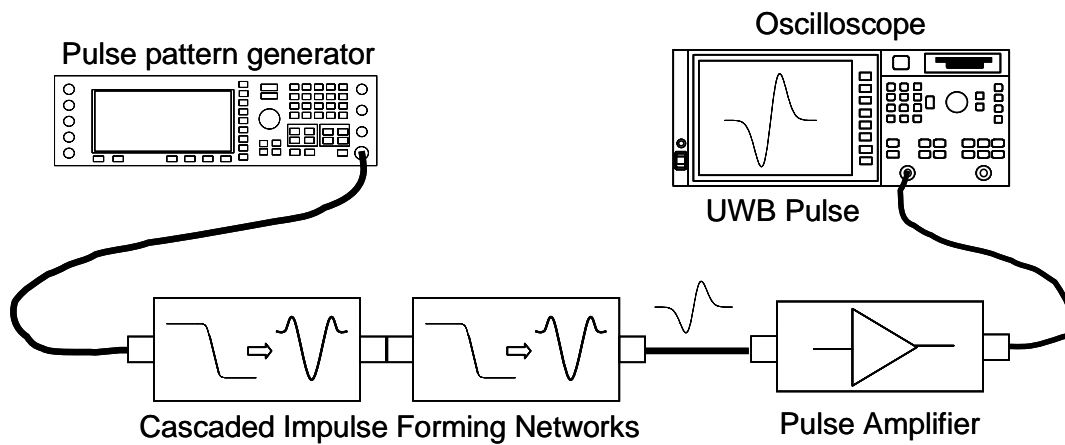


Figure 4.4 Setup for an impulse radio UWB Down link pulse generation

The generated monocycle pulse had a peak to peak voltage of 226 mV and a pulse width of 42 ps with its spectrum satisfying the FCC average spectral emission limit of -41.3 dBm/MHz as shown in figures 4.5 and 4.6

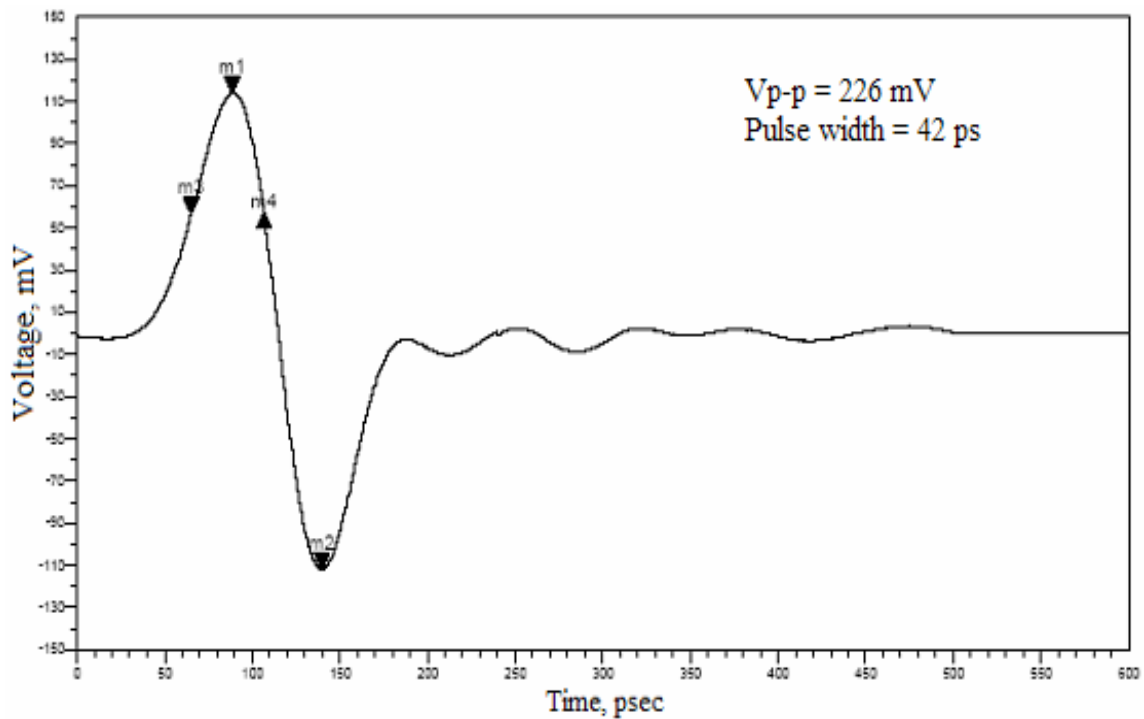


Figure 4.5 UWB downlink source pulse

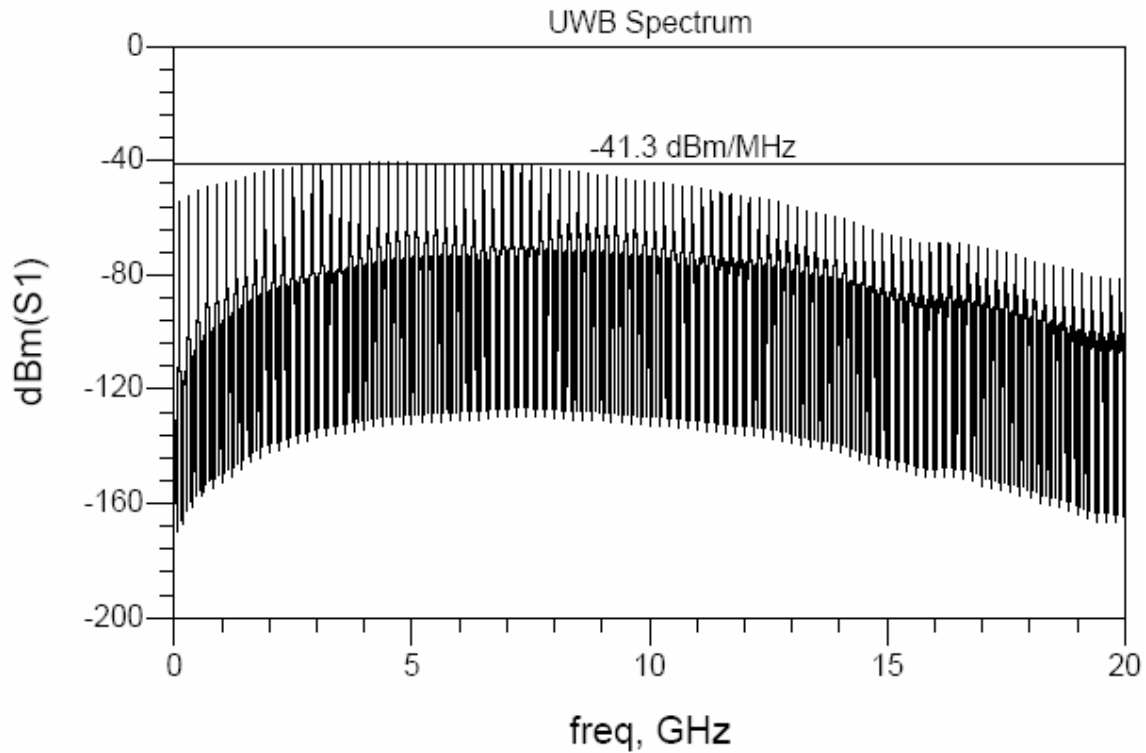


Figure 4.6 UWB pulse spectrum

4.3.2 Temporal Results of UWB downlink pulse over ROF

The above shown UWB pulse is sent across the radio over fiber link of lengths 1 meter, 300 meters and 600 meters. The ROF link is characterized for all these three lengths in Chapter 3. The 1 meter ROF link is used to characterize the distortions induced by the optical transmitter – VCSEL and the photo receiver as a 1 meter MMF would have a negligible modal dispersion and attenuation. Figure 4.7 shows the both experimental and simulated pulse after 1m ROF transmission. It can be seen that the pulse is attenuated by approximately one third of its original amplitude as well as it has undergone a dispersion leading to an increase of approximately 10 ps in the pulse width. This shows that VCSEL and photo receiver modules has not just losses but are of dispersive nature.

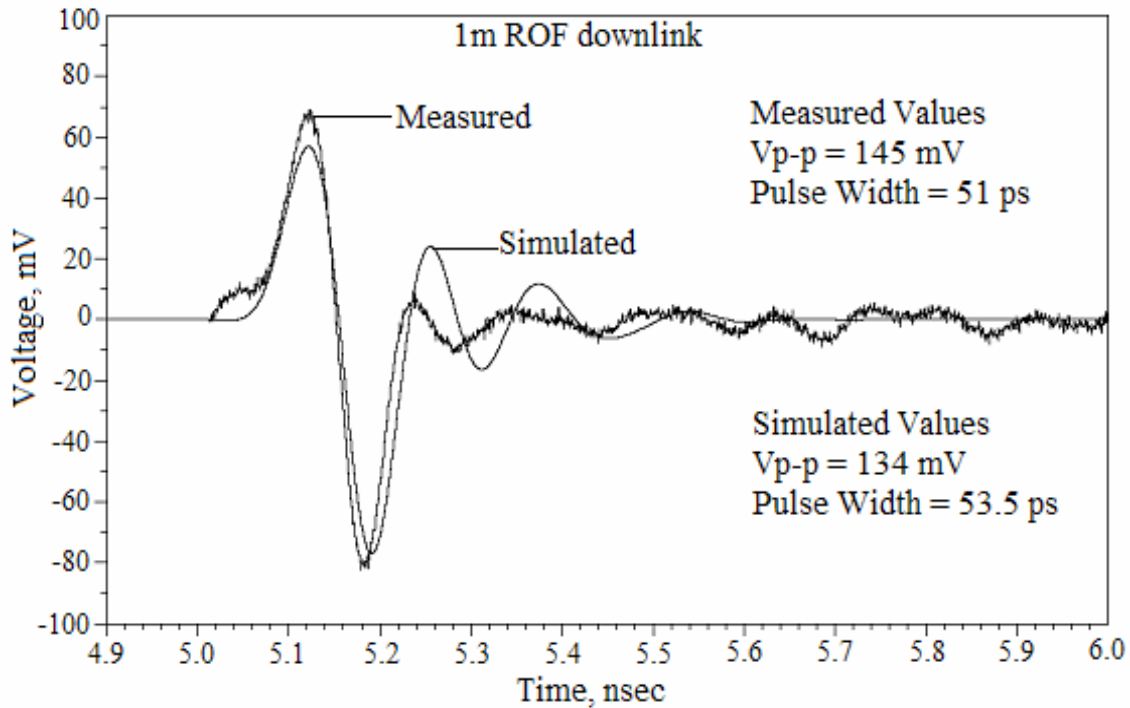


Figure 4.7 UWB downlink pulse after 1 meter ROF

Figure 4.8 shows the attenuation and dispersion undergone by the UWB temporal pulse after transmission over 300 meters ROF. The pulses were adjusted in time domain to overlap for better visualization, even though the group delay predicted by the simulation differs from measurement by 60 ns. It can be seen that the basic pulse shapes roughly match because of the variation of group delay that is the slope of the curves in Figure 3.12 are the same. This group delay variation is responsible for the pulse width variations. It can be recalled from Chapter 3 that for a frequency span of 1 GHz to 10 GHz the group delay variation is measured as well as simulated as ~ 2 ns for 300m ROF link whereas it is negligible for a 1m ROF link. It is important to note that the signal span 3.1 GHz to 10.6 GHz is approximately within the group delay measurement span. This certainly imposes different delays for different frequency components leading to the dispersion of the pulse as seen.

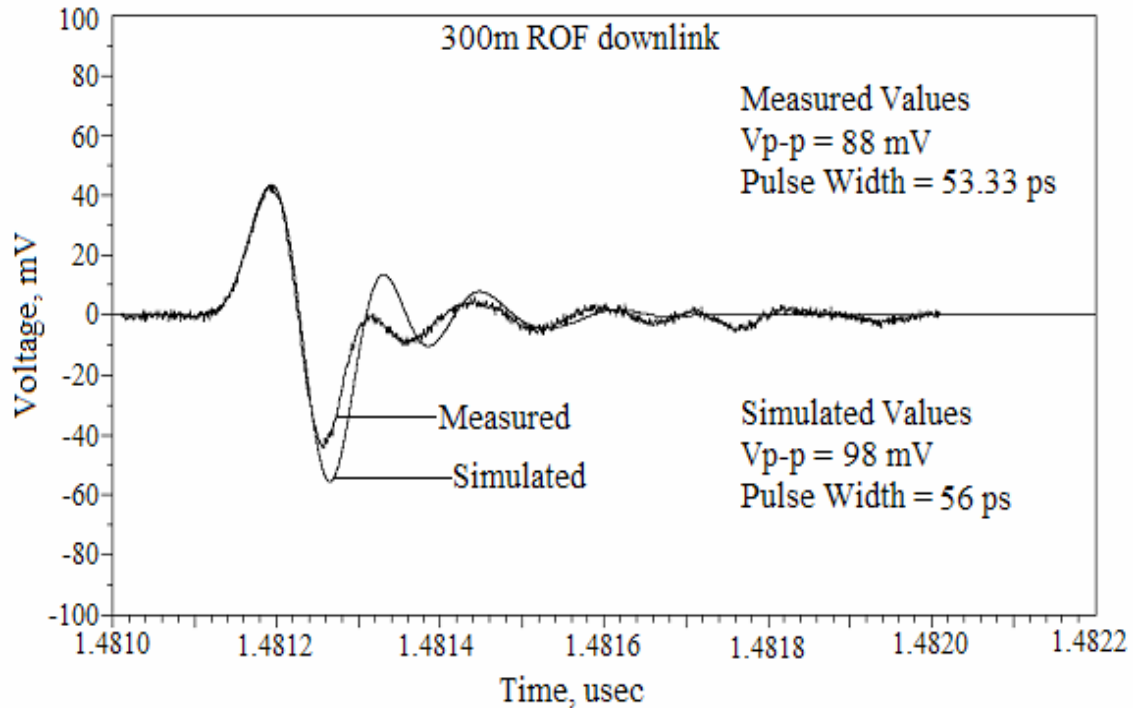


Figure 4.8 UWB downlink pulse after 300 meter ROF

Figure 4.9 shows the UWB temporal pulses after a 600 meter ROF transmission. The pulse width has increased due to some more variation in modal delays. From Chapter 3 it can be learned that the average group delay has approximately doubled which should be the case with the doubled transmission distance. But it can be seen in Figure 3.14 that the slope of the group delay curve is approximately similar to the 300 meter ROF transmission case. So the pulse width variation is not expected to be very high which is reflected in the figure 4.8. It can be seen that the simulation and measured pulse amplitudes differ largely unlike other cases. As mentioned before this is attributed to the modeling error introduced by the single fiber length to represent a segmented and connectorized fiber length in the experimental setup. This error could be rectified if the connector matrix for the modal power distribution is modeled and included in the simulations.

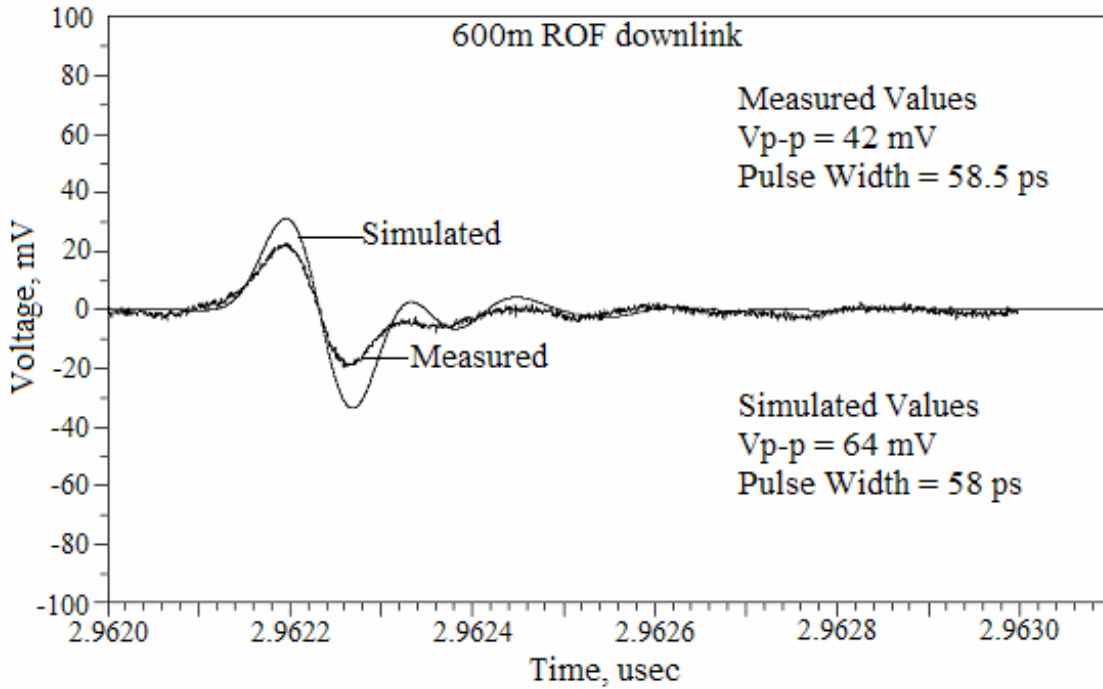


Figure 4.9 UWB downlink pulse after 600 meter ROF

4.3.3 Spectral Results of UWB downlink pulse over ROF

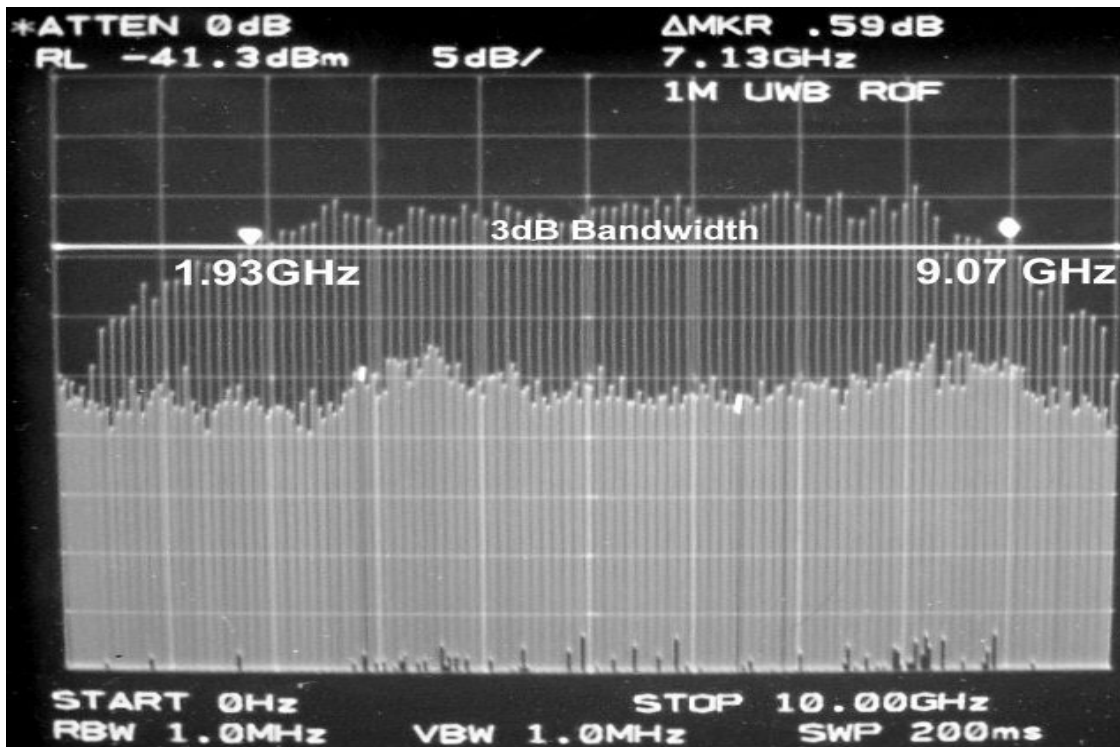


Figure 4.10 Measured downlink spectrum after 1 meter ROF

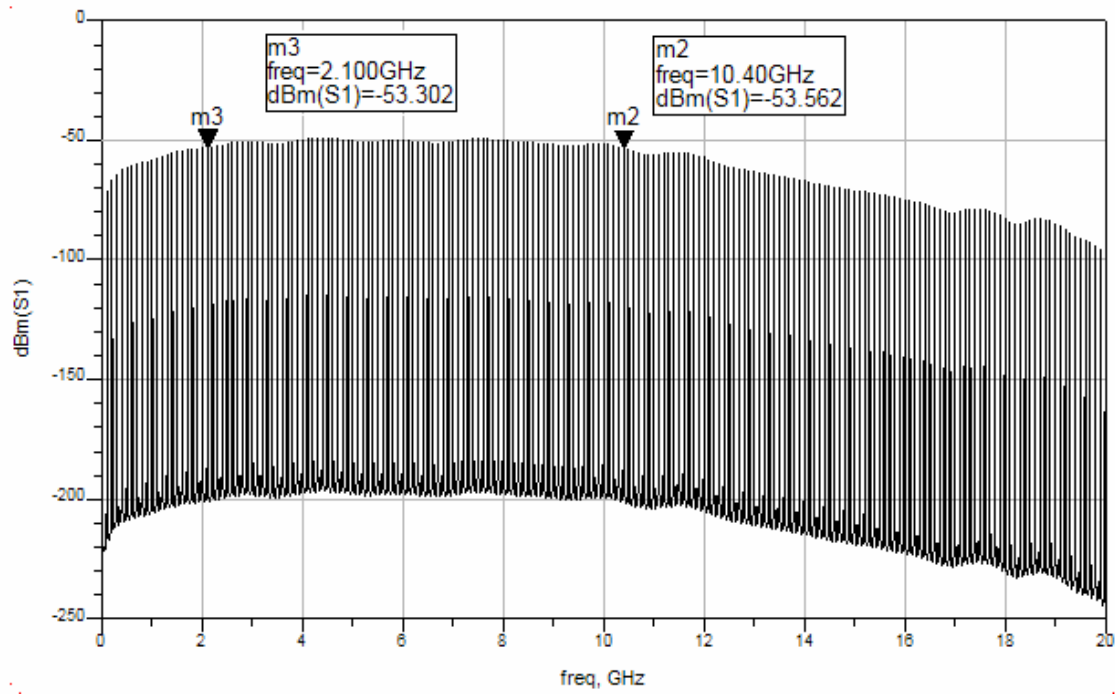


Figure 4.11 Simulated downlink spectrum after 1 meter ROF

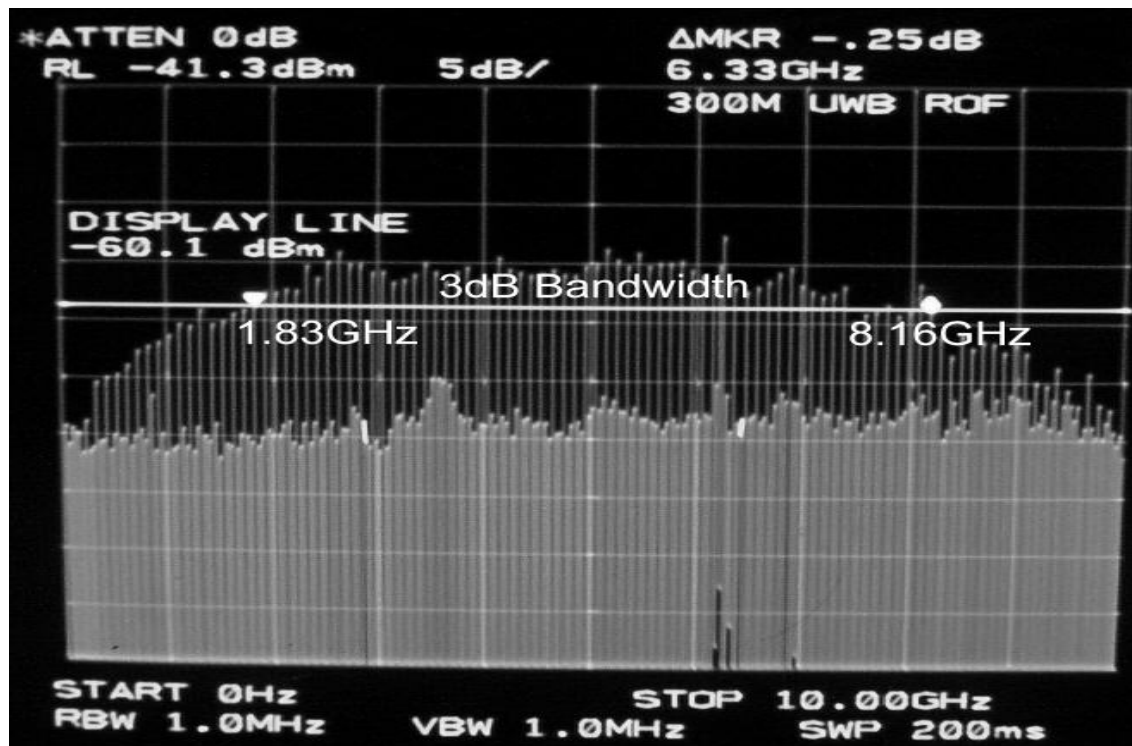


Figure 4.12 Measured downlink spectrum after 300 meter ROF

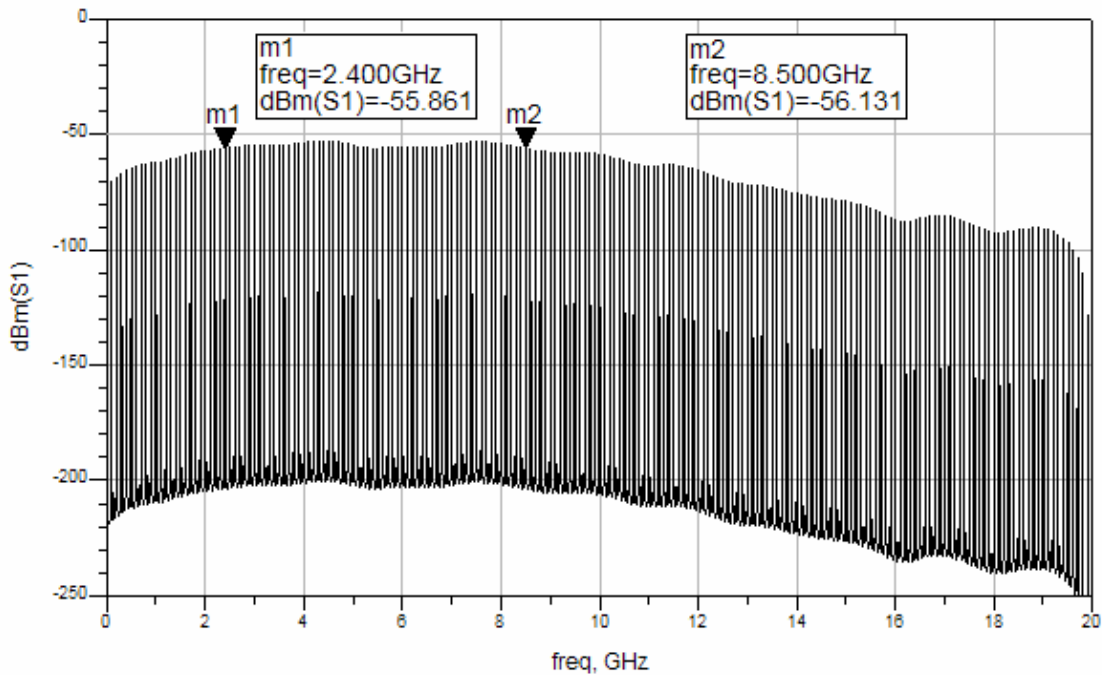


Figure 4.13 Simulated downlink spectrum after 300 meter ROF

The spectrum of the UWB signal after the 1 meter ROF transmission (Figure 4.10 and 4.11) illustrates that the link places constraints on the amplitude as well as the 3 dB bandwidth of the UWB pulse. Also the group delay is minimal for a 1 meter ROF. From the temporal signals it can be seen that the pulse shape is retained and the pulse expansion is minimal. All these suggest that the 1 meter ROF link can be viewed as a pulse compressor and filter which spreads the pulse spectral energy across a broad bandwidth of 7 to 8 GHz and filters out the spectral contents below 2 GHz and above 10 GHz. It can be concluded that the 1 meter ROF link can be used for shaping the UWB pulse to meet the FCC average emission spectral limit. For a 300 meter case the spectrum (Figure 4.12 and 4.13) suggests that the upper limit of the 3 dB band is further down to ~ 8 GHz which relates to the pulse expansion in time domain. Overall the 3 dB bandwidth has reduced to ~ 6 GHz which deteriorates the signal shaping including ringing.

4.3.4 Results of UWB uplink pulse transmission over ROF

For uplink pulse generation, the setup as shown in Figure 4.14 is used. The pulse from a down link setup is amplified and sent over a transmitting and receiving broadband antennae (3-11 GHz) separated by a typical UWB distance of 1 meter. This signal is again amplified as shown in Figure 4.15 and used for transmission over ROF link of 1, 300 and 600 meters.

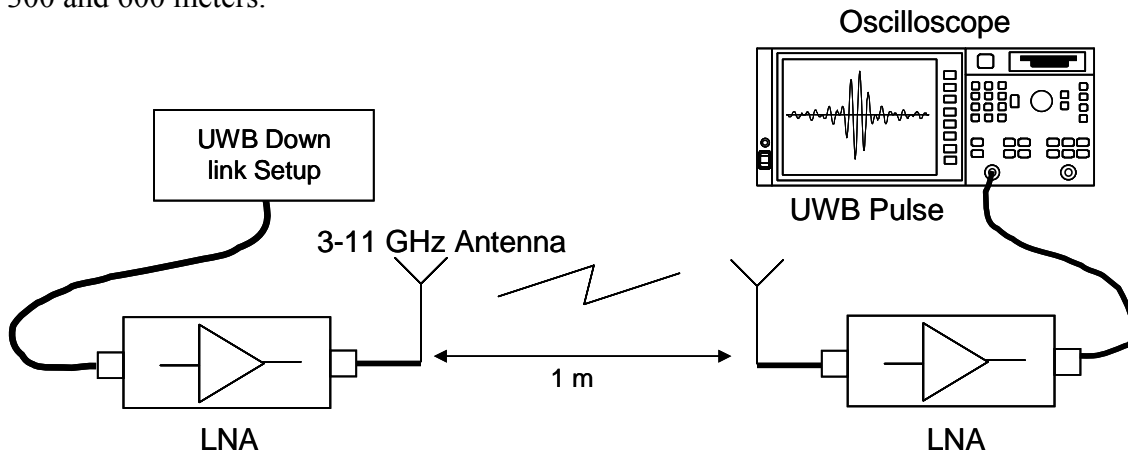


Figure 4.14 Setup for an impulse radio UWB up link pulse generation

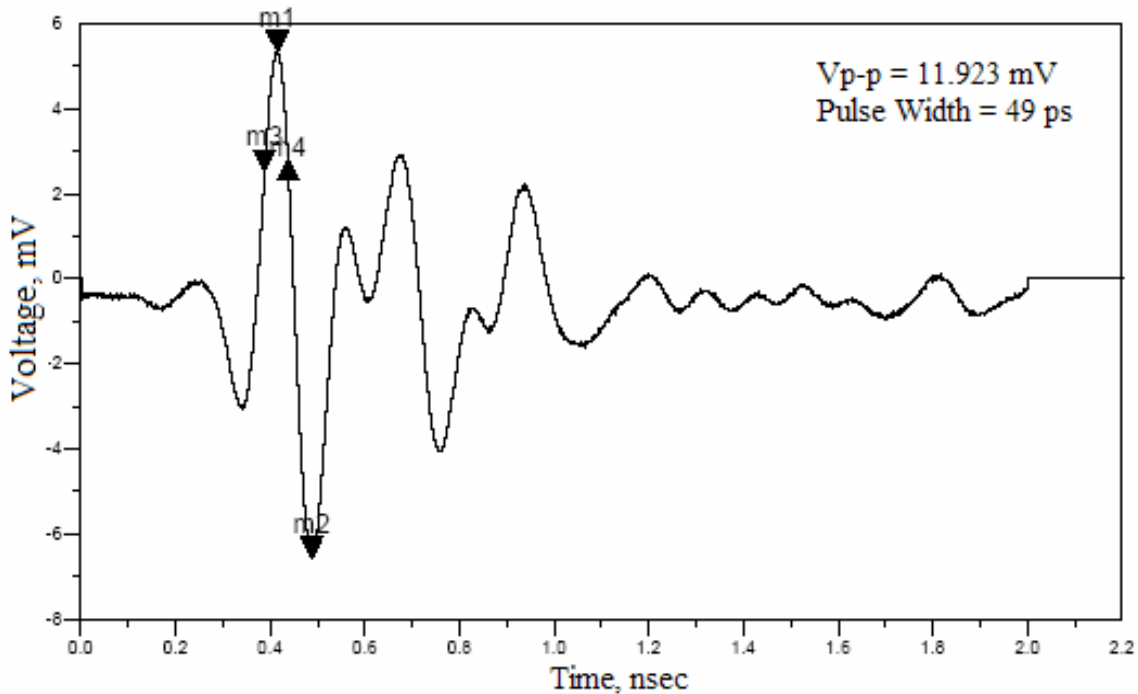


Figure 4.15 UWB uplink source pulse

The results for ROF transmission distances of 1m, 300m and 600m are shown below in Figures 4.16, 4.17, 4.18 .

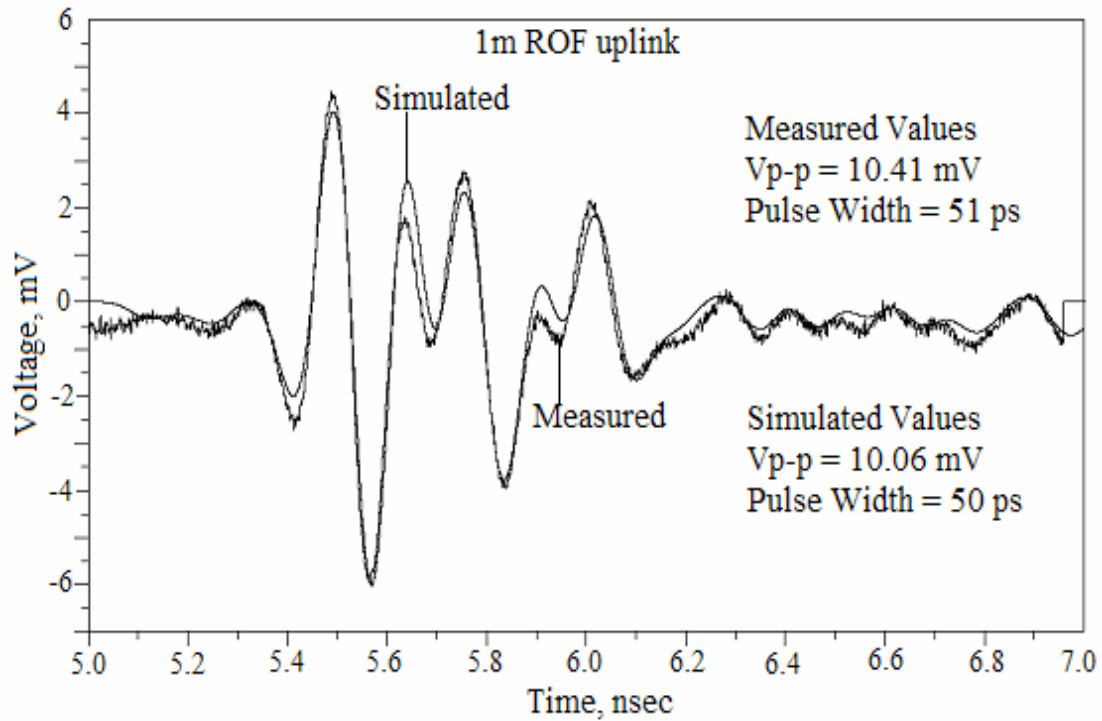


Figure 4.16 UWB uplink pulse after 1 meter ROF

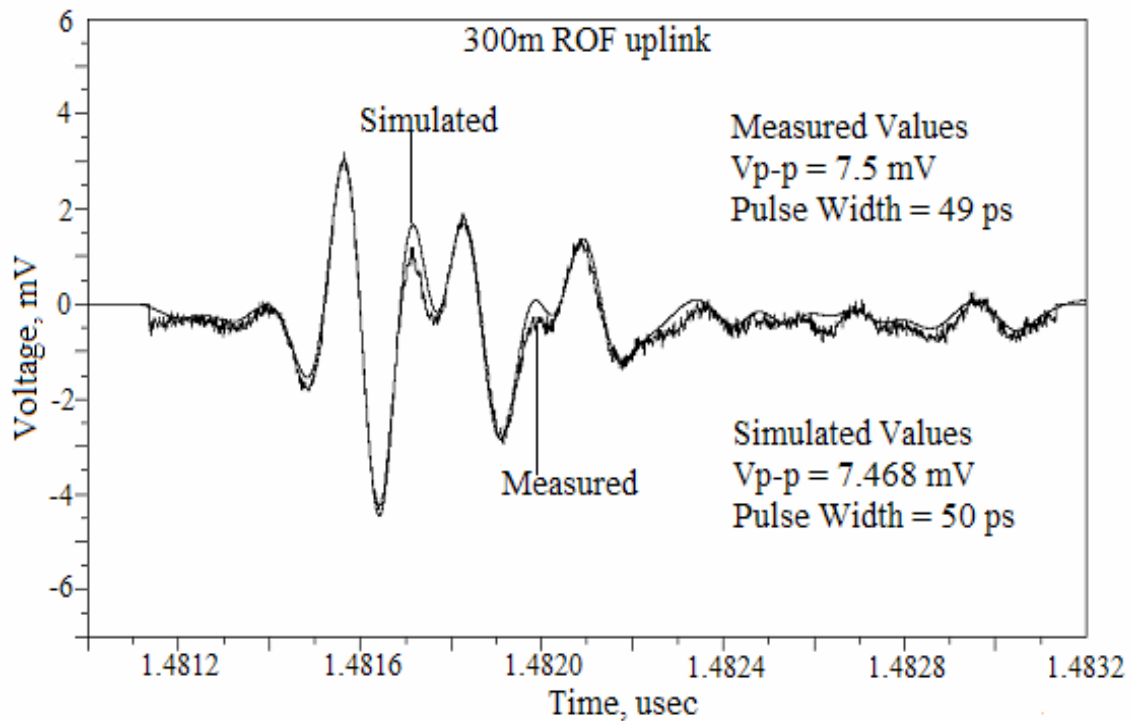


Figure 4.17 UWB uplink pulse after 300 meter ROF

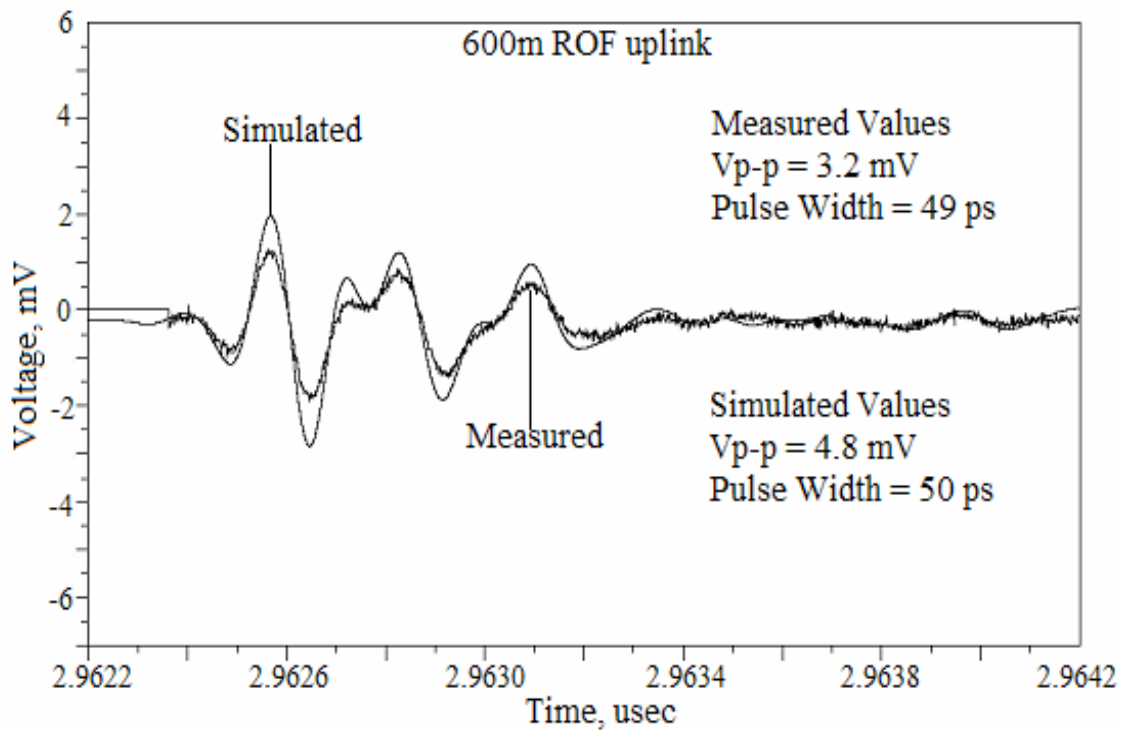


Figure 4.18 UWB uplink pulse after 600 meter ROF

4.4 Summary

This chapter successfully demonstrated the transmission of pulsed UWB signals over a 1m, 300m and 600m VCSEL based MMF links. Both uplink and downlink scenarios were considered and the received temporal signal was analyzed. From the results from chapter 3 as well as chapter 4 it is concluded that 600 meter ROF distance could lead to gross errors due to the inherent connector error in the simulation model as mentioned in chapter 3.

In the next chapter the OFDM WLAN signal transmission over a MMF will be analyzed for 300 meter transmission distance.

5 WLAN transmission over MMF link

5.1 Introduction to Wireless LAN

Wireless LAN is a wireless data communication system designed to extend or replace the functions of a conventional Wired LAN. The IEEE specifications for wireless LAN had both radio channel as well as infra-red channel as access mediums. But the radio channel has become the de facto standard for most of the practical and commercial deployments. This thesis concentrates only on the radio channel based wireless LAN systems. A typical Radio channel based WLAN system is fed by a wired LAN network as shown in Figure 5.1. The access point (AP) is the interface between the wired and wireless LANs which consists of a MAC layer connecting to the bridge of the wired LAN and a physical layer comprising the base station including antenna. This chapter explores about WLAN transmission over MMF link for range extension by conducting simulations and experiment. Also it explores the transmission of WLAN in the presence of UWB signal in the ROF channel.

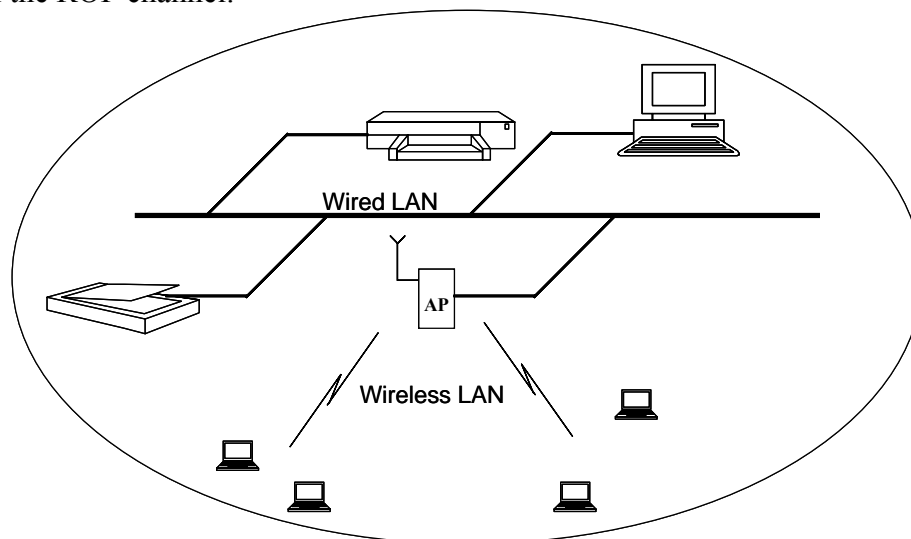


Figure 5.1 A typical Wireless LAN scenario

5.2 WLAN Physical media and access modulations

The IEEE 802.11 standard describes the physical media specifications and the modulation formats. Table 5.1 summarizes the IEEE 802.11a and g standards:

	802.11a	802.11g
Compatibility	802.11a	802.11b
Data rate per channel	54, 48, 36, 24, 18, 12, 9, 6 Mbps	54, 36, 33, 24, 22, 12, 11, 9, 6, 5.5, 2, 1 Mbps
Available Bandwidth	300 MHz	83.5 MHz
Number of Non-Overlapping Channels	4 Indoor (UNII1) 4 Indoor/Outdoor (UNII2) 4 Outdoor (UNII3)	3 (Indoor / Outdoor)
Frequency (GHz)	5.15 – 5.25 (UNII1) 5.25 – 5.35 (UNII2) 5.725 – 5.825 (UNII3)	2.4 – 2.4835 (US & EU) 2.471-2.497 (Japan)
Modulation Type	OFDM BPSK (6, 9 Mbps) QPSK (12, 18 Mbps) 16-QAM (24, 36 Mbps) 64-QAM (48, 54 Mbps)	OFDM/CCK (6,9, 12,18,24,36,48,54) OFDM (6,9,12,18, 24,36,48,54) DQPSK/CCK (22, 33, 11, 5.5 Mbps) DQPSK (2 Mbps) DBPSK (1 Mbps)
Output Power (mW)	40 (UNII1), 200 (UNII2), 800 (UNII3)	100 (EU) ,1000 (US)
Number of Channels	4 (UNII1) , 4 (UNII2) , 4 (UNII3)	
Channel Spacing	20MHz	OFDM - 20MHz, PBCC - 5MHz
Channel Bandwidth	20MHz	OFDM -20MHz, PBCC - 22MHz
Adjacent Channel		25MHz
Sensitivity (dBm)	-82 @PER10% (6Mbps)	OFDM -82 @PER10% (6Mbps) PBCC -76@FER8%
Cutoff level (dBm)	-30@PER10%	OFDM -20@PER10% PBCC -10@FER8%

Table 5.1 WLAN Specifications [7], [8]

5.3 IEEE 802.11a signal generation and testing parameters

The parameters necessary to setup the simulations in ADS using the WLAN library are discussed in Table 5.2 and 5.3:

Information data rate	6, 9, 12, 18, 24, 36, 48 and 54 Mbit/s (6, 12 and 24 Mbit/s are mandatory)
Modulation	BPSK OFDM QPSK OFDM 16-QAM OFDM 64-QAM OFDM
Error correcting code	K = 7 (64 states) convolutional code
Coding rate	1/2, 2/3, 3/4
Number of sub carriers	52
OFDM symbol duration	4.0 μ s
Guard interval	0.8 μ s (T_{GI})
Occupied bandwidth	16.6 MHz

Table 5.2 OFDM Parameters [7]

Parameter	Values
N_{SD} : Number of data sub carriers	48
N_{SP} : Number of pilot sub carriers	4
N_{ST} : Number of sub carriers, total	52 ($N_{SD} + N_{SP}$)
Δ_F : Sub carrier frequency spacing	0.3125 MHz (= 20 MHz/64)
T_{FFT} : IFFT/FFT period	3.2 μ s ($1/\Delta_F$)
$T_{PREAMBLE}$: PLCP preamble duration	16 μ s ($T_{SHORT} + T_{LONG}$)
T_{SIGNAL} : Duration of the SIGNAL BPSK-OFDM symbol	4.0 μ s ($T_{GI} + T_{FFT}$)
T_{GI} : Guard Interval duration	0.8 μ s ($T_{FFT}/4$)
T_{GI2} : Training symbol of GI duration	1.6 μ s ($T_{FFT}/2$)
T_{SYM} : Symbol Interval	4 μ s ($T_{GI} + T_{FFT}$)
T_{SHORT} : Short training sequence duration	8 μ s ($10 \times T_{FFT}/4$)
T_{LONG} : Long training sequence duration	8 μ s ($T_{GI2} + 2 \times T_{FFT}$)

Table 5.3 Timing Parameters [7]

After the signal generation, the signal has to be bench marked. There are many criteria described in IEEE 802.11a for this purpose. In a ROF case, the transmitter criteria are more important as the ROF link could be viewed as a block replacing the power amplifier between the signal generation and the antenna blocks. The transmitter signal has to meet the transmitter spectral mask, the relative constellation error and the Error vector magnitude (EVM) specifications which are described in Figure 5.2 and Table 5.4.

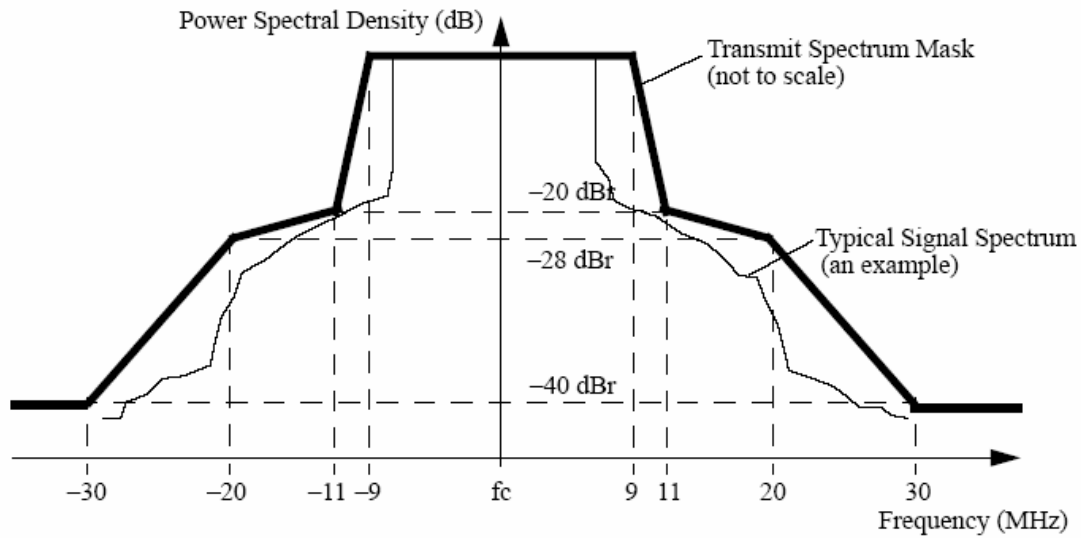


Figure 5.2 IEEE 802.11a Transmitter spectral mask [7]

Data Rate	Relative Constellation Error (dB)	EVM (%rms)
6	-5	56.2
9	-8	39.8
12	-10	31.6
18	-13	22.3
24	-16	15.8
36	-19	11.2
48	-22	7.9
54	-25	5.6

Table 5.4 EVM and constellation error requirements of IEEE 802.11a [7]

5.4 WLAN transmission over Fiber

For exploring the wireless LAN transmission over fiber only the two cases IEEE 802.11a OFDM and IEEE 802.11g OFDM are considered. The WLAN library of the ADS Ptolemy simulator [40] provides a test bench for both the above mentioned cases. The optical components are modeled in ADS circuit simulator [40]. But ADS offers a Co-simulation interface between the Ptolemy and circuit simulators which provides a seamless integration of the WLAN models with optical components. The corresponding experimental setup for WLAN ROF transmission is as shown in figure 5.3 [36]. A control PC generates the necessary pattern of either IEEE 802.11a or 802.11g and loads it into a vector signal generator which drives the ROF link whose output is fed into a vector signal analyzer test set for WLAN which in turn feeds the control PC. The control PC along with its original pattern and received pattern produces EVM results, constellation diagrams, base band spectrum etc.

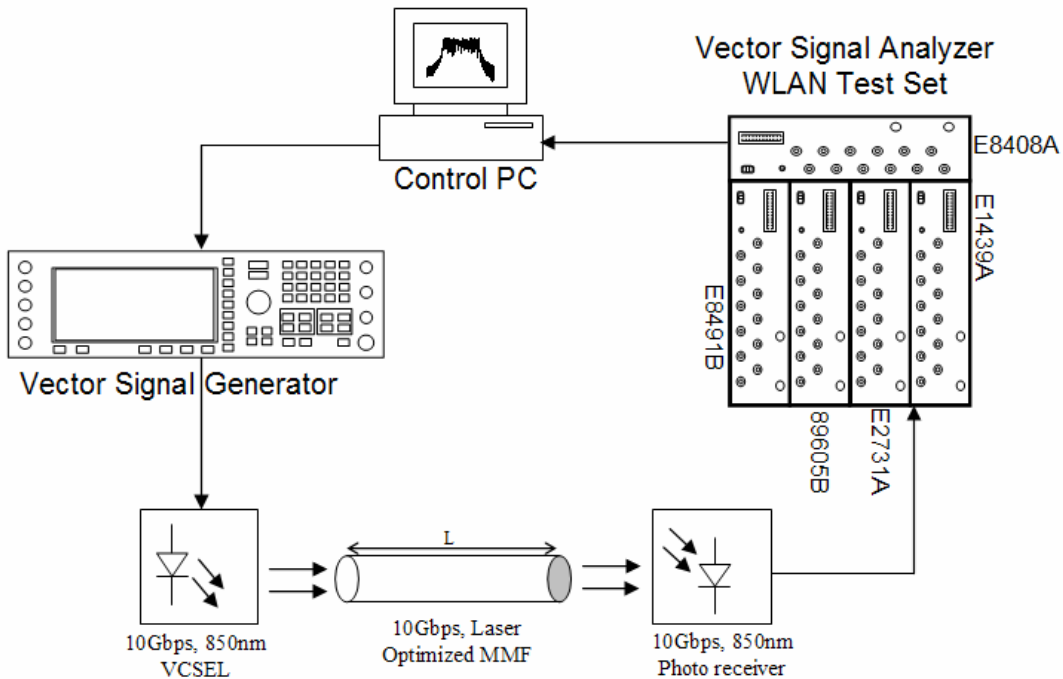


Figure 5.3 WLAN over fiber Setup [36]

5.5 IEEE 802.11a/g ROF transmission performance results

Simulation Parameters							
RF frequency	Data rate	Power	GI	Symbol time	Data time	Signal time	MMF length
5200/2400 MHz	54 Mbps	-10 dBm	0.250	4 μ s	16 μ s	4 μ s	300 meters

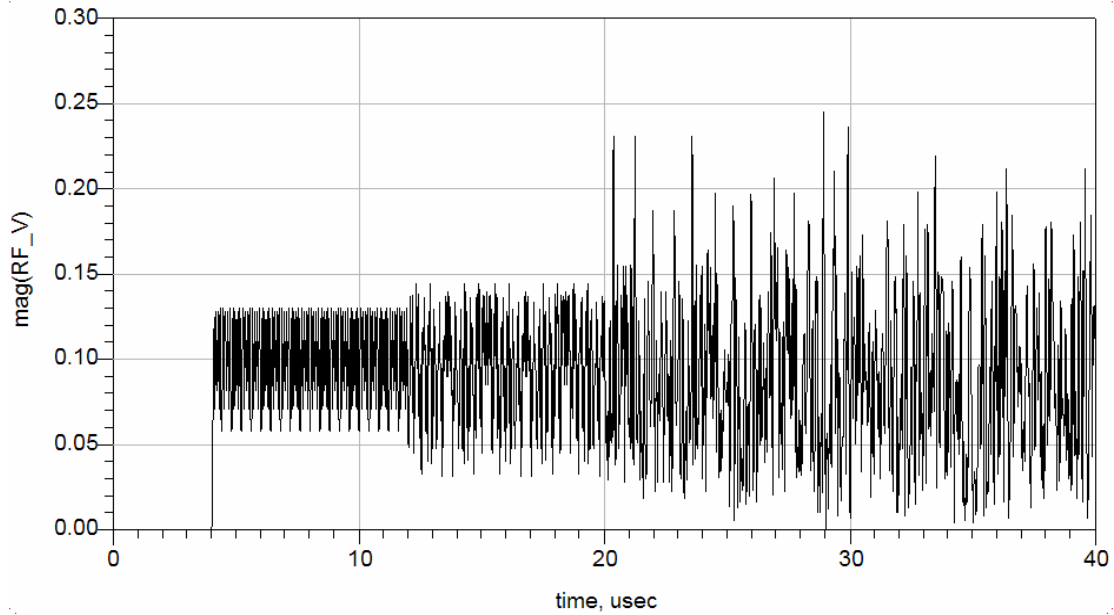


Figure 5.4 IEEE 802.11a signal after 300 meter ROF

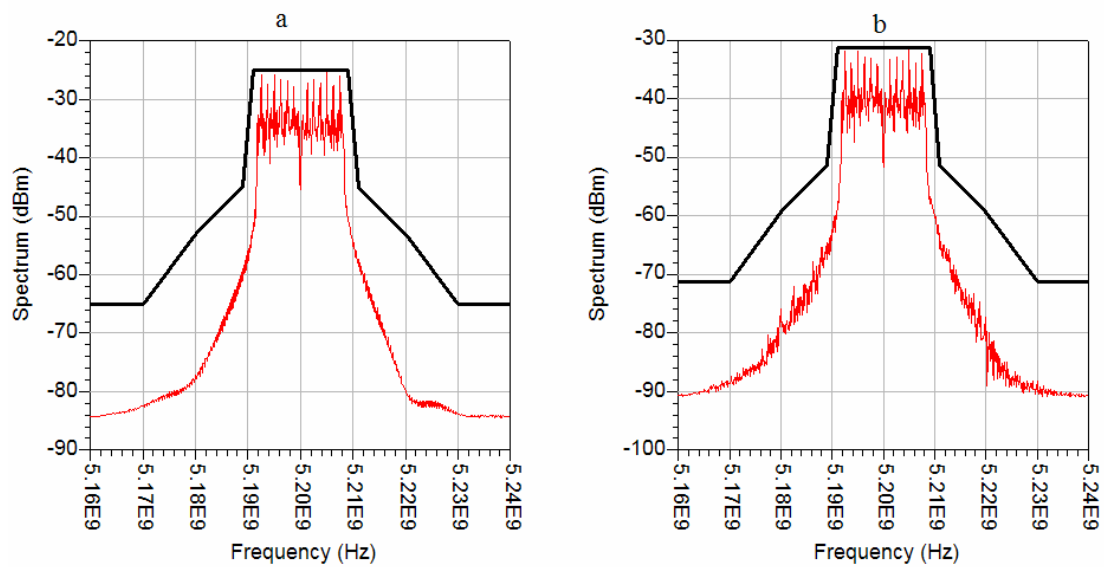


Figure 5.5 IEEE 802.11a signal spectrum a) without ROF b) with ROF

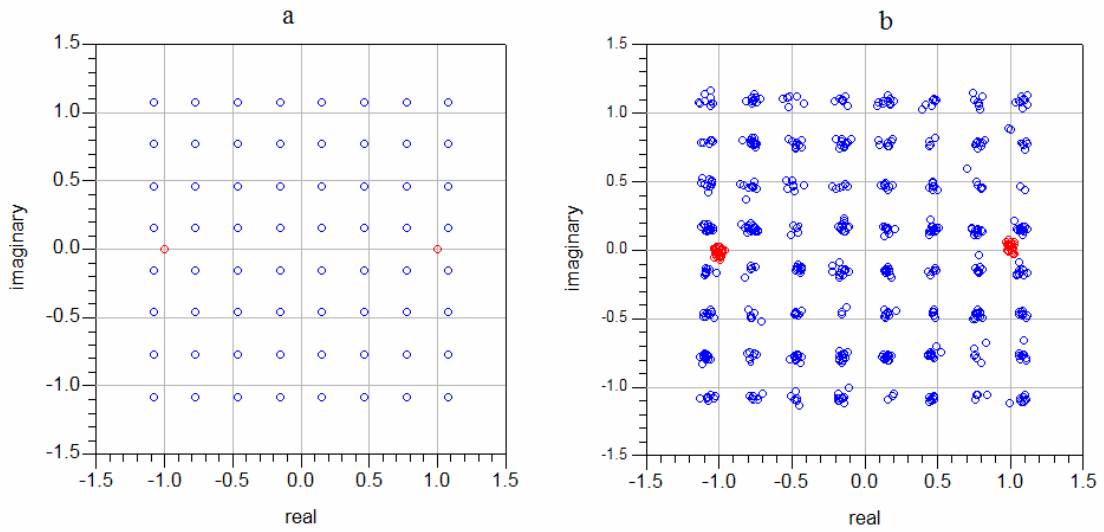


Figure 5.6 IEEE 802.11a constellation a) without ROF b) with ROF

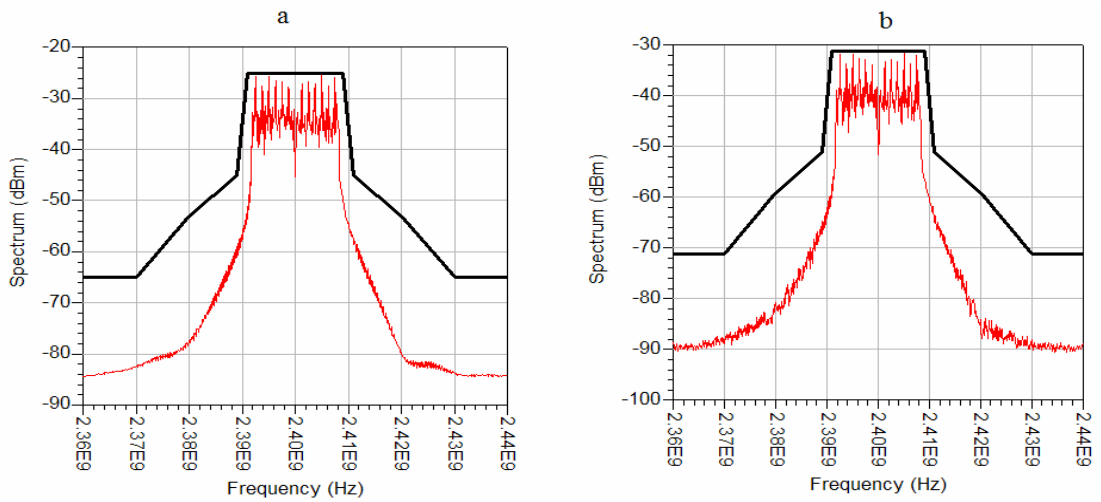


Figure 5.7 IEEE 802.11g signal spectrum a) without ROF b) with ROF

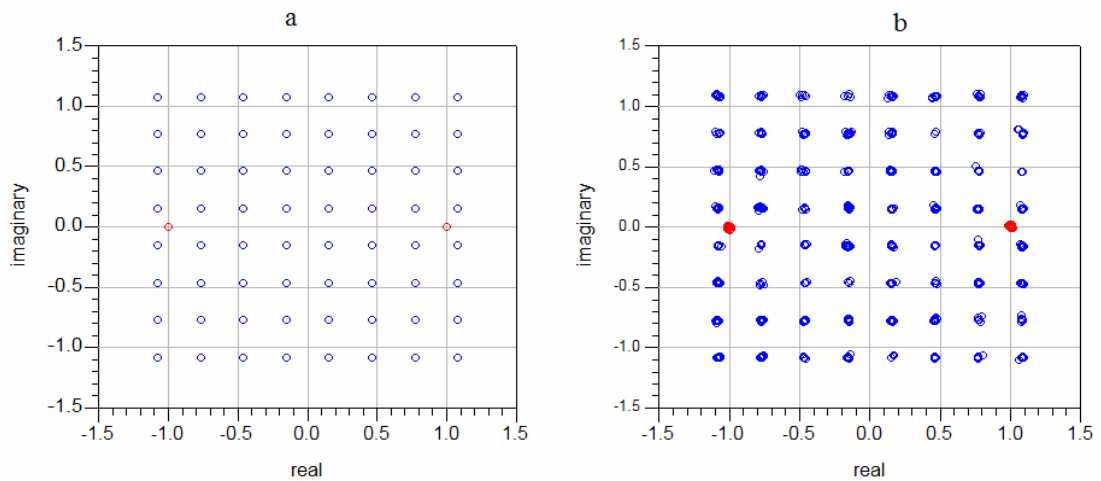


Figure 5.8 IEEE 802.11g constellation a) without ROF b) with ROF

The above results gives an idea about the performance of IEEE 802.11a/g OFDM signals transmitted over a 300 meter ROF link. Figure 5.4 is the temporal WLAN signal after 300m ROF transmission. It can be observed that the spectral measurements in Figure 5.5 and 5.7 have more or less the same performance for 11a and 11g except for the frequency of operation. They are complying excellently with the IEEE spectral mask with a huge margin. The real performance difference gets reflected in the signal constellation diagrams as shown in Figure 5.6 and 5.8. The corresponding constellation error in dB is tabulated in Table 5.5.

Signal	IEEE Relative Constellation Error (dB)	Simulated Relative Constellation Error without ROF (dB)	Simulated Relative Constellation Error with ROF (dB)
IEEE 802.11a (54 Mbps)	-25	-136	-29.425
IEEE 802.11g (54 Mbps)	-25	-136	-38.5

Table 5.5 Relative Constellation Error

From Table 5.5 it can be certainly observed that the constellation error constraints are just met marginally for the ROF case and IEEE 802.11g performs better than IEEE 802.11a. But considering the ROF link as an attenuator block present in between the WLAN transmitter and the antenna in a down link scenario, it is good to examine the error vector measurements and compare it against the IEEE 802.11a requirements. The EVM performances are tabulated below in Table 5.6.

Signal	IEEE EVM %	Simulated EVM % without ROF	Simulated EVM % with ROF	Measured EVM % with ROF
IEEE 802.11a (54 Mbps)	5.6	<< 1	3.38	3.2
IEEE 802.11g (54 Mbps)	5.6	<< 1	1.18	1.1

Table 5.6 EVM Results

The EVM results show that the predicted results from the simulation were consistent with the experimental measurements. Also both IEEE 801.11a/g meet the IEEE transmitter requirements in terms of spectral mask, relative constellation error and error vector magnitude with a 300 meter ROF link augmented with the WLAN transmitter. It should be noted that all these tests were performed with 54 Mbps data rate for which the IEEE requirements are most stringent. Also it was found from the simulation that there is a constraint placed by the ROF link on the transmitter power as -10 dBm as maximum, above which the EVM performance deteriorates heavily. This could be attributed to the VCSEL diode's non-linearity. Later the measurements confirmed the transmitter power constraint.

5.6 WLAN transmission over Fiber in the presence of UWB signal

This section explores the possibilities of the presence of UWB signal in a ROF link used to transmit a WLAN signal. Even in the radio channel the UWB signal occupying a very wide bandwidth leads to a co-existence scenario with WLAN IEEE 802.11a (see Figure 5.9). But this scenario is taken care by the FCC's average EIRP emission limit of -41.3 dBm/MHz for UWB transmitter power [11] [48].

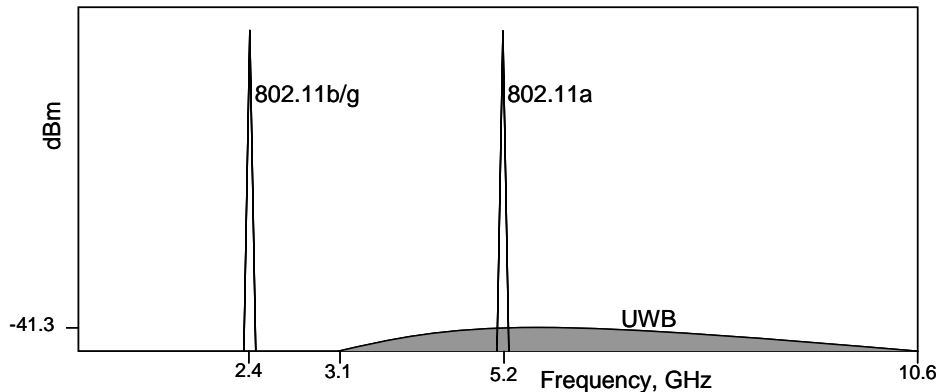


Figure 5.9 Spectrum of IEEE WLAN and UWB

The performance of WLAN signal with UWB presence [37] [38] is evaluated in two scenarios of the ROF link. Only the IEEE 802.11a is chosen as it operates at 5.2 GHz which lies well within the spectral span of UWB and receives a considerable interference as compared with the 2.4 GHz IEEE 802.11b/g. The first scenario is where UWB is added with IEEE 802.11a signal using a RF power combiner and sent across the ROF link before evaluated (Figure 5.10). This scenario can be categorized as UWB presence at the ROF transmitter.

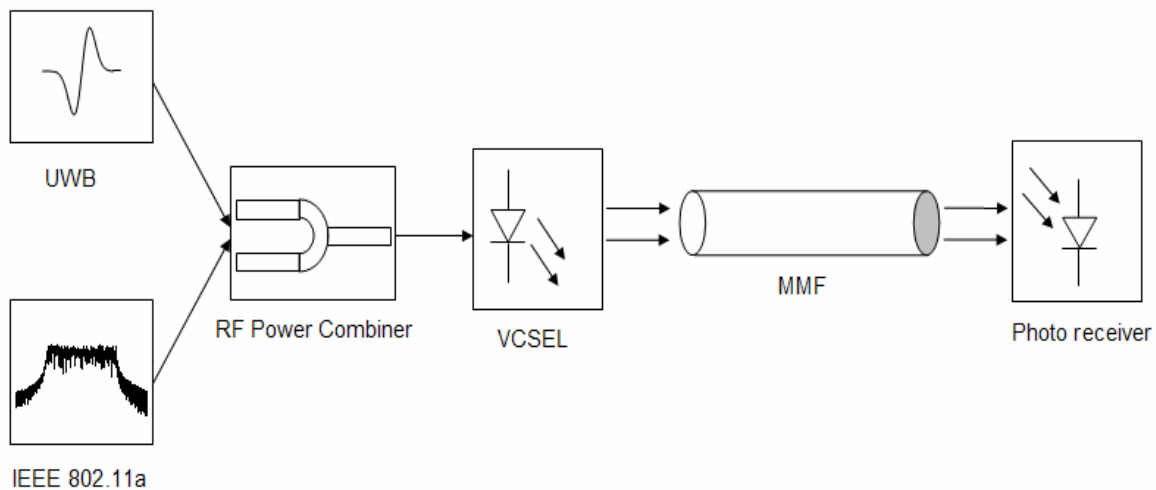


Figure 5.10 WLAN and UWB added using RF combiner

The second scenario is where the UWB and IEEE 802.11a are separately modulated over two VCSEL diodes correspondingly (Figure 5.11) [38]. The VCSEL diodes differ in few nanometers of emission wavelength. Then the optically modulated UWB and WLAN signals are combined with an opto-coupler and sent over the multimode fiber. All the signals are received by a single photo receiver. So, effectively the UWB and WLAN are transmitted over separate optical channels i.e. two different wavelengths before they are added up at the photo receiver. This scenario can be categorized as UWB presence at the ROF receiver.

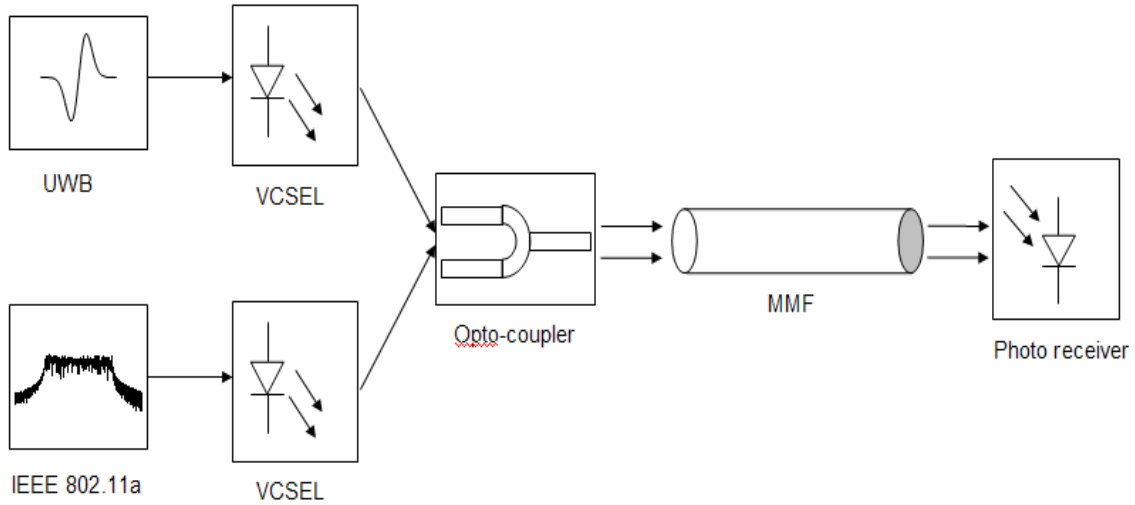


Figure 5.11 WLAN and UWB added using Opto-coupler

5.6.1 Performance results for IEEE 802.11a in the presence of UWB

Scenario 1: UWB presence at ROF transmitter

Simulation Parameters		
IEEE 802.11a	RF Frequency	5200 MHz
	Data rate	54 Mbps
	Transmitter Power	-10 dBm
	GI	0.250
	Symbol time	4 μ s
	Data time	16 μ s
	Signal time	4 μ s
UWB	Vp-p	226 mV
	Pulse width	42 ps
	Data rate	100 Mbps
Others	MMF length	300 meters
	RF combiner loss	3 dB

Table 5.7 Simulation Parameters for UWB presence at ROF transmitter

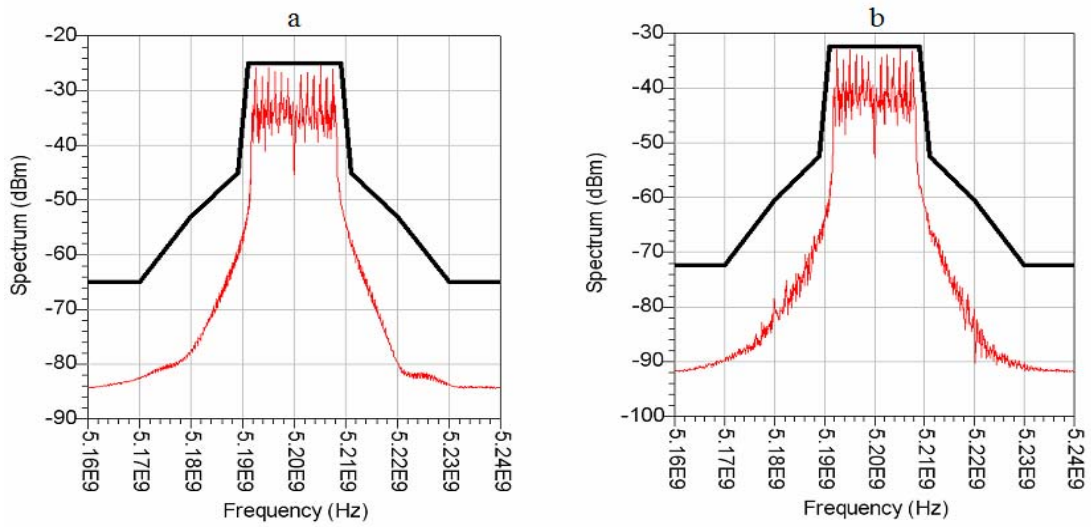


Figure 5.12 IEEE 802.11a signal spectrum a) without UWB b) with UWB at ROF transmitter

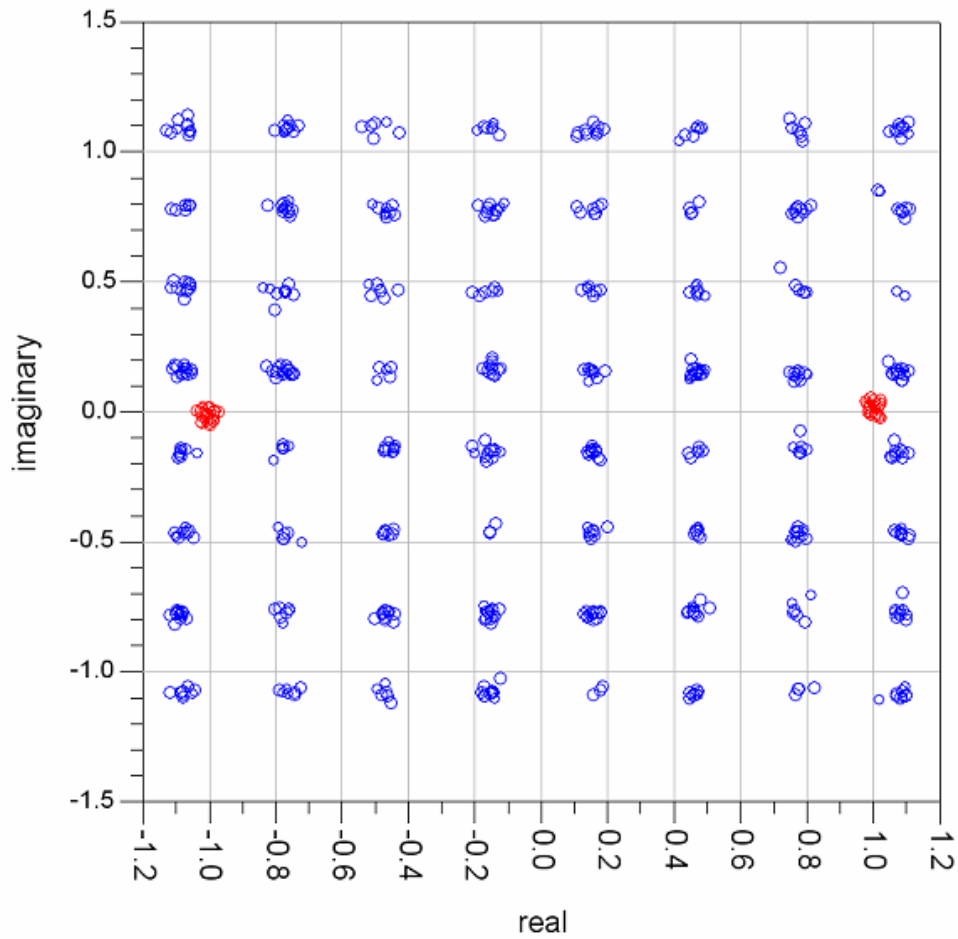


Figure 5.13 IEEE 802.11a constellation with UWB presence at ROF transmitter

Signal	IEEE standard	Simulated	Measured
Relative constellation Error (dB)	-25	-32.17	-31.7
EVM%	5.6	2.46	2.6

Table 5.8 Relative Constellation Error and EVM in dB

From simulated and measured EVM it can be seen that the performance of the IEEE 802.11a is well within the IEEE standard specifications, even in the presence of a downlink UWB signal at the ROF transmitter. The spectrum (Figure 5.12) also confines to the IEEE spectral mask. Figure 5.13 shows the signal constellation diagram. Also it is seen that the EVM performance (Table 5.8) is better than the simple WLAN transmission over fiber. This could be attributed to the fact that the 3 dB RF power combiner decreases the WLAN transmitter power fed into the VCSEL diode. As seen before, this reduces the non-linear effects improving the performance. In the present work there is no facility to evaluate the UWB performance other than temporal qualities of the pulse. Figure 5.14 shows the UWB pulse train added with IEEE 802.11a signal at the photo receiver.

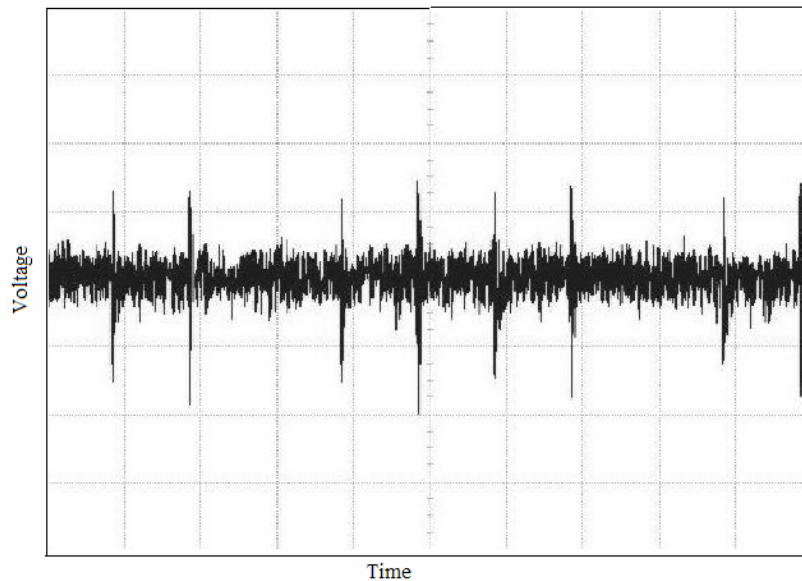


Figure 5.14 UWB pulse train in time domain with WLAN added

Scenario 2: UWB presence at ROF Receiver

The simulation parameters were similar to the Scenario 1 for IEEE 802.11a and UWB. Two VCSEL diodes were used to modulate these two signals separately and added using an opto-coupler.

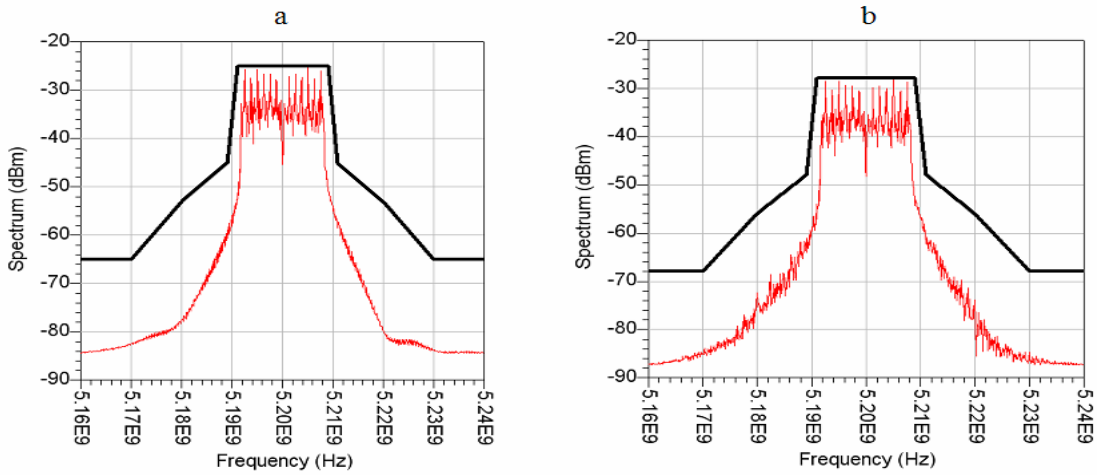


Figure 5.15 IEEE 802.11a signal spectrum a) without UWB b) with UWB

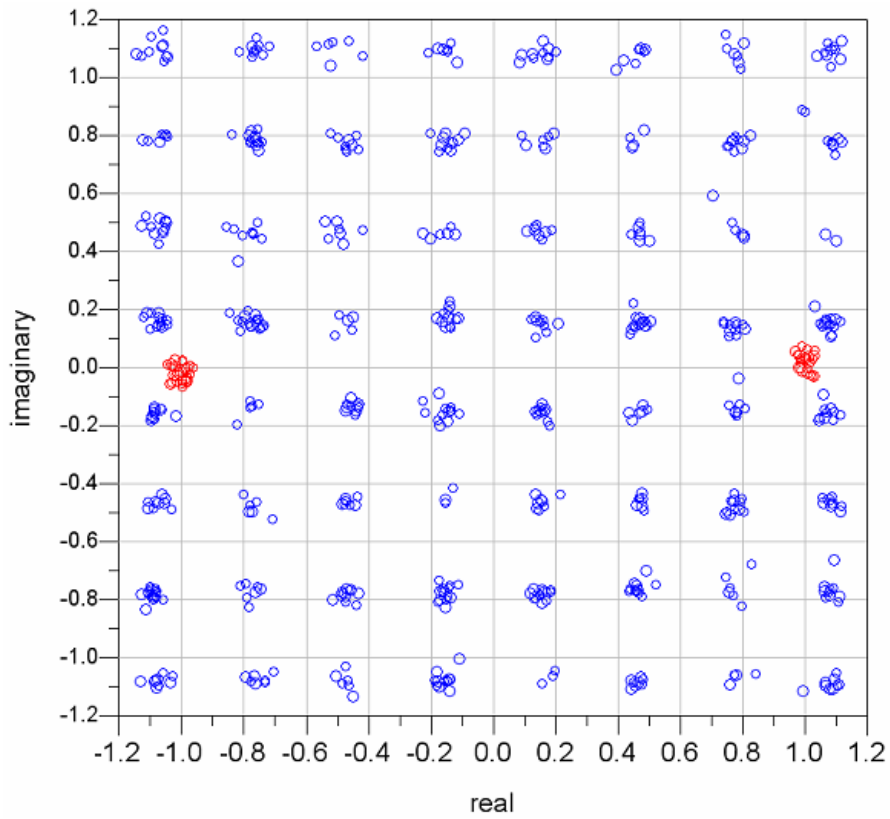


Figure 5.16 IEEE 802.11a constellation with UWB presence at ROF receiver

Signal	IEEE standard	Simulated	Measured
Relative constellation Error (dB)	-25	-29.37	-28.4
EVM%	5.6	3.4	3.8

Table 5.9 Relative Constellation Error and EVM in dB

From simulated and measured EVM it can be seen that the performance of the IEEE 802.11a is well within the IEEE standard specifications, even in the presence of a downlink UWB signal at the ROF Receiver. The spectrum (Figure 5.15) also confines to the IEEE spectral mask. Figure 5.16 shows the signal constellation diagram which is worse than the scenario 1 (Figure 5.13). The EVM performance (Table 5.9) is very much similar to the WLAN transmission over fiber. But this method of having two VCSEL diodes could prove costly. In future, where VCSEL diodes promise a very low cost optical transmitter, this technique could be used to extend the coverage range of two different wireless networks with the same fiber channel. As shown in Figure 5.14 the UWB pulses had a peak-to-peak voltage of 30~40 mV and were heavily distorted. But they could be still detected and a co-existence scenario for UWB and WLAN is possible.

5.7 Summary

This Chapter successfully demonstrated the OFDM WLAN signal transmission over 300 meter MMF links. Also the performance of WLAN in the presence of UWB signal both at the ROF transmitter and ROF receiver were examined successfully.

6 Conclusions and Future directions

6.1 Conclusions

Even though Radio over fiber links were existing in applications like antenna remoting for an earth station or CATV distribution systems, they were predominantly using single mode fiber link as their medium together with DFB or Fabry-Perot lasers as electro-optical transmitters. Also the commercial applications of such links were very limited due to the huge costs involved for single mode fiber based infrastructure.

This thesis proposed a low cost alternative to the existing ROF links based on VCSEL laser diode and the laser-optimized 10Gbps multimode fiber for the transmission of OFDM wireless LAN signals (5 and 2.4 GHz) and pulsed UWB signals (3.1 to 10.6 GHz) for a distance of 300 meters. In Chapter 2 the evolution of multimode fibers as a short distance high speed data link up to 10Gbps was investigated. Also the evolution of VCSEL laser diode towards a reliable electro-optical transmitter at 10Gbps was investigated.

In chapter 3 the VCSEL diode was characterized and modeled based on the measurement of L-I-V DC characteristics and S-parameters. The multimode fiber was characterized as a transfer function based on modal delays calculated from WKB approximation. Based on the individual component models the entire MMF link was characterized based on S21 parameters as well as the group delays. From this the bias settings for the VCSEL diode was chosen for the desired link performance, for UWB as well as WLAN transmission.

6.1.1 Conclusions for UWB

The UWB transmission over MMF link brought the following conclusions:

- A down link UWB pulse sent over a Radio channel of 1 meter undergoes an attenuation of 20 times from its original amplitude.
- A down link UWB pulse sent over a ROF link of 300 meter undergoes an attenuation of 3 times from its original amplitude.
- A down link UWB pulse sent over a ROF link of 600 meter undergoes an attenuation of approximately 4 times from its original amplitude.
- All the above 3 cases introduces ringing and the pulse undergoes temporal expansion of approximately the same width.
- A 300 meter or 600 meter ROF link offers a superlative performance than a 1 m UWB radio channel.
- These ROF links are potential range extension infrastructures for UWB systems.

6.1.2 Conclusions for WLAN

The WLAN transmission over 300m MMF link brought the following conclusions:

- Both IEEE 802.11a and g OFDM signals confined to the transmitter spectral mask.
- The error vector magnitude was well with in the 5.6 % mark set by IEEE for both signals.
- IEEE 802.11g had a better EVM performance than 11a.
- The simulation predictions for IEEE 802.11a EVM performance in the presence of UWB signal at both ROF transmitter and receiver agreed well with the experiments.

- The EVM performance of the both above cases were well with in the IEEE EVM specifications.
- The WLAN added UWB pulse train in time domain shows that a co-existence scenario is possible.

6.2 Future directions of ROF

Millimeter wave systems are the upcoming wireless systems which would constitute much of the next generation networks. With enormous bandwidth available millimeter wave systems could be the solution for the demanding multimedia applications [50]. The 60 GHz band is one of the potential millimeter waveband. For e.g. the IEEE 802.15.3c millimeter wave interest group is exploring the use of the 60 GHz band for wireless personal area networks (WPANs) [51]. A demonstration of wireless LAN at 60 GHz is also available in the literature [52]. Recent literature shows demonstration of 60GHz wireless transceivers [53], [54], [55] and this shows interests growing in the millimeter wave electronics.

However, mm-waves cannot be distributed electrically due to high RF propagation losses. In addition, generating mm-wave frequencies using electrical devices is challenging. This in turn would raise the cost of the system in terms of generation and distribution of the millimeter waves.

Radio over fiber is an ideal solution for generation and distribution of millimeter waves [56] [57]. It's already demonstrated that ROF could be a potential medium for Road-to-Vehicle communication system operating at frequency bands 63-64 GHz and 76-77 GHz [58].

Other than signal generation, photonic systems could be as well used to perform millimeter wave and microwave signal processing [59] [60]. These signal processing functions include filtering, fixing, up conversion and down conversion etc. Including these photonic signal processing functions within a ROF transmission system would make the entire system cost very cheaper especially in the case millimeter waves.

Bibliography

- [1] E.I. Ackerman, and C.H. Cox III, "RF Fiber-Optic Link Performance," IEEE Microwave Magazine, Vol. 2, No 4, pp. 50-58, Dec. 2001
- [2] Djafar K. Mynbaev, Lowell L. Schneiner, "Fiber-Optic Communications Technology," N.J.: Prentice Hall, 2001.
- [3] S. F. Yu, "Analysis and Design of Vertical Cavity Surface Emitting Lasers," (Wiley Series in Lasers and Applications), Wiley-Interscience, 2003.
- [4] GSM specification GSM 05.05: 1994-02 Edition 2 Title: European digital cellular Telecommunications system (Phase 1); Source: SMG 2 Radio transmission and reception Part 1
- [5] DCS specification GSM 05.05-DCS 1994-02 Title: European digital cellular telecommunications system (Phase 1); Source: SMG Radio transmission and reception Part 2: DCS extension
- [6] IEEE Standard 802.11b-1999, "Part 11: Wireless LAN Medium Access Control (MAC) and Physical Layer (PHY) specifications: High-speed Physical Layer Extension in the 2.4 GHz Band," 1999.
- [7] IEEE Standard 802.11a-1999, "Part 11: Wireless LAN Medium Access Control (MAC) and Physical Layer (PHY) specifications: High-speed Physical Layer in the 5 GHz Band," 1999.

- [8] IEEE Standard 802.11g-2003, “Part 18 High Rate direct sequence spread spectrum (HR/DSSS) PHY specification,” 2003.
- [9] UMTS specification <http://www.umtsworld.com/technology/wcdma.htm>
- [10] CDMA 2000 <http://www.umtsworld.com/technology/cdma2000.htm>
- [11] IEEE 802.15.3 WPAN High Rate Alternative PHY Task Group 3a, Available from www.ieee802.org/15/pub/TG3a.html
- [12] James M. Wilson, “The Next Generation of Wireless LAN Emerges with 802.11n,” Technology@Intel Magazine, 2004.
- [13] IEEE 802.20 <http://grouper.ieee.org/groups/802/20/Documents.htm>
- [14] ANSI INCITS 364-2003: Information Technology - Fibre Channel 10 Gigabit (10GFC)
- [15] IEEE Standard 802.3ae-2002: Amendment: Media Access Control (MAC) Parameters, Physical Layers, and Management Parameters for 10 Gbps Operation.
- [16] P. A. Davies, N. J. Gomes, “Subcarrier multiplexing in optical communication networks,” Analogue Optical Fibre Communications, Editors: B. Wilson, Z. Ghassemlooy and I. Darwazeh, IEE, pp 1-28, 1995.
- [17] G. Agrawal, “Fiber-Optic Communication Systems,” 2nd ed., New York: John Wiley & Sons, 1997.
- [18] Max Ming-Kang Liu, “Principles and applications of optical communications,” Irwin Professional Publishing, 1996.
- [19] H.P.A. van den Boom, W. Li, P.K. van Bennekom, I.T. Monroy, Giok-Djan Khoe, “High-capacity transmission over polymer optical fiber,” IEEE Journal of Select. Topics in Quantum Electronics, Vol. 7 , pp. 461-470, 2001

- [20] C.H. Cox III “Analog Optical links: models, measures and limits of performances,” Microwave Photonics, pp. 210-219, edited by Anne vilcot, Beatrice Cabon, Jean Chazelas, Kluwer Academic publishers.
- [21] Siegfried Geckeler, “Optical fiber transmission Systems,” Artech House Inc, 1987.
- [22] “Understanding Optical Communications” IBM Redbook, Lead Author - Harry Dutton
- [23] IEEE 802.3 Gigabit Ethernet Standard, 1000Base-SX for short wavelength transceivers (850 nm) and multimode fiber.
- [24] M.J. Hackert, S.M. Sibley, P.Sendlbach, “Performance of telecommunication-grade multimode fiber at 780 nm,” Journal of Lightwave Technology, Vol. 10, No. 6, pp. 712 - 719, June 1992.
- [25] M. Jungo, “Vertical-Cavity Surface-Emitting Lasers (VCSELs) Characterization and Modeling for Parallel Optical Interconnects Applications - Overview, Characterization and Modelling”
<http://www.ifh.ee.ethz.ch/~jungo/overview.shtml>
- [26] Dave Welch, “Low-cost, Single mode transmission with long wavelength VCSELs,” Lightwave, Feb 1999, pp. 62-67.
- [27] J. Geske, V. Jayaraman, T. Goodwin, M. Culick, M. MacDougal, T. Goodnough, D. Welch, J.E. Bowers, “2.5Gbps Transmission over 50km with a 1.3- μ m Vertical-Cavity Surface-Emitting Laser,” IEEE Photonics Technology Letters, Vol. 12, No. 12, pp. 1707-1709, Dec. 2000.
- [28] Stefan Rapp, “Long-Wavelength Vertical-Cavity Lasers Based on InP/GaInAsP Bragg Reflectors,” Doctoral thesis, Royal Institute of Technology, 1999.

- [29] L. Raddatz, I.H. White, D.G. Cunningham, M.C. Nowell, "An experimental and theoretical study of the offset launch technique for the enhancement of the bandwidth of multimode fiber links," *Journal of Lightwave Technology*, Vol. 16, No. 3, pp. 324 - 331, March 1998.
- [30] FOTP-204 (TIA-455-204), "Measurement of Bandwidth on Multimode Fiber" (Dec. 2000).
- [31] FOTP-203 (TIA-455-203), "Launched Power Distribution Measurement for Graded Index Multimode Fiber Transmitters" (June 2001).
- [32] FOTP-220 (TIA-455-220) "Differential Mode Delay Measurement of Multimode Fiber in the Time Domain" (Dec. 2001).
- [33] W. Stephens, T. Joseph, "System characteristics of direct modulated and externally modulated RF fiber-optic links," *Journal of Lightwave Technology*, Vol. 5, pp. 380- 387, March 1987.
- [34] R.E. Schuh, E. Sundberg, B. Verri, T. Arkner, "Penalty free simultaneous 1 Gbit/s digital and GSM-1800 radio signal transmission over 600 m multimode fibre using 850 nm VCSEL sources," *The 13th IEEE International Symposium on Personal, Indoor and Mobile Radio Communications*, Vol. 5, pp. 2274 – 2276, Sept. 2002.
- [35] R.E. Schuh, E. Sundberg, A. Alping, T. Arkner, "Penalty-free GSM-1800 and WCDMA radio-over-fibre transmission using multimode fibre and 850 nm VCSEL," *Electronics Letters*, Vol. 39, No. 6, pp. 512 – 514, March 2003.

- [36] M.Y.W. Chia, B. Luo, M.L. Yee, E.J.Z. Hao, "Radio over multimode fibre transmission for wireless LAN using VCSELs," *Electronics Letters*, Vol. 39, No. 15, pp. 1143 – 1144, July 2003.
- [37] M.Y.W. Chia and M.L. Yee, "Wireless Ultra Wideband Communications using radio over fiber," *IEEE Conference on UWB Systems and Technology (UWBST)*, pp. 265 – 269, Nov. 2003.
- [38] C. K. Sim, M.L. Yee, B. Luo, L.C. Ong, M.Y.W. Chia, "Performance Evaluation for Wireless LAN, Ethernet and UWB Co-existence on Hybrid Radio-Over-Fiber Picocells," *Optical Fiber Conference*, March 2005.
- [39] C. Carlsson, A. Larsson, A. Alping, "RF transmission over multimode fibers using VCSELs-comparing standard and high-bandwidth multimode fibers," *Journal of Lightwave Technology*, Vol 22, No. 7, pp. 1694 – 1700, July 2004.
- [40] Agilent EEsof, Advanced Designed System, Available from <http://eesof.tm.agilent.com/products/ads2004a.html>.
- [41] P. V. Mena, Sung-Mo Kang, T.A. DeTemple, "Rate-equation-based Laser Models with a Single Solution Regime", *Journal of Lightwave Technology*, Vol. 15, No. 4, pp. 717-730, April 1997.
- [42] P. V. Mena, J. J. Morikuni, S.-M. Kang, A. V. Harton, and K. W. Wyatt, "A Simple Rate-Equation-Based Thermal VCSEL Model," *Journal of Lightwave Technology*, Vol. 17, No. 5, pp. 865-872, May 1999.
- [43] R. Olshansky and D. B. Keck, "Pulse broadening in graded-index optical fibers," *Applied Optics*, vol. 15, no. 2, pp. 483–491, Feb. 1976.

- [44] G. Yabre, "Comprehensive theory of dispersion in graded-index optical fibers," *Journal of Lightwave Technology*, Vol. 18, No. 2, Feb. 2000
- [45] P. Pepeljugoski and D. Kuchta, "Design of optical communication data links," *IBM Journal of Research and Development*, Vol. 47, No. 2–3, Mar.–May 2003.
- [46] P. Pepeljugoski, S. Golowich, J. Ritger, P. Kolesar, and A. Risteski, "Modeling and simulation of the next generation multimode fiber," *Journal of Lightwave Technology*, vol. 21, pp. 1242–1255, May 2003.
- [47] Y. Koyamada and K. Yamashita, "Launching condition dependence of fiber loss and bandwidth," *Journal of Lightwave Technology*, Vol. 6, No. 12, pp. 1866-1871, Dec 1988.
- [48] "First Report and Order in the Matter of Revision of Part 15 of the Commission's Rules Regarding Ultra-Wideband Transmission Systems," FCC, released, ET Docket 98-153, FCC -2-48, April. 22, 2002.
- [49] Picosecond Impulse forming Networks, Available from Picosecond pulse labs.
<http://www.picosecond.com>
- [50] P. Smulders, "Exploiting the 60 GHz Band for Local Wireless Multimedia Access: Prospects and Future directions," *IEEE Communications Magazine*, Vol. 2, No. 1, pp. 140-147, Jan. 2002.
- [51] IEEE 802.15 WPAN Millimeter Wave Alternative PHY Task Group 3c (TG3c)
<http://www.ieee802.org/15/pub/TG3c.html>
- [52] K. Kojucharow, H. Kaluzni, M. Sauer, and W. Nowak, "A Wireless LAN at 60 GHz – Novel System Design and Transmission Experiments," *Microwave Symposium Digest, IEEE MTT-S International*, Vol.3, pp 1513 – 1516, 1998.

- [53] K. Maruhashi, M. Ito, L. Desclos, et al. "Low-Cost 60GHz-Band Antenna-Integrated Transmitter /Receiver Modules Utilizing Multi-Layer Low-Temperature Co-Fired Ceramic Technology," IEEE ISSCC 2000, pp. 324-325, Feb. 2000.
- [54] K. Ohata, K. Maruhashi, M. Ito, et al. "Wireless 1.25 Gb/s Transceiver Module at 60 GHz- Band," ISSCC 2002, pp. 298-299.
- [55] S. Reynolds, B. Floyd, U. Pfeiffer and T. Zwick, "60GHz Transceiver Circuits in SiGe Bipolar Technology," ISSCC 2004, pp. 442-443. Feb. 2004.
- [56] J. J. O'Reilly, P. M. Lane, and M. H. Capstick, "Optical Generation and Delivery of Modulated mm-waves For Mobile Communications," Analogue Optical Fibre Communications, Editors: B. Wilson, Z. Ghassemlooy and I. Darwazeh, IEE, pp 229-256, 1995.
- [57] D. Wake, "Optoelectronics for millimeter-wave radio over fibre systems," Analogue Optical Fibre Communications, Editors: B. Wilson, Z. Ghassemlooy and I. Darwazeh, IEE, pp 202-227, 1995.
- [58] F. Kojima, and M. Fujise, "Multimedia Lane and Station Structure for Road-to-Vehicle Communication System using ROF Techniques," The 11th IEEE International Symposium on Personal, Indoor and Mobile Radio Communications (PIMRC), Vol. 2, pp 969 – 973, 2000.
- [59] B. Cabon, V. Ginod, G. Maury, "Optical generation of microwave functions," Microwave Photonics, pp. 412-430, edited by Anne vilcot, Beatrice Cabon, Jean Chazelas, Kluwer Academic publishers.

- [60] R. Esman “Microwave functions enabled by photonics,” *Microwave Photonics*, pp. 399-412, edited by Anne vilcot, Beatrice Cabon, Jean Chazelas, Kluwer Academic publishers.

Appendix A: Encircled Flux

Encircled Flux is a measurement quantity of the optical power emitted by an optical transceiver coupled with a multimode fiber. It is the percentage of optical power confined within a given radial distance from the center of the fiber. The encircled flux calculation determines the fraction of optical power that is contained within a given radial distance r relative to the guided power contained in the entire fiber. This is expressed as given in the equation 1 as defined in FOTP-203:

$$EF(r) = \frac{\int_0^{2\pi} \int_0^r dP(r', \theta)}{\int_0^{2\pi} \int_0^{r_{\max}} dP(r', \theta)} = \frac{\int_0^{2\pi} \int_0^r I(r', \theta) dA}{\int_0^{2\pi} \int_0^{r_{\max}} I(r', \theta) dA} = \frac{\int_0^{2\pi} \int_0^r I(r', \theta) r' dr' d\theta}{\int_0^{2\pi} \int_0^{r_{\max}} I(r', \theta) r' dr' d\theta} = \frac{2\pi \int_0^r r' I(r') dr'}{2\pi \int_0^{r_{\max}} r I'(r') dr'} \quad (1)$$

Where

r - the radial distance from center of fiber

r_{\max} - fiber core radius

P - Power guided into the fiber

I - 2D Intensity distribution where the angular dependence is integrated by scaling with

2π making it a 1D distribution

The denominator represents the total guided power P_{\max} within the fiber. Hence the

equation reduces to:

$$EF(r) = \frac{2\pi}{P_{\max}} \int_0^r r' I(r') dr' \quad (2)$$

Appendix B: Modes of carrier operation in WLAN

FHSS – Frequency Hopping Spread Spectrum is a modulation technique where the data packets are transmitted in different frequency channels according to a pseudo random frequency hopping scheme. The transmissions are spread over frequency with time, this way the data is spread over a large bandwidth.

DSSS – Direct Sequence Spread Spectrum is a modulation technique where the "data" is multiplied with a Spreading Sequence (PN Sequence), of much higher frequency than the data, which spreads the signal over a wider bandwidth. A bandwidth of 25 MHz is used, which makes room for three different non-overlapping locations of the DSSS spectrum within the ISM band. CCK (Complementary Code Keying) is mandatory, while PBCC (Packet Binary Convolutional Coding) may be added.

CCK – Complementary Code Keying is based on complementary codes and was chosen over other modulations for its superior performance regarding multi path and its good autocorrelation and cross-correlation properties. This is used to increase IEEE 802.11b's peak data rate from 2 to 11 Mbps, while still using QPSK (Quadrature Phase Shift Keying) modulation.

PBCC – Packet Binary Convolutional Coding This scheme is optional for IEEE 802.11b and 802.11g. It makes use of Forward Error Correction to improve the link performance when noise is the limitation.

OFDM – Orthogonal Frequency Division Multiplexing is a multi-carrier modulation technique. The single high-rate bit stream is converted to low-rate N parallel bit streams. Each parallel bit stream is modulated on one of N sub-carriers. Each sub-

carrier can be modulated differently, e.g. BPSK, QPSK or QAM. To achieve high bandwidth efficiency, the spectrums of the sub-carriers are closely spaced and overlapped. Nulls in each sub-carrier's spectrum land at the center of all other sub-carriers.